

Pre-clinical Development of Anthocyanins Colorectal Cancer Chemopreventive Agents

Darren Cooke

(Supervisors:

Dr T H Marczylo

Prof. A J Gescher)

UMI Number: U238385

All rights reserved

INFORMATION TO ALL USERS

The quality of this reproduction is dependent upon the quality of the copy submitted.

In the unlikely event that the author did not send a complete manuscript and there are missing pages, these will be noted. Also, if material had to be removed, a note will indicate the deletion.



UMI U238385

Published by ProQuest LLC 2013. Copyright in the Dissertation held by the Author.
Microform Edition © ProQuest LLC.

All rights reserved. This work is protected against
unauthorized copying under Title 17, United States Code.



ProQuest LLC
789 East Eisenhower Parkway
P.O. Box 1346
Ann Arbor, MI 48106-1346

Abbreviation List

ACF	Aberrant crypt foci
ADME	Absorption, distribution, metabolism and elimination
AIN93G	American Institute of Nutrition mouse diet, number 93G
APC	Adenomatous polyposis coli
C3G	Cyanidin-3-glucoside
COX	Cyclooxygenase
CPS	Counts per second
CRC	Colorectal cancer
DMH	Dimethyl hydrazine
DMSO	Dimethyl Sulphoxide
EGFR	Epidermal growth factor receptor
F.A.	Formic acid
FAP	Familial adenomatous polyposis coli
FRAP	Ferric reducing ability of plasma
G.I.	Gastrointestinal
GCLP	Good clinical laboratory practise
GST	Glutathione-S-transferase
HPLC	High-performance liquid chromatography
LC/MS/MS	Liquid chromatography tandem mass spectrometry
LOD	Limit of detection
LOQ	Limit of quantitation
M1dG	Malondialdehyde-1-deoxyguanosine
MAM	Methylazoxymethanol
MDA	Malondialdehyde
MIN	Multiple intestinal neoplasia
MRM	Multiple reaction monitoring
NSAID	Non-steroidal anti-inflammatory drug
ORAC	Oxygen radical absorbance capacity
PBS	Phosphate buffered saline
PCV	Packed cell volume
PI	Propidium iodide
PK	Pharmacokinetic
ROS	Reactive oxygen species
SMAD4	Mothers against decapentaplegic homolog 4 (a class of genes downstream of TGF- β)
SPE	Solid phase extraction

TAC	Total anthocyanin content
TEAC	Trolox equivalent antioxidant capacity
TGF-β	Transforming growth factor-β
UDPGA	Uridine 5'-diphosphoglucuronic acid

ACKNOWLEDGMENTS.....	vi
ABSTRACT	vii
LIST OF FIGURES	lix
LIST OF TABLES.....	xv
1. INTRODUCTION	1
1.1. Colorectal Carcinogenesis	1
1.1.1 Mutagenesis	1
1.1.2 Carcinogenesis.....	2
1.1.3 Colorectal Carcinogenesis	4
1.1.4 Role of COX Enzymes in Carcinogenesis.....	7
1.1.5 Role of Oxidation in Carcinogenesis	8
1.1.6 Role of Epidermal Growth Factor Receptor in Carcinogenesis	9
1.2 Rodent Models of Colorectal Carcinogenesis	11
1.2.1 Chemically Induced Models	11
1.2.2 Genetic Mouse Models of Colorectal Carcinogenesis	15
1.2.3 Xenograft Models	18
1.3 Cancer Chemoprevention	19
1.3.1 Current Cancer Treatment and the Need for Prevention	19
1.3.2 Development of Cancer Chemopreventive Agents	20
1.3.3 Chemopreventive Agents	21
1.3.4 Mechanisms of Cancer Chemoprevention	22
1.4 Anthocyanins	26
1.4.1 Occurrence and Dietary Levels	26
1.4.2 Chemical Properties of Anthocyanins	27
1.4.3 Metabolism of Anthocyanins in Humans	30
1.4.4 Metabolism of Anthocyanins in Animals.....	31

1.4.5 In vitro Metabolism	37
1.4.6 Pharmacokinetics of Anthocyanins	39
1.4.7 Health Effects of Anthocyanins	41
1.4.8 Cancer Chemopreventive Properties of Anthocyanins in Animals.....	41
1.4.9 Anticarcinogenic Mechanisms of Anthocyanins from In Vitro Studies in Cultured Cells	45
1.5 Aims.....	60
 2. MATERIALS AND METHODS	 63
2.1 Materials	63
2.1.1 Sources of Anthocyanins and Method of Purification of Anthocyanins from Berries	63
2.1.2 Chemicals Used	63
2.1.3 Polymerase Chain Reaction (PCR) Materials Used.....	64
2.2 Analytical Methods	65
2.2.1 HPLC Method for the Separation of 15 Anthocyanins Present in Mirtoselect	65
2.2.2 HPLC Method for the Separation of Cyanidin-3-Glucoside and its Metabolites from Biomatrices	66
2.2.3 LC/MS/MS Methods (Short and Long)	66
2.3 Polymerase Chain Reaction (PCR) for Confirming Presence of APC Mutation in Tissue Samples from Apc^{MIN} Mice.	73
2.3.1 DNA Extraction	73
2.3.2 PCR of DNA to Detect the APC Mutation	74
2.4 Animal Experiments	76
2.4.1 Feeding Study Design	76
2.4.2 Oral Pharmacokinetic Study.....	77
2.4.3 Intravenous Pharmacokinetic Study.....	77
2.4.4 Sample Collection	77
2.4.5 Packed Cell Volume Measurement.....	79

2.4.6 Pharmacokinetic and Bioavailability Calculations	80
2.5 Solid-Phase Extraction of Anthocyanins from Biological Samples	82
2.5.1 Plasma and Urine	82
2.5.2 Mucosa, Bile and Brain	82
2.6 Liquid-Liquid Extraction of Murine Tissues	84
2.7 Determination of Malondialdehyde-1-deoxyguanosine (M1dG) Adducts in DNA.....	85
2.7.1 DNA Extraction from Adenoma Tissue	85
2.7.2 Determining DNA Concentration	86
2.7.3 Immunoslot-blot for Determination of M1dG Adduct Concentration	86
2.7.4 Calculation of M1dG Concentrations	88
2.8 Statistics.....	89
 3. DEVELOPMENT AND OPTIMISATION OF METHODS FOR THE EXTRACTION AND ANALYSIS OF ANTHOCYANINS IN BIOLOGICAL SAMPLES.....	 91
3.1 Method Development for Separation of Anthocyanins in Mirtoselect	91
3.1.1 Aims.....	91
3.1.2 Literature Methods for the Separation of Anthocyanins by HPLC	92
3.1.3 Selection of Stationary Phase	94
3.1.4 Optimisation of Mobile Phase Compositions and Elution Gradient.....	96
3.2 Method Development for the Separation of Cyanidin-3-Glucoside and Its Metabolites.....	103
3.3 Development of Techniques for the Extraction of Anthocyanins from Biological Samples.....	105
3.3.1 Liquid-liquid Extraction of Anthocyanins	105
3.3.2 Solid-Phase Extraction of Anthocyanins	107

3.4 Validation of Methods.....	110
3.4.1 Validation of Acetone Precipitation Extraction Method Using Cyanidin-3-Glucoside	110
3.4.2 Validation of Solid-Phase Extraction Method Using Cyanidin-3-Glucoside	112
3.4.3 Validation of SPE and HPLC-Vis Methods for Extraction and Measurement of Mirtoselect	115
 4. EFFECT OF ANTHOCYANINS ON COLORECTAL CARCINOGENESIS IN THE APC^{MIN} MOUSE.....	118
4.1 Introduction.....	118
4.2 Effect of a 0.1% Dietary Dose of Anthocyanins on Adenoma Development in Apc ^{MIN} Mice.....	120
4.3 Effect of Different Doses of Anthocyanins on Adenoma Development in Apc ^{MIN} Mice.....	125
4.3.1 Mirtoselect	125
4.3.2 Cyanidin-3-Glucoside	130
4.4 Modulation of M1dG Adduct Levels in Colorectal Adenomas by Anthocyanins	135
4.5 Discussion	141
 5. METABOLISM AND PHARMACOKINETICS OF ANTHOCYANINS IN MICE.....	146
5.1 Introduction.....	146
5.2 Steady-State Levels of Anthocyanins in Tissues of Apc ^{MIN} Mice Following Intervention with Anthocyanins.....	148

5.2.1 Mirtoselect	148
5.2.2 Cyanidin-3-Glucoside	153
5.3 Tissue Distribution and Pharmacokinetics of Cyanidin-3-Glucoside and Its Metabolites in Mice Following an Oral Bolus Dose	157
5.4 Tissue Distribution and Pharmacokinetics of Cyanidin-3-Glucoside In Mice Following I.V. Injection	162
5.5 Anthocyanin Metabolite Identification by HPLC and LC/MS/MS Following an Administration via Oral Bolus.....	167
5.5.1 HPLC Identification of Anthocyanins from Tissues of Mice Dosed with Cyanidin-3-Glucoside.....	167
5.5.2 LC/MS/MS Identification of Anthocyanin Metabolites from Tissues of Mice Dosed with Cyanidin-3-Glucoside.....	170
5.6 Bioavailability of Cyanidin-3-Glucoside	174
5.7 Discussion	175
5.7.1: Levels of Anthocyanins in Animals.....	175
5.7.2: Bioavailability of Anthocyanins	177
5.7.3: Anthocyanin Metabolism	180
5.7.4: Comparison of Target Tissue Anthocyanin Levels with In Vitro Efficacy	182
6. DISCUSSION.....	186
6.1 Contribution to Knowledge of Chemopreventive Efficacy.....	187
6.2 Contribution to Knowledge of Anthocyanin ADME	188
6.3 Contribution to Knowledge of Anthocyanin Pharmacodynamics	191
6.4 Considerations for Clinical Trials Using Mirtoselect.....	192
7. BIBLIOGRAPHY	195

Acknowledgments

Completing my PhD has been an extremely challenging yet rewarding process. It would have been considerably more difficult were it not for the help, guidance, and friendship of my supervisor Dr Timothy Marczylo. Tim helped me in all of the ways a good supervisor should, but also became a good friend as well; your patience, help and guidance were invaluable, thanks Tim! My second supervisor, Professor Andreas Gescher, also provided invaluable wisdom, encouragement and help. Andy, and the laboratory he provided, was always fun and productive, and through persuasion we always had the best equipment available! I would especially like to thank Andy for his help during the writing stage of my PhD – our meetings were intense, yet enjoyable – thanks for your patience Andy.

I would also like to thank my colleagues for being themselves, they made the time spent at Leicester enjoyable and the memories they helped build will be with me forever.

Finally, I would like to thank my family and partner; their support throughout my academic life, their desire for my success and their pride in my achievements are what drove me. In many ways the PhD I have achieved is for them – thank you all.

Abstract

Anthocyanins, from soft fruits and berries possess cancer chemopreventive effects in carcinogen-induced models of colorectal cancer. The aim of the work described here was to improve our understanding of their potential efficacy as colorectal cancer chemopreventive agents and their pharmacokinetics and pharmacodynamics. The hypothesis was tested that dietary Mirtoselect, a standardised mixture of 15 anthocyanins, or the isolated anthocyanin cyanidin-3-glucoside (C3G) affect adenoma development in the Apc^{MIN} mouse, a genetic model of colorectal cancer. Anthocyanins were added to the diet at 0.03, 0.1 or 0.3% (w/w) for the animals' life time. Adenoma number and size were measured at the end of the experiment (week 16). Both interventions reduced adenoma number/burden in a dose-dependent fashion. A potential mechanism by which anthocyanins are thought to exert cancer chemoprevention is anti-oxidation. Anti-oxidant effects of the interventions were investigated in DNA from Apc^{MIN} murine adenoma tissue by analysis of the pyrimidopurinone adduct of deoxyguanosine M1dG, a product of the reaction of DNA with malondialdehyde. At the dietary dose of 0.3% C3G and Mirtoselect significantly reduced levels of M1dG, suggesting that antioxidation may contribute to anthocyanin-mediated interference with adenoma development.

C57BL mice, the Apc^{MIN} background strain, received C3G po or I.V. at 500 or 1 mg/kg, respectively. Levels of anthocyanins in plasma and tissue were measured using a newly developed HPLC method. C3G bioavailability was 3.28%, consistent with literature values after ingestion of berries/fruits. Anthocyanin species were detected in the plasma, urine, mucosa, liver, kidneys,

heart, lung, gall bladder and brain. Absorption, distribution and excretion in the urine were rapid. The mean time of peak levels for all tissues studied was ~26 min.

The work described here defines further the potential role of anthocyanins in colorectal cancer chemoprevention. It also describes pharmacokinetic and pharmacodynamic features which may help optimise future clinical chemoprevention trials.

List of Figures

Figure 1.1: The multistage process of carcinogenesis. (The dark cellular core represents damaged DNA).....	3
Figure 1.2: Potential mechanism of colorectal carcinogenesis (route 'B').....	5
Figure 1.3: The histopathology of colorectal cancer, a multistage process.....	6
Figure 1.4: Formation of M1dG by reaction of malondialdehyde (MDA) and deoxyguanosine (dG) (Leuratti et al., 1998).....	9
Figure 1.5: A simplified schematic of the EGFR transmembrane glycoprotein depicting mitogen-activated protein kinase signal transduction cascade to the nucleus.....	10
Figure 1.6: Dietary phytochemicals that block or suppress multistage carcinogenesis.....	25
Figure 1.7: Structures of common anthocyanidins, existing as glycosides in nature.....	27
Figure 1.8: Absorptivities relating to pH 1 values for the chloride salts of the six major anthocyanidin-3-glucosides (1.0×10^{-4} M) after 1h of dissolution (taken from Cabrita <i>et al.</i> , 2000).....	28
Figure 1.9: pH-Dependent conformational rearrangement of the anthocyanin molecule, shown here for anthocyanins bearing a sugar ("Gl") on C-3.....	29
Figure 1.10: Fate of cyanidin-3-glucoside in biological systems (humans, rats etc).....	34

Figure 1.11: Degradation of anthocyanidins and formation of the corresponding phenolic acids.....	38
Figure 2.1: Representation of a blood sample, after centrifugation. The dark area shows the PCV.....	79
Figure 2.2: The equations used for calculating the AUC, AUC_{INF} and bioavailability following oral and I.V. bolus dosing.....	81
Figure 3.1: HPLC method employed by Nielsen et al (2003a) for the separation of anthocyanins from commercial blackcurrant juices.....	92
Figure 3.2: Example chromatogram for the separation of the anthocyanin components of Mirtoselect (Indena SpA).....	93
Figure 3.3: The ability of different stationary phases to separate 15 anthocyanins from Mirtoselect, using the method described in Figure 3.1.....	95
Figure 3.4: Effect of formic acid concentration of mobile phase A on the separation of anthocyanins from Mirtoselect.....	96
Figure 3.5: Chromatograms showing the separation of anthocyanins in Mirtoselect under varying HPLC conditions.....	98
Figure 3.6: Chromatograms showing the effect of changing channel B from acetonitrile (chromatogram i) to methanol (chromatogram ii) for the separation of anthocyanins in Mirtoselect.....	99

Figure 3.7: Representative HPLC chromatogram of optimal Mirtoselect separation.....	101
Figure 3.8: Representative HPLC chromatograms of C3G and its metabolites in urine. Channel A in both cases is 10% formic acid in water.....	104
Figure 3.9: Effect of increasing methanol concentration on the elution of cyanidin and C3G from Oasis HLB 1cc, 30mg SPE cartridges.....	108
Figure 3.10: Standard curve of - Unextracted standards, Extraction 2, Extraction 1 and Extraction 3 from Table 3.3.....	114
Figure 4.1: Effect of Mirtoselect or C3G (0.1% in the diet) on total numbers of intestinal adenomas in Apc ^{MIN} mice, male and female data combined.....	121
Figure 4.2: Lack of effect of Mirtoselect or C3G (0.1% in the diet) on mean packed cell volume.....	121
Figure 4.3: Effect of Mirtoselect and C3G (0.1% in the diet) on number and size of adenomas.....	122
Figure 4.4: Effect of Mirtoselect and C3G at a dietary concentration of 0.1% on number and size of adenomas compared with control animals.....	124
Figure 4.5: (A) Effect of Mirtoselect at three dietary concentrations (0.03, 0.1 and 0.3%) on total numbers of intestinal adenomas in Apc ^{MIN} mice. (B) An inverse correlation between adenoma decrease and dose was demonstrated by least mean square analyses.	125

Figure 4.6: Lack of effect of Mirtoselect at three dietary concentrations (0.03, 0.1 and 0.3%) on mean PCV.....	126
Figure 4.7: Effect of Mirtoselect at three dietary concentrations (0.03, 0.1 and 0.3%) on number and size of adenomas throughout the entire intestine (proximal, medial, distal small intestines and colon combined).	127
Figure 4.8: Effect of Mirtoselect at three dietary concentrations (0.03, 0.1 and 0.3%) on number and size of adenomas in the Apc ^{MIN} mouse compared with control animals.....	128
Figure 4.9: Effect of Mirtoselect at three dietary concentrations (0.03, 0.1 and 0.3%) on tumour burden in the Apc ^{MIN} mouse intestine.....	129
Figure 4.10: (A) Effect of C3G at three dietary concentrations (0.03, 0.1 and 0.3%) on total numbers of intestinal adenomas in Apc ^{MIN} mice. (B) An inverse correlation between adenoma decrease and dose was demonstrated by least mean square analyses.....	130
Figure 4.11: Lack of effect of C3G at three dietary concentrations (0.03, 0.1 and 0.3%) on mean PCV.....	131
Figure 4.12: Effect of C3G at three dietary concentrations (0.03, 0.1 and 0.3%) on number and size of adenomas throughout the entire intestine (proximal, medial, distal small intestines and colon combined).....	132
Figure 4.13: Effect of C3G at three dietary concentrations (0.03, 0.1 and 0.3%) on number and size of adenomas in the Apc ^{MIN} mouse compared with control animals.....	133
Figure 4.14: Effect of C3G at three dietary concentrations (0.03, 0.1 and 0.3%) on tumour burden in the Apc ^{MIN} mouse intestine.....	134

Figure 4.15: M1dG immunoslot blot standard curve completed as described in 2.7.3.....	136
Figure 4.16: An example of an immuno-slot blot of DNA extracted from adenoma tissue from the small intestine of Apc ^{MIN} mice.....	137
Figure 4.17: An example of a standard curve for the quantitation of M1dG adduct levels.....	138
Figure 4.18: Effects of Mirtoselect or C3G at 0.1 and 0.3% in the diet, on M1dG adduct formation in adenoma tissue of the Apc ^{MIN} mouse.....	139
Figure 5.1: HPLC–Vis chromatograms of Mirtoselect extracts from various tissues of the Apc ^{MIN} mouse which received 0.3% Mirtoselect over 12 weeks (0.3% w/w in diet).....	150
Figure 5.2: HPLC–Vis chromatograms of C3G extracts from various tissues of Apc ^{MIN} mice.....	155
Figure 5.3: Plasma, urine and tissue concentration versus time curves for C3G and total anthocyanin content in C57BL mice which received C3G (500 mg/kg) via oral gavage.....	158
Figure 5.4: Plasma, urine and tissue concentration versus time curves for C3G and total anthocyanin content in C57BL mice which received C3G (1 mg/kg) via I.V. injection.....	164
Figure 5.5: Example chromatograms of various biomatrices from male C57BL mice dosed orally with C3G via gavage (see 5.3).....	169
Figure 5.6: HPLC and LC/MS/MS chromatograms of urine from the cyanidin-3-glucoside oral bolus study (see section 5.3).....	171

Figure 5.7: HPLC and LC/MS/MS chromatograms of mucosa from the cyanidin-3-glucoside oral bolus study (see section 5.3).....	172
------------------------------------------------------------------------------------------------------------------------------------	-----

List of Tables

Table 1.1: Rodent models of chemically induced CRC using indirect-acting carcinogens.....14

Table 1.2: Varying levels of anthocyanins in common fruits and wine.....26

Table 1.3: Metabolites identified in bio-matrices after dosing with anthocyanins.....35

Table 1.4: Plasma levels of anthocyanins after oral dosing in humans.....40

Table 1.5: Summary of growth inhibitory effects of anthocyanins and anthocyanin-rich extracts.....50

Table 1.6: Summary of evidence of underlying mechanisms responsible for the chemopreventive efficacy of anthocyanins.....55

Table 2.1: Transitions employed for the detection of parent anthocyanin ions present in Mirtoselect and cyanidin-3-glucoside and for their corresponding aglycons, in mouse biomatrices.....68

Table 2.2: Transitions employed for the detection of the glucuronide metabolites of anthocyanins present in Mirtoselect and cyanidin-3-glucoside, in mouse biomatrices.....69

Table 2.3: Transitions employed for the detection of the methylated metabolites of anthocyanins present in Mirtoselect and cyanidin-3-glucoside, in mouse biomatrices.....70

Table 2.4: Transitions employed for the detection of the sulphated metabolites of anthocyanins present in Mirtoselect and cyanidin-3-glucoside in mouse biomatrices.....	71
---------------------------------------------------------------------------------------------------------------------------------------------------------------------------------	----

Table 2.5: Transitions employed for the detection of the conjugated metabolites of anthocyanins present in Mirtoselect and cyanidin-3-glucoside, in mouse biomatrices.....	72
-----------------------------------------------------------------------------------------------------------------------------------------------------------------------------------	----

Table 2.6: Master mix composition for PCR of mouse DNA for identifying mutation of the APC gene.....	74
-------------------------------------------------------------------------------------------------------------	----

Table 2.7: PCR Cycling sequence used for the amplification of the Apc ^{MIN} gene sequence (* = repeat steps 2 – 4, 35 times).....	74
---------------------------------------------------------------------------------------------------------------------------------------------------	----

Table 3.1: Assessment of liquid-liquid methods for the extraction of C3G from human plasma.....	106
--------------------------------------------------------------------------------------------------------	-----

Table 3.2: Validation of the acidified acetone extraction method.....	111
------------------------------------------------------------------------------	-----

Table 3.3: Validation of the SPE method of C3G extraction from human plasma. Values shown are extraction efficiencies (%).....	113
---------------------------------------------------------------------------------------------------------------------------------------	-----

Table 3.4: Reproducibility of Retention Time (tR) and Retention Index (iR) relative to C3G for anthocyanins in the standardized bilberry extract Mirtoselect.....	117
--------------------------------------------------------------------------------------------------------------------------------------------------------------------------	-----

Table 5.1: Anthocyanins identified by LC/MS/MS analysis of urine and intestinal mucosa samples from Apc ^{MIN} which received Mirtoselect (0.3%) with their diet.....	152
--------------------------------------------------------------------------------------------------------------------------------------------------------------------------------------	-----

Table 5.2: Total anthocyanin and C3G T_{MAX} and C_{MAX} values for a range of tissues from mice orally dosed with 500 mg/kg C3G. C_{MAX} concentrations in nmol/ml or nmol/g depending on biomatrix.....	160
Table 5.3: Pharmacokinetic data derived from a range of tissues from mice dosed with C3G (500 mg/kg) by oral gavage.....	161
Table 5.4: Total anthocyanin and C3G T_{MAX} and C_{MAX} values for a range of tissues from mice dosed intravenously through the tail vein with 1 mg/kg C3G. C_{MAX} concentrations in nmol/ml or nmol/g depending on tissue type.....	165
Table 5.5: Pharmacokinetic data derived from a range of tissues from mice dosed by I.V. injection.....	166
Table 5.6: Metabolite identification for metabolites present in tissues after oral bolus dose of C3G (500 mg/kg).....	174
Table 5.7: AUC and dose values necessary to calculate the bioavailability of both C3G and total anthocyanin content (TAC).....	175

1. Introduction

1.1. Colorectal Carcinogenesis

Colorectal cancer (CRC) is one of the most common forms of cancer in industrialised countries, accounting for 15% of all malignant neoplasms. The lifetime colorectal cancer risk in the general population is 5% (Fodde *et al.*, 2001), but this figure rises dramatically with age: by the age of 70 approximately half the Western population will have developed an adenoma, which may or may not progress to become malignant (Fodde *et al.*, 2001). Prognosis is poor with a 5 year survival rate between 40 – 50% (Kobaek-Larsen *et al.*, 2000). Nearly all cases of colorectal cancer in humans are adenocarcinomas, with the majority (97%) sporadic, and the remaining 3% due to one of two autosomal inherited diseases: hereditary non-polyposis colorectal cancer (HNPCC, 2%) or familial adenomatous polyposis coli (FAP, 1%). Cancer occurs as a result of DNA damage at a cellular level, a process termed mutagenesis.

1.1.1. Mutagenesis

There are three main types of mutagenesis (Weinberg *et al.*, 2006):

- Single point mutations
- Structural chromosomal aberrations
- Genome mutations.

These three types of mutagenesis can be initiated by a range of sources including chemical carcinogens, oncogenic viruses, electromagnetic radiation (UV, X-Ray), free radicals and DNA replication errors. Exposure to these initiators can result in any of the three types of mutagenesis resulting in faulty DNA replication which, if not corrected or removed by the genes necessary for DNA-damage repair, will potentially lead to carcinogenesis (Weinberg *et al.*, 2006). Cells can repair damaged DNA in three ways, by:

- Excision repair – can be base or nucleotide excision
- Mismatch repair – repairs incorrectly linked bases
- Translesion synthesis - last resort (error prone) DNA repair

Each of these systems is in place to limit the duplication of DNA damage, and as such, should these mechanisms become damaged, the risk of cancer is increased.

1.1.2. Carcinogenesis

Carcinogenesis, the process which leads to the development of cancer, is caused by mutations of the genetic material of normal cells, which upsets the balance between proliferation and cell death. It is a multistage process that develops from a DNA mutation, through promotion before finally resulting in the progression of cells to form a tumour (Figure 1.1).

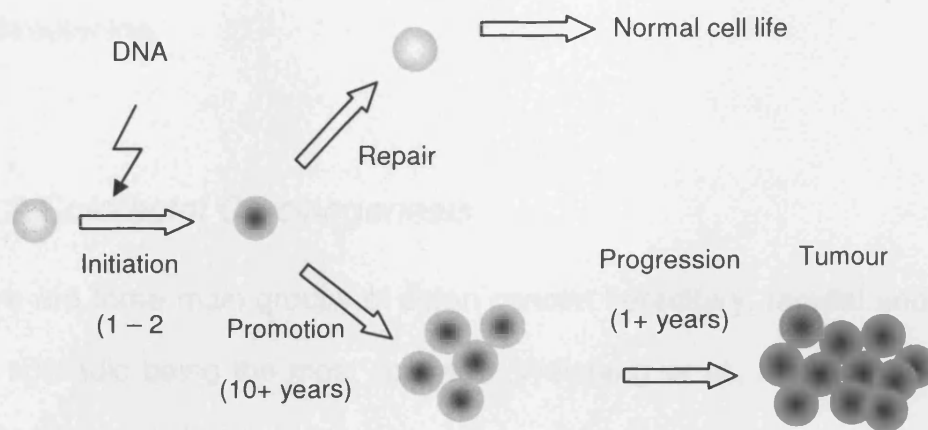


Figure 1.1: The multistage process of carcinogenesis. (The dark cellular core represents damaged DNA) (Surh, 2003).

Normally, the balance between proliferation and programmed cell death is tightly regulated to ensure the integrity of organs and tissues. Mutations in DNA that lead to cancer disrupt these normal processes. Disregulated genes (oncogenes) cause uncontrollable proliferation of cells. DNA repair is controlled by tumour suppressor genes, which discourage cell growth or halt division to enable DNA repair. Mutations in the protooncogenes can lead to signals for the release of excessive cell growth and mutations in tumour suppressor genes can cause an increase in cell proliferation and hinder or inhibit DNA repair. The net result is that cells are either dividing at a rate greater than that of DNA repair, or normally dividing cells are not being checked for DNA damage. There are many backup processes which duplicate the functions of both protooncogenes and tumour suppressor genes, and as such both types of mutations are required for carcinogenesis to occur. The tumours produced in this situation can either be benign or malignant. Benign tumours do not pose a direct threat to life, unless directly impinging on vital areas. Malignant tumours can invade

other organs, spread to distant areas of the organism (metastasis) and become life threatening.

1.1.3. Colorectal Carcinogenesis

There are three main groups of colon cancer: hereditary, familial and sporadic, with sporadic being the most common (Weinberg *et al.*, 2006). Most of these colonic cancers involve mutations in the APC gene (adenomatous polyposis coli), a tumour suppressor gene. The APC gene produces a protein which plays a critical role in many cellular processes that determine whether a cell may develop into a tumour, and normally works through association with other proteins.

The luminal surface of the gastrointestinal (G.I.) tract consists of villi (extrusions) and crypts (area between villi) (Figure 1.2). This arrangement creates a very high surface area through which nutrients can be absorbed. The surface created by the villi is coated with epithelial cells which are routinely shed and replaced with new cells produced from stem cells located in the base of the crypts (Fodde *et al.*, 2001). If everything is functioning normally the cells would proliferate as in Figure 1.2 via the 'A' route. Current theories of colorectal carcinogenesis suggest that these stem cells can undergo an APC mutation which is then passed onto the progeny and gets incorporated into the new epithelial cells (route 'B' in Figure 1.2) (Fodde *et al.*, 2001 and Lamprecht *et al.*, 2002). These epithelial cells then move up the lateral surface of the villi replacing the cells which have been shed at the apex. However, due to the APC mutation these abnormal epithelial cells are shed less easily, and over

time can accumulate with new epithelial cells supplementing their numbers. The normal process of epithelial renewal takes 3-6 days (Fodde *et al.*, 2001 and Kay *et al.*, 2005) and cell mitotic rates should equal rate of loss. Intestinal tumours are the result of an increase in this gain:loss ratio (Fodde *et al.*, 2001).

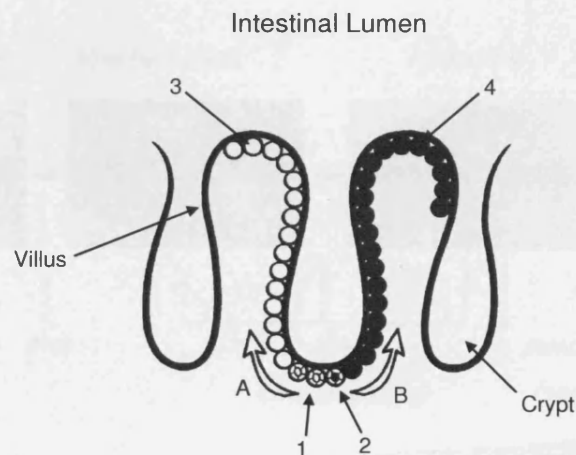


Figure 1.2: Potential mechanism of colorectal carcinogenesis (route 'B'). Stem cells (1) develop an APC mutation (2) in the base of the crypt. These proliferate up the crypt onto the surface of the villus generating epithelial cells carrying the APC mutation (4). Instead of being shed as healthy epithelial cells (3) would, they can accumulate to form adenomas – modified from Lamprecht *et al.*, 2002.

The earliest signs of colorectal neoplasms are aberrant crypt foci (ACF). ACFs are recognized as being early preneoplastic lesions and have consistently been observed in experimentally-induced colon carcinogenesis in laboratory animals (McLellan *et al.*, 1991). Pretlow *et al.* (1992) have also shown that these lesions are present in the colonic mucosa of patients with colon cancer and have suggested that aberrant crypts are putative precursor lesions from which adenomas and carcinomas develop within the colon. ACF express mutations in

the *Apc* gene and *Ras* oncogene that appear to be biomarkers of colon cancer development (Jen *et al.*, 1994). ACF can be composed of cells of normal morphology (nondysplastic) or dysplastic cells. Dysplastic cells are more likely to become a polyp – a benign tumour mass protruding into the lumen (Fodde *et al.*, 2001 and Talavéra *et al.*, 2005) (see Figure 1.3).

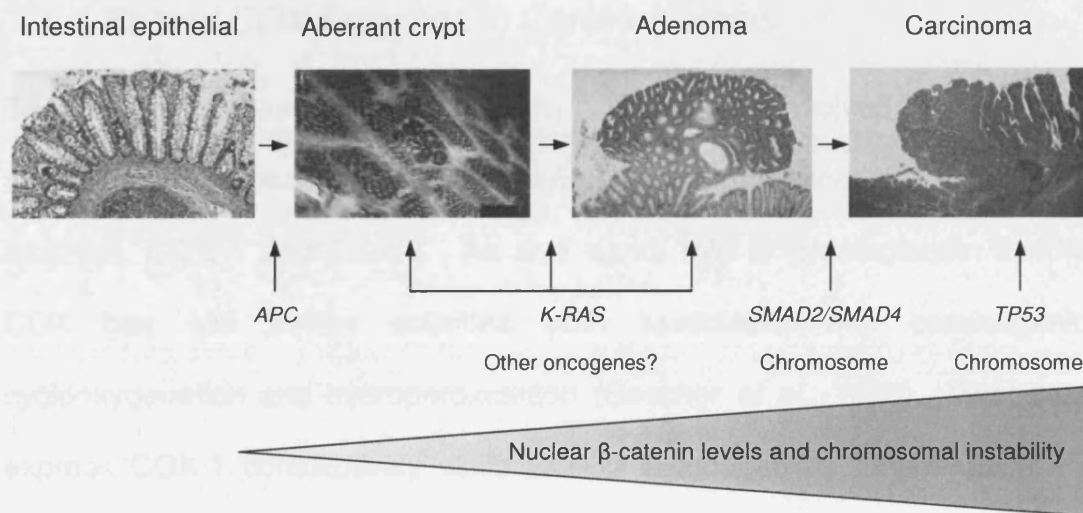


Figure 1.3: The histopathology of colorectal cancer, a multistage process. The model shows genetic alterations and pathological changes for the transformation of normal colonic cells into colorectal carcinomas. The details of the transformation are discussed in the text (Fodde *et al.*, 2001).

K-RAS mutations and mutations of other oncogenes lead to promotion of ACF into adenomas. The tumour-suppressor genes centrally involved in colorectal tumorigenesis are *APC*, *p53* and *SMAD4* (Fodde *et al.*, 2001). Adenomas can exist as two types – hyperplastic and adenomatous (dysplastic), the dysplastic polyps are more likely to develop into carcinomas (Figure 1.3). Loss of *p53* function, a tumour suppressor gene, is involved in this late-stage progression rather than initiation (Vogelstein *et al.*, 1988 and Cao *et al.*, 2001). The role of

β -catenin in carcinogenesis is as a binding partner for APC (Su *et al.*, 1993 and Rubinfeld *et al.*, 1993). Once β -catenin has been activated it binds to DNA-binding proteins in the cell nucleus to serve as an essential activator of transcription resulting in increased cellular proliferation (Fodde *et al.*, 2001).

1.1.4. Role of COX Enzymes in Carcinogenesis

The prostanoid, cyclooxygenase (COX) is an enzyme involved in prostaglandin synthesis and is expressed in numerous types of cancer. It exists in two isoforms, COX-1 and COX-2. As well as its role in prostaglandin synthesis COX has two further activities both associated with carcinogenicity: cyclooxygenation and hydroperoxidation (Gescher *et al.*, 1998). Most tissues express COX-1 constitutively while COX-2 is induced by inflammation. The COX-2 gene is an immediate, early response gene that is induced by growth factors, oncogenes, carcinogens, and tumour-promoting phorbol esters such as TPA (12-*O*-tetradecanoylphorbol ester) (Subbaramaiah *et al.*, 1996 and Kelley *et al.*, 1997). COX-2 is upregulated in transformed cells and in malignant tissue (Subbaramaiah *et al.*, 1996, Kelley *et al.*, 1997, Herschman *et al.*, 1996, Kutchera *et al.*, 1996, Eberhart *et al.*, 1994, Ristimaki *et al.*, 1997 and Hida *et al.*, 1998), and has been shown to be selectively overexpressed in human colon, gastric (Ristimaki *et al.*, 1997) and breast cancer (Brueggemeier *et al.*, 1999). In addition to the genetic evidence implicating COX-2 in tumorigenesis, the majority of studies investigating the role of prostanoids in epithelial malignancy have concentrated on colon cancer and suggest that COX-2 expression and prostaglandin production are crucial to the growth and development of these tumours (Taketo, 1998 and Gustavson-Svard *et al.*,

1997). The role of COX-2 in carcinogenesis has been evidenced in a study which showed COX-2 knock-out mice are resistant to colonic tumorigenesis caused by a mutation in the APC gene (Oshima *et al.*, 1996b).

1.1.5. Role of Oxidation in Carcinogenesis

There has been increasing interest in recent years in the role of oxidation in carcinogenesis and antioxidation as a mechanism by which chemopreventive agents exert their activity (Sardas, 2003). Oxidative stress arises from both endogenous and exogenous sources in the form of reactive oxygen species (ROS). These can consist of either oxygen radicals, highly reactive species with one or more unpaired electrons which can exist independently, or non-radical derivatives of oxygen (Sharma *et al.*, 2004), both of these are produced constantly under normal conditions. As a result of their constant production, antioxidant systems, both endogenous and dietary, are present to limit the damage they may cause, but cell damage through ROS is still ubiquitous (Sardas, 2003). As a result of this damage, ROS have been described as an important class of carcinogens (Sardas, 2003).

Techniques for measuring the extent of DNA damage caused as a result of ROS are becoming more abundant and include immuno-slot blot, comet assay and enzyme-linked immunosorption assay (ELISA). DNA adducts investigated primarily include malondialdehyde-deoxyguanine (M1dG) and 8-oxodeoxyguanosine (8-oxo-dG). Malondialdehyde is a product of lipid peroxidation and prostaglandin biosynthesis. It is mutagenic and carcinogenic and reacts with DNA to form M1dG (Leuratti *et al.*, 1998). It has been detected

in the mucosa of healthy humans in the range of $2 \rightarrow 120$ adducts per 10^8 nucleotides (Sharma *et al.*, 2004). The endogenous formation of malondialdehyde in humans and the data describing its genotoxicity and mutagenicity suggest that it may play an important role in human carcinogenesis. Figure 1.4 shows the reaction involved in producing M1dG.

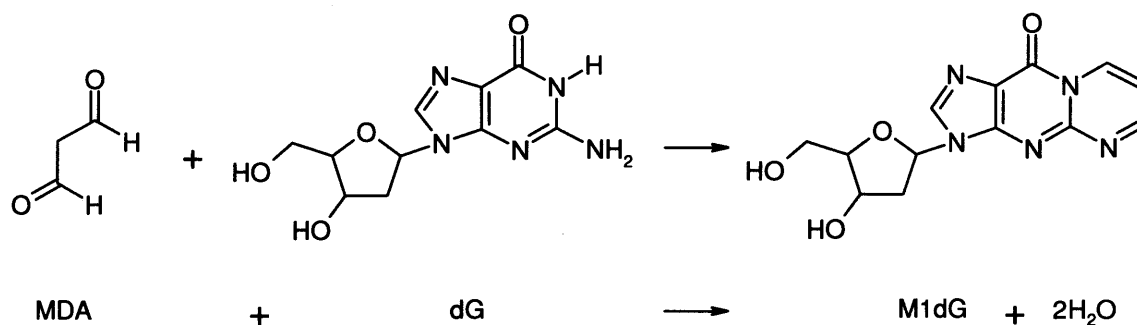


Figure 1.4: Formation of M1dG by reaction of malondialdehyde (MDA) and deoxyguanosine (dG) (Leuratti *et al.*, 1998).

1.1.6 Role of Epidermal Growth Factor Receptor in Carcinogenesis

Another key element in carcinogenesis is the role of epidermal growth factor receptor (EGFR). EGFR, which is also known as HER-1, is a transmembrane receptor for epidermal growth factor (EGF) and is a member of the ErbB family of tyrosine kinases (Herbst, 2004). Compatible ligands for the EGFR include EGF and transforming growth factor- α (TGF- α). Ligand-binding to EGFR results in autophosphorylation of receptor tyrosine kinases and subsequent activation of signal transduction pathways that are involved in regulating cellular proliferation, differentiation and survival, for example the signalling pathway involving mitogen activated protein kinase (MAPK) (Herbst, 2004). EGFR is overexpressed in the majority of solid tumours including colorectal cancer

(Herbst *et al.*, 2002). Overexpression of this intensity initiates down-stream signalling pathways, resulting in cells with aggressive growth and invasive characteristics (Figure 1.5) (Ethier, 2002).

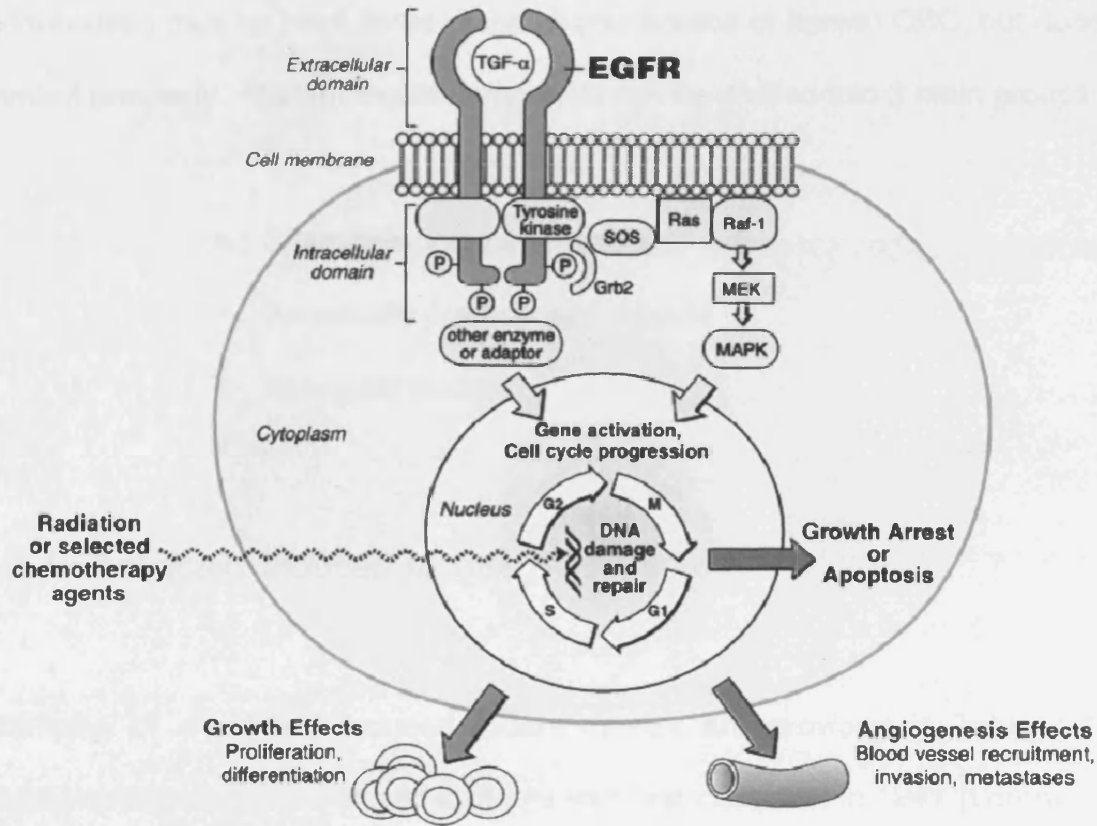


Figure 1.5: A simplified schematic of the EGFR transmembrane glycoprotein depicting mitogen-activated protein kinase signal transduction cascade to the nucleus. Once phosphorylated the tyrosine kinase initiates a downstream effect on other pathways which go on to affect the cell cycle (Adapted from Ethier, 2002).

1.2 Rodent Models of Colorectal Carcinogenesis

Animal models have been increasingly incorporated into CRC research to allow a better understanding of the onset and progression of the disease. Rodent models used thus far have some of the characteristics of human CRC, but none mimic it precisely. Rodent models employed can be divided into 3 main groups:

- Chemically induced models
- Genetically predisposed models
- Xenograft models

1.2.1 Chemically Induced Models

Examples of chemically induced rodent models are provided in Table 1.1. Chemical induction of colorectal tumours was first observed in 1941 (Lorenz *et al.*, 1941). 1,2,5,6-Dibenzanthracene and 20-methylcholanthracene were orally administered to mice, which developed intestinal tumours. Hydrazines have also been shown to be potential colonic carcinogens. An oral dose of the hydrazine cycasin from cycad flour showed effective tumorigenesis in the colon of rats (Laquer, 1964). Cycasin is metabolised *in vivo* to methylazoxymethanol (MAM). 1,2-Dimethylhydrazine (DMH), which is also metabolised to MAM in the liver, also gives rise to tumours with a distribution mainly in the distal region of rat colon (Druckrey *et al.*, 1967). Azoxymethane (AOM), a more widely used hydrazine carcinogen, is another precursor of MAM, and is excreted at much lower levels in the urine whilst still being an effective inducer of colonic tumours

in rodents (Wakabayashi *et al.*, 1992 and D'Agostino *et al.*, 1995). Hydrazines also give rise to the formation of aberrant crypt foci (ACF) (Rao *et al.*, 1999).

2-Amino-1-methyl-6-phenylimidazo[4,5-*b*]pyridine (PhIP), a heterocyclic amine, is a rodent carcinogen (Wakabayashi *et al.*, 1992, Sugimura *et al.*, 1997 and Ito *et al.*, 1997). PhIP is present in broiled meats and fish, and the dose shown to be carcinogenic would be present in 400 – 500 kg of overcooked beef (Kobaek-Larsen *et al.*, 2000) (400 ppm dose in Table 1.1). PhIP models have very long latency periods – as long as 104 weeks in rat and display a low incidence of CRC (Ito *et al.*, 1997 and Esumi *et al.*, 1989).

DMH, AOM and PhIP are indirect acting carcinogens; metabolism is required to produce the carcinogen. Genotoxic carcinogens, which directly interact with DNA can also be employed in carcinogenesis studies. A single, large, oral dose of *N*-methyl-*N*-nitrosourea (MNU) will induce tumours in the gastrointestinal tract (Leaver *et al.*, 1969). *N*-Methyl-*N*-nitro-*N*-nitrosoguanidine (MNNG) is a carcinogen when administered to Sprague-Dawley rats intra-rectally (Zusman *et al.*, 1991). After 52 weeks three types of tumours were detected: polypoid adenomas, intraepithelial carcinomas and small carcinomas.

The route of administration of a particular carcinogen also has a significant effect on CRC incidence (examples are shown in Table 1.1). Dietary administration gives a variable but low incidence of CRC (Thorup *et al.*, 1992 and 1994) whereas subcutaneous injection gives a higher incidence (Maskens, 1976, Rubio *et al.*, 1994 and D'Agostino *et al.*, 1995), although there are exceptions (Nordlinger *et al.*, 1991). These differences may be due to the

carcinogen being activated or deactivated by metabolism in the liver, as a result of the first-pass effect. After a drug is swallowed it is absorbed by the digestive system and enters the hepatic portal system, which transports it directly to the liver, before it enters the general circulation. The first-pass effect does not occur with other routes of administration.

Table 1.1: Rodent models of chemically induced CRC using indirect-acting chemical carcinogens. DMH = 1,2-dimethylhydrazine; AOM = azoxymethane; PhIP = 2-amino-1-methyl-6-phenylimidazo[4,5-*b*]pyridine; SC = subcutaneous injection; IM = intramuscular injection (Adapted from Kobaek-Larsen *et al.*, 2000).

Species/Sex	Strain	Chemical	Dose Regimen	Colon Tumour Incidence	Reference
Rat	BD	DMH	21 mg/kg, SC x 20 weeks	100%	Druckrey, 1967
Rat/male	F344	DMH	30 mg/kg, SC x 1	10%	Glauert, 1989
Rat/male	Sprague-Dawley	DMH	20 mg/kg, SC x 20 weeks	100%	Tsunoda, 1992
Rat/male	F344	AOM	8 mg/kg, IM x 12 weeks	80%	Shamsuddin, 1981
Rat/male	Wistar	AOM	10 mg/kg, SC x 12 weeks	35%	Nordlinger, 1991
Rat/male	Wistar	AOM	15 mg/kg, SC x 6 weeks	100%	D'Agostino, 1995
Mice/female	Shrew	MNU	1.5 mg/mouse, 16 x biweekly	100%	Yang, 1996
Rat/male	F344	PhIP	100 ppm (diet)	43%	Ito, 1997
Rat/male	F344	PhIP	400 ppm (diet)	55%	Ito, 1997
Mice/both	CDF1	PhIP	0.04% (diet)	0%	Esumi, 1989

One advantage of using chemical carcinogens for the induction of colorectal cancer is the high incidence of colonic tumours observed, however, one disadvantage is the hazard to the investigators through the handling of carcinogens. This problem is further enhanced by the excretion of these carcinogens and their metabolites in the urine, increasing the risk of aerosol inhalation. The hazard associated with inhalation of excreted carcinogens or their metabolites can be partly reduced by using safer alternatives – in the case of hydrazines, AOM is safer than MAM for example. Another disadvantage is the lack of relevance of this model to human carcinogenesis; the very high doses of carcinogen administered bear little physiological relevance to the human situation.

1.2.2 Genetic Mouse Models of Colorectal Carcinogenesis

CRC mouse models have been created by interfering with the adenomatous polyposis coli (APC) gene, and as such these mice spontaneously develop adenomas along the intestinal tract, mimicking the inherited condition of familial adenomatous polyposis coli (FAP) in patients (Su *et al.*, 1992). The advantage of these models is that they reflect parts of the pathogenesis of CRC in humans (Heyer *et al.*, 1999).

The most common model is the multiple intestinal neoplasia (Apc^{MIN}) mouse. This model was derived by treating male mice with ethylnitrosourea, causing a germline mutation at the Min locus, and then mating these Min/+ mice with C57BL/6J females – this method produced a 50% transference to the offspring (Moser *et al.*, 1990 and Su *et al.*, 1992). With the presence of the Min mutation

the mice develop adenomas primarily in the small intestine. The adenomas which develop do not undergo metastasis and occur in a range of sizes up to approximately 4 mm in diameter. The life expectancy of these mice is approximately 18 weeks, and the mice can develop an adult-onset progressive anaemia characterized by a decreasing red cell count and an increasing proportion of reticulocytes, symptoms typical of anaemia due to chronic blood loss. The mice become anaemic after 60 days of age and anaemia is probably the cause of death by 120 days of age in most affected mice. The anaemia is presumably secondary to the development of multiple adenomas, which can bleed into the intestinal lumen (Moser *et al.*, 1990). The model mimics FAP in humans – the murine APC (*mAPC*) gene has been shown to be closely linked with the Min locus, and sequence comparison of *mAPC* between normal and APC^{MIN} mice identified a nonsense-mutation in the APC^{MIN} mice – analogous to those found in FAP patients (Su *et al.*, 1992).

APC^{MIN} mice are not the only genetic mouse model for spontaneous colorectal carcinogenesis. Knockout mouse models enable alteration or removal of specific genes. One example of a knockout mouse is the APC 716 knockout model. These mice are characterised by having truncated APC polypeptides (Kobaek-Larsen *et al.*, 2000). Research with this model on the C57BL murine background showed the development of multiple polyps throughout the gastrointestinal tract; this development was exacerbated by treatment with heterocyclic amines (Oshima *et al.*, 1996a). APC1638N is another knockout model which showed the spontaneous growth of adenomas, adenocarcinomas and polyploid hyperplasia (Fodde *et al.*, 1994, Sorensen *et al.*, 1997 and Yang

et al., 1997). The APC1638N model is heterozygous for a targeted frameshift mutation at codon 1638 of the APC gene.

Human colorectal tumours arising from APC mutations are found to have other mutations in other genes, including: K-RAS, TGF- β , SMAD2, SMAD4 and TP53. Methods to determine the effect these gene changes have on colorectal carcinogenesis have involved the use of genetically manipulated mice. APC mutations were combined with these gene mutations and the effect this has on adenoma formation in the mice was determined (Kinzler *et al.*, 1996 and Heyer *et al.*, 1999). With SMAD4, a tumour suppressor gene downstream of TGF- β , mutations in the presence of an APC mutation it was shown that tumour progression was enhanced and the endpoint was more malignant than mice with the APC mutation alone (Takaku *et al.*, 1998). As a result, SMAD4^{+/-} mice have been bred which develop intestinal lesions. Heterozygous SMAD4 mice develop polyps in the duodenum and stomach from 1 year of age (Taketo *et al.*, 2000).

The main advantage of these models is their correlation with the processes observed in human CRC, and the genes involved. The weakness of these genetic models is that they do not reflect the human situation exactly. In the case of the APC^{MIN} model, mice develop adenomas and the mice die before the adenomas develop into carcinomas, whilst in humans adenocarcinomas are the final malignancy. Another problem with the models is that they principally develop tumours of the small intestine, which does not reflect the human situation of primarily colonic tumours.

1.2.3 Xenograft Models

Xenograft models require a host animal to support the growth of the inserted colon cancer cell lines. If a wild type animal were to be used its immune system would suppress the cell growth and reject the foreign cells. With this in mind a strain of mice called nude mice have been bred; these mice have a suppressed immune system with no body hair, hence the moniker “nude mouse”, or athymic nude mouse. Generally, the cells are injected subcutaneously, which means the micro-environment will be considerably different to the target organ, but tumour development can then be monitored without surgical intervention, and tumour growth is normally recorded as a measured tumour volume. More recently orthotopic injection of the cells is being used, which is injection into the relevant tissue of the model. Almost any cancer cell line could be used, but as a rule cell lines which grow best in the lab would be used for subcutaneous injection for a xenograft experiment; the colon cells most commonly used are: HT29, HCT116, SW620 and CaCo-2.

The advantage of xenograft models is the rapid growth of cells implanted, providing a rapid means of screening chemopreventive agents. However, the disadvantages are again the lack of relevance to the human situation, whereby the steps leading to carcinogenesis are not representative of the normal situation required for tumour initiation. The microenvironment the cells exist in does not match the environment in which the cells would develop in the real cancer. Also, the cancer cell lines are often derived from metastatic tissue and differ significantly from tumour cells developing into a primary tumour.

1.3 Cancer Chemoprevention

1.3.1 Current Cancer Treatment and the Need for Prevention

Cancer chemoprevention refers to the administration of medication for the purpose of preventing or delaying cancer. Cancer treatment involves the use of radiotherapy, chemotherapy or surgery to attempt to cure patients (Tsao *et al.*, 2004). In some instances a combination of all three is required. These methods of cancer treatment, whilst able to kill a proportion of the cancer cells, also often cause the patient serious side effects (Sporn *et al.*, 2005). Once treated, recurrence of disease is not uncommon, and in this case a second treatment is not always possible; radiotherapy for example cannot be used over a certain dose in each tissue. Because treatment in many cases is not successful there is a role for chemoprevention of cancer (Tsao *et al.*, 2004).

Disease prevention has had both medical and financial success in other areas – cardiovascular disease has been massively decreased following the release of the chemopreventive statins (Sporn *et al.*, 2005), for example. Sporn and Su (2000) hypothesised that we need to consider that cancer is ultimately the end stage of a chronic disease process. Prevention has been managed effectively in cardiovascular patients through healthier living and the use of preventive agents, and this approach may also be beneficial to healthy humans at a higher risk of developing cancer. With this in mind, we should be treating the causes of cancer as opposed to its effects. The latter are only visible at a late stage; to achieve this we would need to target future patients before they show signs of cancer (Sporn *et al.*, 2000). In high risk groups this is possible, and these people would be the major beneficiaries of a chemopreventive agent. A high

risk is determined by a genetic defect or a lifestyle which increases risk. For example genetic defects which lead to a predisposition of colorectal cancer include FAP, a truncation of the Apc gene, or hereditary nonpolyposis colorectal cancer (HNPCC) or glutathione S-transferase (GSTnull) mutations (Ozturk *et al.*, 2003).

1.3.2 Development of Cancer Chemopreventive Agents

Potential cancer chemopreventive agents are generally identified through epidemiological studies investigating diet and cancer incidence. From these studies, environmental, lifestyle and dietary differences which may lead to potentially protective effects are proposed. Certain medications, such as non-steroidal anti-inflammatory drugs (NSAIDs) used as anti-inflammatory agents, are also being investigated as potential chemopreventive agents, and are thought to work through their inhibition of the COX family of enzymes (Hilmi *et al.*, 2006).

Once the potential agent is identified, investigations into the effect of the agent *in vitro*, including its effects on cell proliferation, its ability to induce apoptosis and its ability to induce senescence are studied. If the agent is shown to possess properties which are related to cancer chemoprevention and appears safe, *in vivo* studies will be carried out. When investigating an agent *in vivo*, both the toxicity of the drug and its effect on cancer progression are monitored. An example experiment for testing the chemopreventive ability of a CRC drug *in vivo* is to use Apc^{MIN} mice to monitor the effect of that drug on intestinal adenoma number and size. Once any chemopreventive effect has been

determined, pharmacokinetic (PK) studies would be undertaken to determine the type and route of metabolism, agent tissue concentrations, and distribution throughout the animals. PK studies also help determine the efficacious dose suitable for humans. Pharmacodynamic studies are also undertaken to determine the physiological effects, and mechanisms of the drug *in vivo*.

Once efficacy and toxicity have been determined in animals, chemopreventive agents can be entered into clinical trials. These consist of several phases and normally start with a small number of volunteers (often healthy ones) at a range of doses (phase I) to determine safety and pharmacokinetics. Once the initial safety of the therapy has been confirmed in phase I trials, phase II trials are carried out on larger groups designed to assess clinical efficacy of the therapy, as well as to continue phase I safety assessments in a larger group of volunteers and patients. Phase III studies are randomized, controlled trials on large patient groups and are aimed at being the definitive assessment of the efficacy of the new therapy, and a determination of the long term safety effects.

1.3.3 Chemopreventive Agents

The family of non-steroidal anti-inflammatory drugs (NSAIDs) show great promise for the prevention of colon cancer. Classically, they have shown potential due to their ability to inhibit the COX family of enzymes (section 1.1.4). An early example of a NSAID used in chemoprevention trials was sulindac, which caused regression of adenomatous polyps in Gardner's syndrome patients (Waddell *et al.*, 1983). Another example is aspirin, which has shown evidence of reducing the risk in men and women for cancers of the colon and

rectum (Mandel *et al.*, 1993). However, early NSAIDs which inhibit COX-1 and 2 have severe side-effects, including gastrointestinal (G.I.) bleeding, G.I. perforation and renal toxicity (Hilmi *et al.*, 2006). With the release of the new NSAIDs celecoxib and rofecoxib, which are highly selective COX-2 inhibitors, the G.I. side-effects were minimised, whilst offering the same chemopreventive efficacy in the G.I. tract. However, increased cardiovascular and renal complications (Drazen, 2005) mean their use as chemopreventive agents is not advised (Hilmi *et al.*, 2006). NSAIDs have also been tested in combination with other potential chemopreventive agents, such as sulindac in conjunction with tea extracts, where a significant synergistic decrease was observed when both treatments were applied compared to treatment of sulindac or tea individually (Orner *et al.*, 2003).

Other compounds investigated as cancer chemopreventive agents occur naturally in our diet. As stated earlier, candidates are identified through epidemiological studies and varying incidences of cancer around the world, and the diet these populations consume. Examples of such phytochemical chemopreventive agents investigated are: resveratrol, curcumin, indole-3-carbinol, epigallocatechin gallate (EGCG), theaflavin and quercetin.

1.3.4 Mechanisms of Cancer Chemoprevention

Potential mechanisms of action of chemopreventive agents have been elucidated to a great extent. One mechanism for preventing colorectal carcinogenesis is to inhibit the enzymes involved in initiation or promotion. One example of this is inhibition of the COX family of enzymes. Traditional NSAIDs and now selective COX-2 inhibitors have been successful at inhibiting

cyclooxygenase, and thus preventing or delaying the onset, or limiting the malignancy of tumours. Some phytochemicals used in chemoprevention (section 1.3.3) act as free-radical scavengers and thus can prevent oxidative damage leading to cancer cell growth. *Wattenberg* (1979, 1983 and 1985) showed retardation of benzo(a)pyrene-induced neoplasia in lungs of mice by dietary antioxidants, but the mechanism of anti-carcinogenicity by antioxidants is not fully understood. It has been hypothesised that the most plausible mechanisms are scavenging of ROS, limiting the formation of “activated” carcinogenic species by phase I biotransformation and through detoxifying ROS by inducing phase II detoxification enzymes (Sardas, 2003). Five large scale clinical trials have provided differing conclusions about the effects of antioxidants on cancer (Blot *et al.*, 1993, Heinonen *et al.*, 1994, Omenn *et al.*, 1994, Hennekens *et al.*, 1996 and Lee *et al.*, al 1999). The Alpha-Tocopherol (vitamin E)/Beta-Carotene Cancer Prevention Study (ATBC) showed no effect on lung cancer occurrence in Finnish male smokers (Heinonen *et al.*, 1994). The 1996 Physicians' Health Study I (PHS) found no change in cancer rates associated with beta-carotene and aspirin taken by U.S. male physicians (Hennekens *et al.*, 1996). Bjelakovic *et al* (2006) conducted a meta-analysis on the effect of anti-oxidants on colorectal adenoma adverse events. This meta-analysis reviewed eight randomized clinical trials incorporating 17,620 participants, and compared antioxidant supplements with placebo or no intervention. The result of this meta-analysis found no convincing evidence that antioxidant supplements had a significant beneficial effect on primary or secondary prevention of colorectal adenoma incidence (Bjelakovic *et al.*, 2006). So the exact role of antioxidants in cancer chemoprevention is unresolved.

It has been suggested that chemopreventive agents act as either blocking or suppressing agents (Figure 1.6) (Wattenberg, 1985 and Surh, 2003). Blocking agents prevent carcinogens from reaching the target sites and suppressing agents inhibit the malignant transformation of initiated cells. It has also been noted that the use of the terms “blocking” and “suppressing” agents may be an over simplification, and a better understanding of the events occurring at the cellular level in carcinogenesis is now available (Gescher *et al.*, 1998, Milner *et al.*, 2001 and Manson, 2003). Surh *et al* (2003) highlighted the many cellular signalling molecules targeted by phytochemicals in chemoprevention. These include: NF- κ B and AP1, NRF, MAPK, JNK and β -catenin.

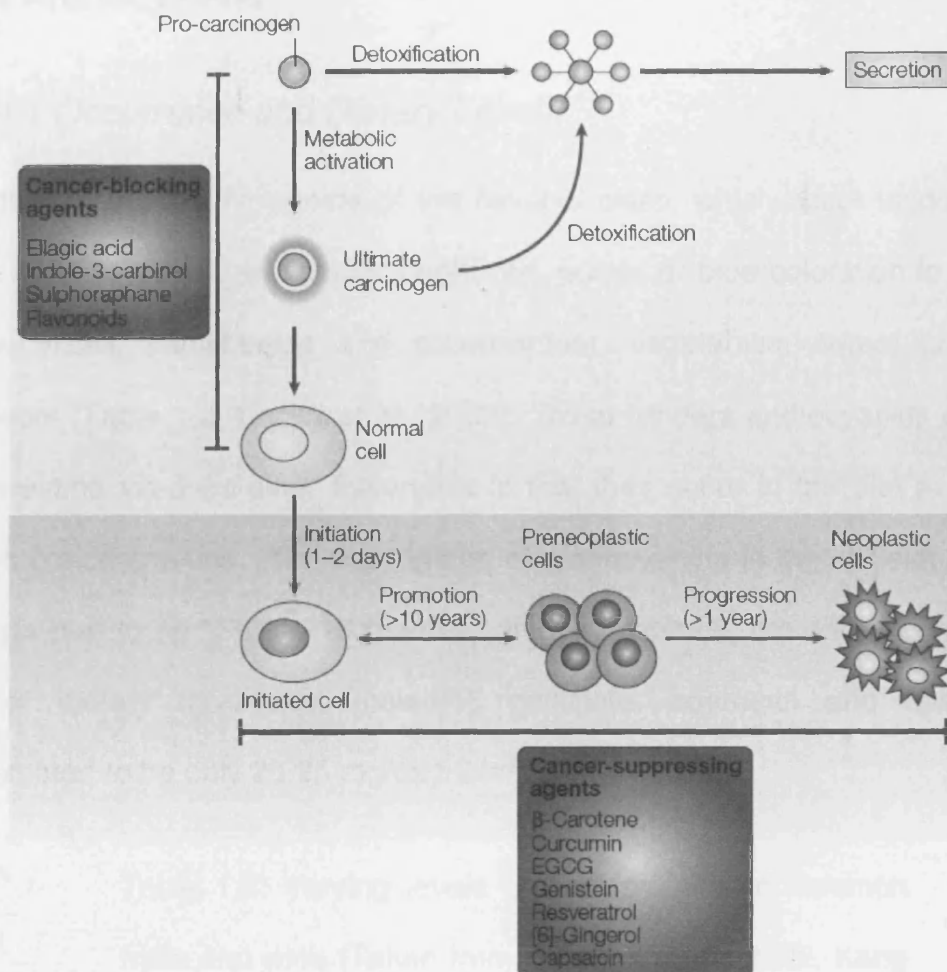


Figure 1.6: Dietary phytochemicals that block or suppress multistage carcinogenesis (see 1.1.2). Chemopreventive agents can act as blocking or suppressing agents (see 1.3.4). Figure adapted from Surh, 2003.

1.4 Anthocyanins

1.4.1 Occurrence and Dietary Levels

Anthocyanins are flavonoids of the flavanol class, which occur ubiquitously in the plant kingdom, and confer bright red, purple or blue coloration to fruits (eg blueberries, blackberries and strawberries), vegetables, cereal grains and flowers (Table 1.2, Cooke *et al.*, 2005). What renders anthocyanins especially interesting *vis-à-vis* other flavonoids is that they occur in the diet at relatively high concentrations. The daily intake of anthocyanins in the US diet has been suggested to be 180 to 215 mg/day, whilst in contrast, the daily intake of most other dietary flavonoids, including genistein, quercetin and apigenin, is estimated to be only 20-25 mg/day (Hertog *et al.*, 1993).

Table 1.2: Varying levels of anthocyanins in common fruits and wine (Taken from Felgines *et al.*, 2002, Kang *et al.*, 2003 and Kay *et al.*, 2005)

Anthocyanin Containing Foodstuff	Anthocyanin (mg) per 100 g Foodstuff
Chokeberry	200 - 1000
Aubergine	750
Orange	~ 200
Blackberry	~ 115
Blueberry	80 - 420
Raspberry	10 - 60
Cherry	350 - 400
Redcurrant	80 - 420
Red grape	30 - 750
Red wine	24 - 35

Anthocyanidin is the name of the aglycon analogue of anthocyanins. In higher plants, anthocyanidins comprise cyanidin, delphinidin, malvidin, pelargonidin, peonidin and petunidin (for structures see Figure 1.7), which occur exclusively conjugated with sugar moieties as anthocyanins. Their distribution in nature is 50, 12, 12, 12, 7 and 7%, respectively (Zhang *et al.*, 2005). The most common sugar components of anthocyanins are glucose, galactose and arabinose, which are usually conjugated to the anthocyanidin *via* the C-3 hydroxyl group in ring C of the molecule. Some anthocyanins comprise multiple sugar moieties involving hydroxyl functionalities of the molecule other than that at C-3.

1.4.2 Chemical Properties of Anthocyanins

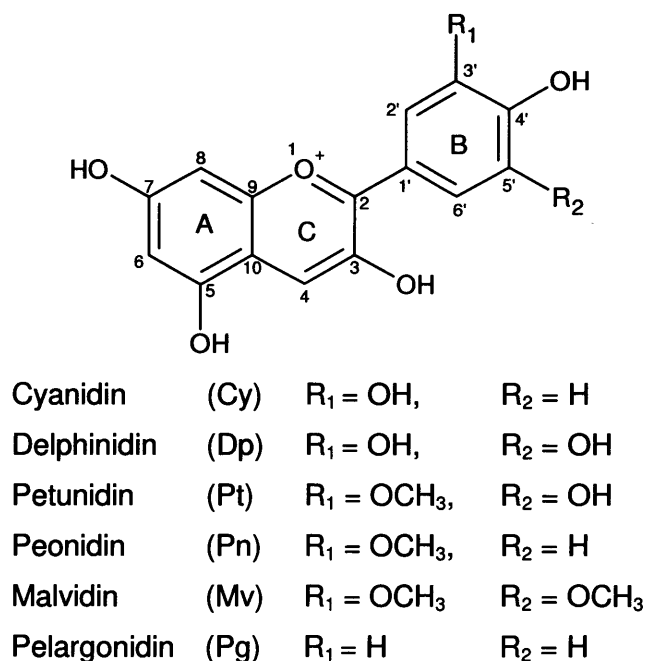


Figure 1.7: Structures of common anthocyanidins, existing as glycosides in nature.

Anthocyanins are water soluble and each anthocyanin displays subtle differences in how they respond to changes in pH (Figure 1.8). At $\text{pH} < 3$ anthocyanins possess a charged middle ring (ring C), forming a highly-coloured

flavilium cation (Figure 1.9). Anthocyanins are usually intensely coloured at pH 1 - 4 and pH > 8 but less coloured at pH 5 - 7 (Lapidot *et al.*, 1999 and Cabrita *et al.*, 2000). The colour changes are the corollary of reversible conformational changes (see Figure 1.9).

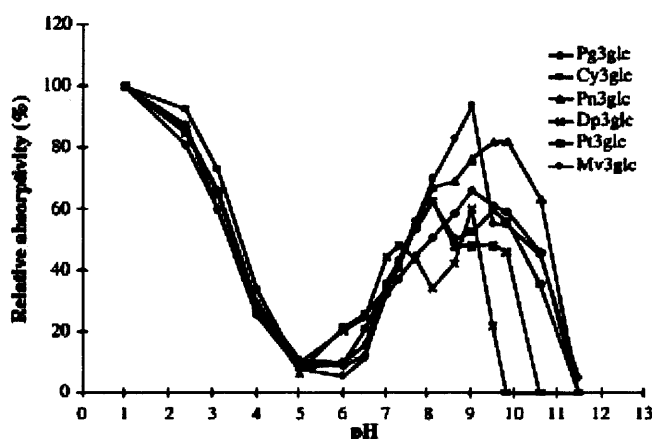


Figure 1.8: Absorptivities relating to pH values for the chloride salts of the six major anthocyanidin-3-glucosides (1.0×10^{-4} M) after 1h of dissolution (taken from Cabrita *et al.*, 2000)

The stability of the flavilium cation as judged by UV/visible absorbance is compromised by increasing pH (Lapidot *et al.*, 1999 and Cabrita *et al.*, 2000). The implications of the different conformational manifestations of anthocyanins, found under different pH conditions, for pharmacological activity are unclear. Cabrita *et al.*, (2000) have shown that all anthocyanins retain >70% stability after 60 days at pH 1-3 (10°C) but lose stability with increasing pH. Cabrita *et al.* also noted that anthocyanins with only 1 free hydroxyl group on the B ring (pelargonidin, peonidin & malvidin) showed the greatest stability at high pH - further enhanced by the presence of additional methoxy groups. Anthocyanins containing three oxygen functional groups on ring B (delphinidin & petunidin) possess *ortho*-hydroxyl groups, and their stability is not as good as that of pelargonidin, petunidin & malvidin at pH 8-9. The stability of cyanidin, which has only 2 oxygen-containing functional groups, but still an *ortho*-hydroxyl

group, seems to behave similarly to the former group of anthocyanins (pelargonidin, peonidin & malvidin) at high pH. Minimal stability of anthocyanins was observed at pH 3.3 – 4.5 (Nielsen *et al.*, 2003a).

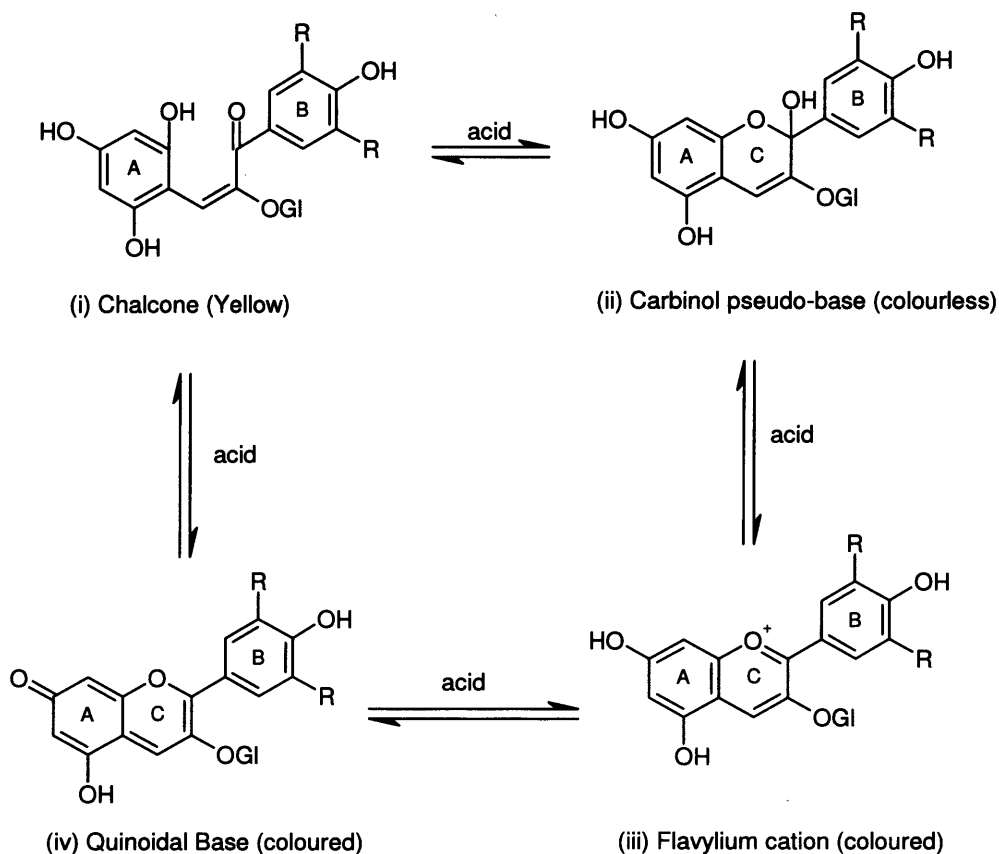


Figure 1.9: pH-Dependent conformational rearrangement of the anthocyanin molecule, shown here for anthocyanins bearing a sugar ("Gl") on C-3. Anthocyanins exist in several freely interchangeable structural forms, which form predominates is dependent upon pH. Around neutral pH anthocyanins occur as chalcones, with the anthocyanin ring C open (i). Under mildly acidic conditions the ring is closed to form a carbinol pseudo base (ii). In strong acid (pH 2) ring C acquires aromaticity involving a charged ring oxygen, forming a coloured flavylium cation (iii). In alkali, oxidation of ring A generates a quinon which is also coloured, eliminating the charge (iv). The ring-opened chalcone can be reformed at neutral pH.

1.4.3 Metabolism of Anthocyanins in Humans

The studies carried out in healthy volunteers usually involve oral dosing with either an extracted (freeze-dried) mixture or through eating/drinking the fruit itself (either as berries, juice or wine). Some anthocyanin sources thus far investigated are: black raspberries, blackberries, elderberries, bilberries, chokeberries, boysenberries and grapes. As would be expected all of these sources contain a mixture of different anthocyanins.

All studies show similar metabolite profiles for anthocyanins, and can be broken down into three major pathways: methylation, glucuronidation and deglycosylation. Further anthocyanin metabolism can yield methylated glucuronides, anthocyanidin glucuronides, methyl anthocyanidins etc. There is also limited evidence for the formation of sulphated metabolites, but these are in the minority (Felgines *et al.*, 2005). Anthocyanins also undergo bacterial degradation in the gut to phenolic acids, but these acids would not be detected at the wavelength used with anthocyanins (Fleschhut *et al.*, and Keppler *et al* 2006).

Kay *et al* (2005) have shown that after a dose of cyanidin-3-glycosides (from chokeberry extract) in humans, 7 major metabolites (from 4 parent compounds) were present. The metabolites were glucuronides (1), methylated (3) or methylated glucuronides (3) of starting materials, and both mono and di methylation was observed. Kay *et al* (2004) showed the extent of metabolism when they repeated the chokeberry study. This study revealed that ~68% of excreted anthocyanins (in serum and urine) were glucuronidated or methylated metabolites with the remaining 32% being parent anthocyanins.

Felgines *et al* (2005) investigated the consumption of blackberries, and discovered 10 unique cyanidin-derived metabolites in urine. Of these metabolites 2 were unknown, 3 were glucuronides, 1 was a methylated metabolite and 3 were methylated glucuronides. The remaining 2 were aglycons, which had undergone deconjugation. Two aglycons were observed despite blackberry containing only cyanidin glycosides. This is due to the methylation of cyanidin. From the structures of cyanidin and peonidin (Figure 1.7) it is clear that methylation of the OH group at position 3' in cyanidin would result in the formation of peonidin. Methylation on the 4' hydroxyl group would result in a methyl cyanidin possessing many of the characteristics of peonidin, and which would be indistinguishable by HPLC or LC/MS/MS, assuming a similar retention time. The presence of these aglycons in urine may be a consequence of the presence of β -glucuronidases in the urine and kidney, as opposed to deconjugation in tissues (Galvano *et al.*, 2004 and Felgines *et al.*, 2005).

There are many earlier literature reports showing only parent compound in urine after anthocyanin consumption (Bub *et al.*, 2001 and Milbury *et al.*, 2002), but most recent publications show a pattern of metabolites similar to that described above involving glucuronidation and/or methylation or deconjugation.

1.4.4 Metabolism of Anthocyanins in Animals

The sites of anthocyanin metabolism in animals can be identified, as individual tissues can be analysed to follow changes in metabolic profile. Another benefit of using animals is that different routes of administration can be investigated.

Table 1.3 shows the major metabolites observed in experimental animals. It is apparent that this metabolism (methylation, glucuronidation or deconjugation) is consistent between animal species – and parallels that observed in humans. Figure 1.10 summarises the fate of an anthocyanin-glycoside after oral dosing to humans and animals.

Ichinani *et al* (2005a) compared the metabolic profiles obtained after oral and I.V administration of cyanidin-3-glucoside. When dosed intravenously, cyanidin-3-glucoside produced only 2 major metabolites – monomethylated analogues of cyanidin-3-glucoside. After oral administration the same monomethylated cyanidin-3-glucosides were present, but alongside these a glucuronide of the cyanidin aglycon and of the methylated cyanidin-3-glucoside were also detected. The presence of cyanidin glucuronide in the plasma suggests that deconjugation only occurs when the parent glucoside is dosed orally. The sites of deconjugation are most likely the gut villi.

Talavéra *et al* (2003) have shown that the stomach plays an essential role in the absorption of anthocyanins. When administered by intragastric injection the glucoside and galactoside of cyanidin were absorbed quickly, quicker than the rutinoside, with total absorption being ~25%. However, the rats used in this study were anaesthetised, and therefore gut motility may have been compromised with loss of peristalsis. This may have the effect of the anthocyanins remaining longer in the stomach creating a bias towards gastric absorption. Detection of parent compound in the gastric tissue has been shown to be as early as 15 min after oral gavage (Tsuda *et al.*, 1999). It has been hypothesised (Passamonti *et al.*, 2002) that the speed of absorption is in part

due to the presence of the anion carrier bilitranslocase, although this transporter can become saturated at higher doses. It was also evident from a study using a bilberry extract (Talavéra *et al.*, 2003) that the rate of absorption followed the extent of hydroxylation of the compound. The bilberry mixture used contained the glucosides, galactosides and arabinosides of 5 anthocyanins delphinidin, cyanidin, petunidin, peonidin and malvidin, which were absorbed in the proportions as expected for increasing hydrophilicity.

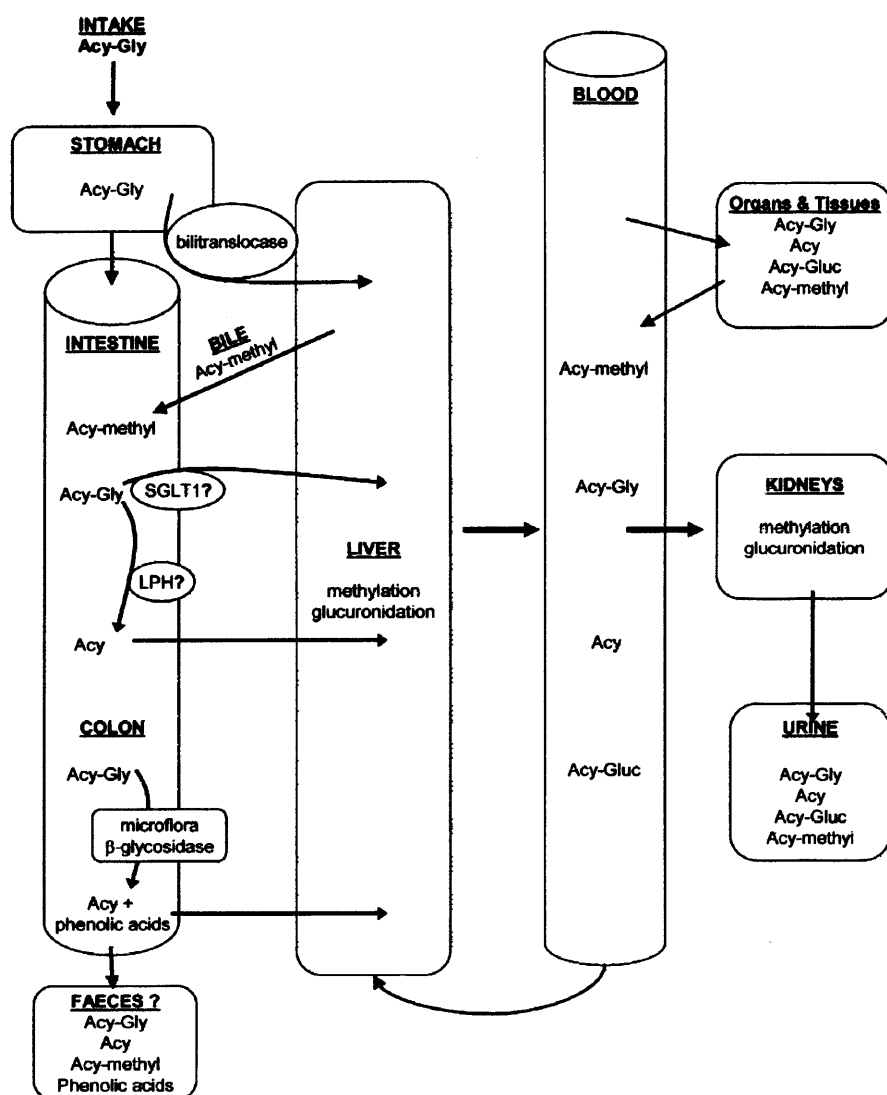


Figure 1.10: Fate of anthocyanidin-3-glycosides in biological systems (humans, rats etc). Abbreviations: Acy-gly = anthocyanin-glycoside; Acy = anthocyanin aglycon; Acy-methyl = methylated metabolite; Acy-Gluc = glucuronidated metabolite; SGLT1 = sodium dependent glucose transporter; LPH = lactase phloridzin hydrolase. Figure adapted from McGhie *et al.*, 2007.

Table 1.3: Metabolites identified in bio-matrices after dosing with anthocyanins.

Dose	Animal Model	Matrix Studied	Metabolites Found (Or Type of Metabolism)	Ref
Marionberry extract (78% C3G)	Pig (In feed)	Urine	C3G-glucuronide methylated C3G methylated C3G glucuronide cyanidin glucuronide methylated cyanidin glucuronide	Wu, 2004
		Plasma	C3G C3G-glucuronide	
Blackberry (4 x cyanidin glycosides)	Rat (In feed)	Stomach	parent compounds	Talavéra, 2005
		Jejunum	methylation glucuronidation methylated glucuronides cyanidin (aglycon)	
		Liver	methylation (high proportion) glucuronidation methylated glucuronides	
		Kidney	glucuronidation	
		Plasma	methylation & glucuronidation	
Cyanidin-3-glucoside	Rat (oral)	Plasma	methylation & glucuronidation	Ichianagi, 2005a

Cyanidin-3-glucoside	Rat (I.V.)	Plasma	methylation	Ichiyonagi, 2005a
Delphinidin-3-glucoside	Rat (in feed)	Plasma	parent & methylated	Ichiyonagi, 2004
Cyanidin-3-glucoside	Rat (oral)	Plasma	parent	} Ichiyonagi, 2005b
			4 x glucuronides	
			6 x methyl glucuronides	
			2 x methylated	
Chokeberry extract	Rat (in feed)	Plasma & urine	parent & methylated	He, 2006
Chokeberry extract	Rat (in feed)	Fecal & caecal	parent & methylated	He, 2005
Red orange anthocyanins	Rat (in feed)	Urine	parent & methylated	Felgines, 2006
Cyanidin-3-glucoside	Rat (oral)	Plasma	parent & methylated	Miyazawa, 1999
Delphinidin-3-rutinoside	Rat (oral & I.V.)	Plasma & Urine	parent & methylated	Matsumoto, 2006
Blackberry extract	Rats, Gastric	Plasma	parent only	Talavéra, 2003
	administration	Bile	parent & methylated	

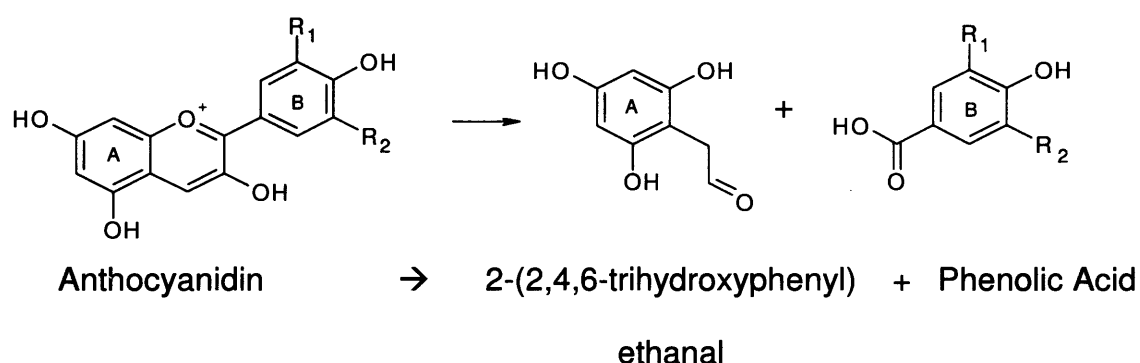
1.4.5 *In vitro* Metabolism

Incubation of anthocyanins and anthocyanidins with rat liver microsomes and nicotinamide adenine dinucleotide phosphate (NADP, NADPH in reduced form) is a model to investigate metabolism catalysed by cytochrome P450 enzymes (Fleschhut *et al.*, 2006). When anthocyanins and anthocyanidins were tested in this system there were no metabolites produced. Incubation of cyanidin with rat liver microsomes and UDPGA resulted in the formation of two mono glucuronides, after the same incubation, but with C3G replacing cyanidin, four glucoside-mono glucuronide metabolites were identified (Fleschhut *et al.*, 2006). The reason for this discrepancy is probably due to the instability of the aglycon or the stability of the glucuronides of the aglycon. In Figure 1.7 there are 5 potential sites of glucuronidation – C3, C5, C7, C6' and C4'. Fleschhut *et al.* (2006) hypothesised that glucuronidation at any site other than 3 or 4' of the aglycon will result in the formation of an unstable glucuronide (Fleschhut *et al.*, 2006). In C3G the C3 position is occupied by the glucoside, so only four sites are available – all of which produce stable glucuronides.

A model utilising gut microflora from the caecum of pigs was used to investigate the stability of glycosides under physiological conditions (Keppler *et al.*, 2005). This study focused on cyanidin, peonidin and malvadin aglycons and their glucosides and rutinosides. All glycosides were hydrolysed to some extent between 20 min and 2 h; glucosides were easily hydrolysed, with most hydrolysis complete after 20 min, whereas hydrolysis of the rutinosides was much slower – taking up to 2 h. Deglycosylation of diglycosides was also much

slower than their equivalent monoglycosides. The aglycons released are inherently unstable and rapid metabolic degradation was observed. The phenolic acid degradation products are shown in Figure 1.11.

Fleschhut *et al* (2006) have also studied metabolism using intestinal microflora. They incubated anthocyanins from red radish anaerobically with a human faecal suspension. Their results showed that both glycosylated and acylated anthocyanins metabolically degrade to the same products as those described by Keppler *et al* (2006). The chemistry for this breakdown is highlighted in Figure 1.11.



Anthocyanidin	Corresponding Phenolic Acid
cyanidin	protocatechuic acid
malvidin	syringic acid
peonidin	vanillic acid
pelargonidin	4-hydroxybenzoic acid
petunidin	3-O methyl gallic acid
delphinidin	gallic acid

Figure 1.11: Degradation of anthocyanidins and formation of the corresponding phenolic acids

1.4.6 Pharmacokinetics of Anthocyanins

Detailed anthocyanin pharmacokinetics (PK) have been reported in both human volunteers and rodents. Absorption into the plasma and excretion into the urine are both rapid. A sample of the data collected in humans thus far is shown in Table 1.4. This table shows the percentage of dose absorbed unchanged to be low, ranging from 0.004 - 0.11%, with a T_{MAX} of between 0.75 – 2.8 h. This range in absorption time may be due to structural differences of anthocyanins. Keppler *et al* (2005) showed how differing sugar moieties affected the rate of degradation, and that the polarity difference between delphinidin and malvidin may also play a role in speed of absorption.

There have also been pharmacokinetic studies in rats (Talavéra *et al.*, 2003 and Ichiyanagi *et al.*, 2004, 2005a, 2005b and 2006) and the results correlate well with the human data, with low levels of absorption and rapid clearance from plasma being observed. Absorption through the stomach and jejunum has also been observed in rats (Ichiyanagi *et al.*, 2004).

Table 1.4: Plasma levels of anthocyanins after oral dosing to humans

Anthocyanin Treatment	Dose (mg)	T_{MAX} (h)	% of Dose Absorbed	Ref
Chokeberry (extract)	721	2.8	N/A	Kay, 2005
Chokeberry (extract)	1300	2	N/A	Kay, 2004
Black raspberry (freeze dried)	45 000 x 7 days	1–2	<1%	Stoner, 2005
Blackcurrant Juice	1200	0.75	0.05 – 0.07%	Nielsen, 2003b
Blackcurrants	3.6	1.25 – 1.75	0.06 – 0.11%	Matsumoto, 2001
Elderberry extract	720	-	0.077% (6h)	Wu, 2002
Blueberry	690	-	0.004% (6h)	Wu, 2002
Red wine	68	0.83	0.016% (3h)	Bub, 2001
Red grape juice	117	2	0.019% (6h)	Bub, 2001

1.4.7 Health Effects of Anthocyanins

In a cohort of elderly individuals who consumed large amounts of strawberries the odds ratio for developing cancer at any site was 0.3, compared to subjects who refrained from high berry consumption (Colditz *et al.*, 1985). Consumption of coloured fruits and vegetables have also been associated with a reduced risk of human breast cancer (Adlercreutz, 1998) and colorectal polyp recurrence (Almendingen *et al.*, 2004). Anthocyanin-containing foodstuffs have been associated with a decreased risk of coronary heart disease and with vasoprotection, and have been shown to have beneficial effects in many parts of the organism, including the central nervous system and the eye (Detre *et al.*, 1986). They are suspected to account, at least in part, for the “French paradox” i.e., the decreased risk of cardiac disease, despite a high-fat diet in individuals living in France.

1.4.8 Cancer Chemopreventive Properties of Anthocyanins in Animals

There are to my knowledge nine reports in which the ability of anthocyanins to interfere with carcinogenesis in animals have been described (Koide *et al.*, 1996, Harris *et al.*, 2001, Hagiwara *et al.*, 2001, Hagiwara *et al.*, 2002, Kang *et al.*, 2003, Singletary *et al.*, 2003, Bobe *et al.*, 2006, Afaq *et al.*, 2005 and Lala *et al.*, 2006).

In a comparative investigation in the Apc^{MIN} mouse (Kang *et al.*, 2003), animals received either a mixture of anthocyanins at 800 mg/L or pure cyanidin at 200 mg/L with the drinking water or tart cherries added to the diet (200 g/kg diet).

These amounts correspond to doses of approximately 2.4 mg and 0.6 mg anthocyanins/animal/day and 600 mg of tart cherries/animal/day, respectively. In mice which received anthocyanins or tart cherries, the number of caecal adenomas was reduced compared with animals on control diet or those which received the non-steroidal anti-inflammatory drug sulindac (Kang *et al.*, 2003). The number of colonic and intestinal adenomas was not significantly influenced by anthocyanins.

In a similar study (Bobe *et al.*, 2006) Apc^{MIN} mice were fed anthocyanin-rich tart cherry extracts at a range of amounts (375, 750, 1500 or 3000 mg tart cherry extract/kg of diet). These amounts correspond to doses of 1.125, 2.25, 4.5 and 9 mg anthocyanins/mouse/day, and each dose diet contained 100 mg/kg of sulindac (0.3 mg/mouse/day), which has previously been shown to be effective at preventing adenoma formation (Waddell *et al.*, 1983). There were no treatment groups with anthocyanins exclusively, and only the effect of anthocyanins with sulindac on adenoma formation was determined. The numbers of adenomas observed was not significantly affected by anthocyanin content, and the largest difference to control of 26% was achieved by the highest and lowest doses alike.

In a xenograft model in which Balb/C mice were inoculated intraperitoneally with syngeneic Meth/A lymphoma cells, animals receiving a diet of anthocyanin-containing red glutinous rice showed evidence of prolonged life expectancy compared to those animals fed normal rice or control diet (Koide *et al.*, 1996).

Commercially available anthocyanin-rich extracts of chokeberry, bilberry or grape were compared in terms of their effects on azoxymethane-induced colonic aberrant crypt foci in rats (Lala *et al.*, 2006). In animals that received these extracts (4 g/kg diet, 30-40 mg anthocyanins/animal/day) for one week before the carcinogen, the numbers of aberrant crypt foci were significantly reduced compared to control rats after 14 weeks of study. The reductions in aberrant crypt foci numbers and multiplicities were accompanied by inhibition of cyclooxygenase-2 gene expression (Lala *et al.*, 2006).

Female rats, previously exposed to 7,12-dimethylbenzanthracene to induce the formation of mammary tumours, were administered Concord grape juice that contained 15 different anthocyanins (making up 12% of the total phenolics), at three concentrations in the drinking water, representing approximately 10, 15 and 20 mg anthocyanins/rat/day) (Singletary *et al.*, 2003). Consumption of the grape juice reduced mammary tumour incidence, multiplicity and final mean tumour mass significantly (Singletary *et al.*, 2003). This study was designed with suitable control animals so as to eliminate any potential preventive effect of sugars and organic acids contained in the grape juice, so that efficacy was likely to be mediated only by the anthocyanins contained in the juice.

Purple sweet potato, red cabbage and purple corn are rich in anthocyanins and have also been shown to inhibit chemical carcinogenesis in rats (Hagiwara *et al.*, 2001 and 2002). Colonic adenomas and adenocarcinomas were induced by treatment with 1,2-dimethyl hydrazine and their incidence increased by supplementing the diet with the food-derived heterocyclic amine PhIP (2-amino-1-methyl-6-phenylimidazo[4,5-*b*]pyridine) a known carcinogen. Purple sweet

potato, purple corn and red cabbage extracts were fed to rats at approximately 490mg, 233mg and 620 mg anthocyanins/rat/day in the diet concurrently with PhIP (0.02%). Treatment with these anthocyanin-containing vegetables was responsible for a significantly decreased incidence and multiplicity of adenomas and adenocarcinomas in the dimethyl hydrazine/PhIP group, compared to rats receiving no intervention (Hagiwara *et al.*, 2001 and 2002). Furthermore, purple corn and red cabbage extracts also inhibited PhIP-induced aberrant crypt formation in the non-dimethyl hydrazine-initiated groups (Hagiwara *et al.*, 2001 and 2002).

Significant decreases in azoxymethane-induced aberrant crypt foci (21-36%) and adenocarcinoma (28 - 80%) multiplicities were observed in rats fed lyophilized black raspberries (approximately 0.38g, 0.75g and 1.5g/animal/day). The marked protective effect was paralleled by significant reduction in urinary levels of 8-hydroxy-2'-deoxyguanosine, a marker of oxidative DNA damage (Harris *et al.*, 2001).

Female CD-1 mice that were subjected to topical application of anthocyanins-containing pomegranate extract demonstrated a delay in onset and decreased incidence and burden of TPA-promoted (12-*O*-tetradecanoyl-phorbol-13-acetate), DMBA-initiated (7,12-dimethylbenz(a)anthracene) skin tumours (Afaq *et al.*, 2005). Topical application of the pomegranate extract inhibited TPA-induced phosphorylation of ERK1/2, p38 and JNK1/2, activation of NFκB and IKK, and degradation of IκB (Afaq *et al.*, 2005).

1.4.9 Anticarcinogenic Mechanisms of Anthocyanins from In Vitro Studies in Cultured Cells

Studies, in which the effects of anthocyanins on cell growth or on cellular events germane to tumour promotion or progression have been investigated, are summarised in Tables 1.5 and 1.6. In terms of inhibition of cancer cell survival, anthocyanidins have demonstrated more potent growth-inhibition than their glycosylated counterparts. Anthocyanidins confounded survival in the 10^{-5} - 10^{-4} M concentration range, whilst the glycosides were hardly growth-inhibitory at concentrations below 10^{-4} M. Anthocyanidins have demonstrated growth inhibitory effects upon cancer cells derived from numerous human tissues (see Table 1.5) including; lung, breast, uterine and vulva carcinomas, colon adenoma and in embryonic fibroblasts (Meiers *et al.*, 2001, Hou *et al.*, 2003, Katsube *et al.*, 2003, Hyun *et al.*, 2004, Lazze *et al.*, 2004 and Zhang *et al.*, 2005). Among the anthocyanidins, delphinidin frequently displayed the most potent growth-inhibitory activity. This finding hints at a structural determinant of pharmacological activity, suggesting a dependence of growth-inhibitory potency on the presence of hydroxyl groups on ring B of the anthocyanidin. A notable exception to this rule is that malvidin demonstrated equivalent or greater potency to delphinidin in some cell lines implying more than one structural determinant is implicit in ascribing efficacy to anthocyanidins (Hou *et al.*, 2003, Katusbe *et al.*, 2003, Galvano *et al.*, 2004 and Hyun *et al.*, 2004). Interestingly, anthocyanin-containing extracts of grapes, bilberries or chokeberries at 50 or 75 $\mu\text{g/ml}$ inhibited the growth of human malignant HT29 colon cancer cells, but not that of non-malignant colon-derived NCM460 cells (Zhao *et al.*, 2004).

Anthocyanins have been shown to interfere with biochemical activities relevant to promotion or progression of malignancies, such as those mediated by COX enzymes, tyrosine kinases and phosphodiesterases. All three systems play key roles in tumorigenesis (Cross *et al.*, 1991, Mestre *et al.*, 1999 and Marko *et al.*, 2004). Several anthocyanins have demonstrated COX-inhibiting activities (Wang *et al.*, 1999, Seeram *et al.*, 2001a and 2003). For example, anthocyanidins (40 μ M) inhibited activities of COX-1 and COX-2 enzyme preparations from ram seminal vesicles and insect cell lysate (Seeram *et al.*, 2003). Cyanidin is the most potent inhibitor of COX-1 and COX-2 demonstrating inhibitory activities of 52.2% and 74.2%, respectively (Seeram *et al.*, 2003). Despite the limited inhibitory activity of purified anthocyanins, several extracts from berries demonstrated comparable COX-2 inhibitory activities to cyanidin and the positive controls ibuprofen and naproxen (Seeram *et al.*, 2001a). Lipopolysaccharide-induced expression of COX-2 mRNA and protein in mouse macrophage RAW264 cells has been suggested, by some authors, to be inhibited by delphinidin or bilberry extract, but details have not been provided (Hou *et al.*, 2004a). Delphinidin-mediated COX-2 down-regulation may have been, at least in part, the consequence of its ability to suppress lipopolysaccharide- and TPA-induced I κ B degradation and IKK and NF κ B activation (Afaq *et al.*, 2004 and Hou *et al.*, 2004a).

Cyanidin, delphinidin and malvidin have been shown to possess IC₅₀ values of 42, 18 and 61 μ M, respectively for the inhibition of tyrosine kinase activity in the epidermal growth factor receptor (EGFR) isolated from EGFR over-expressing A431 cells (Meiers *et al.*, 2001). The same study showed similar, but less potent inhibition of LXFL529L cells with IC₅₀ values of 73 and 33 μ M for cyanidin and

delphinidin, respectively. Malvidin was inactive against LXFL529L cells. In a more recent investigation of EGFR from A431 cells the ability of anthocyanidin molecules to inhibit EGFR tyrosine kinase decreased in the order delphinidin = cyanidin > pelargonidin > peonidin > malvidin (Marko *et al.*, 2004), suggesting that potency seemed to be positively correlated with the presence of hydroxyl functions in positions 3' and 5' of ring B of the anthocyanidin molecule, and inversely with the presence of methoxyl groups. Similarly, greater inhibition of TPA-induced activator protein 1 (AP1), a transcription factor with an integral role in carcinogenesis (Hsu *et al.*, 2000), activity, and ERK and JNK phosphorylation, was observed with the anthocyanidins hydroxylated at positions 3' and 5' of ring B (Hou *et al.*, al 2004b). In contrast, inhibition by anthocyanidins of phosphodiesterase activity in cytosol from HT29 cells displayed the inverse molecular structure-activity relationship, as borne out by a decreasing rank order of potency of malvidin > peonidin > pelargonidin = cyanidin > delphinidin (Marko *et al.*, 2004). This phenomenon suggests that phosphodiesterase-4-inhibitory potency was positively correlated with number of methoxy moieties and inversely with number of hydroxyl groups in positions 3' and 5' in ring B. The complex interaction with these two crucial growth regulatory signalling events resulted in the following rank order of growth-inhibitory properties in HT-29 cells: delphinidin \approx malvidin > cyanidin > peonidin > pelargonidin, with approximate IC₅₀ values of 20, 25, 60, 90 and 225 μ M, respectively (Marko *et al.*, 2004). Despite malvidin being a weak EGFR tyrosine kinase inhibitor it dose-dependently decreased phosphorylation of Elk 1, a signalling component downstream of EGFR, in A431 cells (Meiers *et al.*, 2001). It has been proposed that the latter mechanism occurs through cross-talk between the cAMP pathway and EGFR signalling whereby inhibition of

phosphodiesterase 4 by malvidin is responsible for an increase in protein kinase A activity that in turn deactivates the serine/threonine kinase Raf-1 so blocking signal transduction from EGFR to Elk-1 (Marko *et al.*, 2004).

In terms of their effect on cell cycle, anthocyanidins interrupt the cell cycle machinery at the G₁ or G₂/M phases, and such inhibition might elicit, or contribute to, initiation of apoptosis and limitation of proliferation (see Table 1.6) (Singletary *et al.*, 2003, Hou *et al.*, 2003, Hyun *et al.*, 2004, Fimognari *et al.*, 2004a and 2004b). Once again, increasing number of hydroxyl groups attached to the B-ring of the anthocyanidin molecule correlates with increased apoptotic activity (Hou *et al.*, 2003).

Lastly, several berry extracts demonstrate potent antioxidant activities that correlate with anthocyanin content (Nielsen *et al.*, 2003a, Zheng *et al.*, 2003, Olsson *et al.*, 2004 and Heo *et al.*, 2005). Anthocyanins are powerful antioxidants and may exert anti-carcinogenicity via this property (Rice-Evans *et al.*, 1996, Mazza *et al.*, 2002, Nielsen *et al.*, 2003a, and Galvano *et al.*, 2004). Using the ferric reducing ability of plasma (FRAP) technique, delphinidin-3-glucoside, petunidin-3-glucoside and malvidin-3-glucoside have been shown to be 2 – 2.5 times more potent antioxidants than ascorbic acid (Garcia-Alonso *et al.*, 2004). Similarly, anthocyanins have 3-6 fold greater activities than the reference antioxidant trolox when investigated using the trolox equivalent antioxidant capacity (TEAC) and oxygen radical absorbing capacity (ORAC) techniques. The pattern emerging from these and other studies (Seeram *et al.*, 2002, Noda *et al.*, 2002 and Galvano *et al.*, 2004) is that antioxidant activity appears to increase with increasing degree of hydroxylation of the B-ring of

anthocyanins. The antioxidant capacities of cyanidin and cyanidin-3-glucoside were found to be similar to that of α -tocopherol in systems in which oxidation was studied in linoleic acid, liposomes, rabbit erythrocyte membranes and rat liver microsomes (Tsuda *et al.*, 1994). Similar antioxidant capacity has been demonstrated in vitamin E-depleted rats fed anthocyanin-rich extract in the diet. Plasma antioxidant capacity increased and hepatic 8-Oxo-dG (see section 1.1.5) concentrations declined (Ramirez-Tortosa *et al.*, 2001).

Table 1.5: Summary of growth inhibitory effects of anthocyanins and anthocyanin-rich extracts

Treatment	Cell Line	Effect	Reference
Anthocyanidins			
Delphinidin	CaCo-2	Growth inhibition (20%), 200 μ M	Lazze, 2004
	HeLa S3	IC ₅₀ 200 μ M	“
	H.E.F	Growth inhibition (10%), 200 μ M	“
	LXFL529L	IC ₅₀ 33 μ M	Meiers, 2001
	A431	IC ₅₀ 18 μ M	“
	HT29	IC ₅₀ 35 μ M	Marko, 2004
	MCF-7	Growth inhibition (66%), 200 μ g/ml	Zhang, 2005
	HL60	Growth inhibition (88%), 100 μ M	Katsube, 2003
		↑Apoptosis, 200 μ M	“
	HCT116	Growth inhibition (64%), 100 μ M	“
Cyanidin	CaCo-2	No effect	Lazze, 2004
	HeLa S3	No effect	“
	H.E.F	No effect	“
	U937	IC ₅₀ 60 μ g/ml	Hyun, 2004
	HT29	IC ₅₀ : 63 μ M	Kang, 2003
		IC ₅₀ 57 μ M	Marko, 2004
	HCT-116	IC ₅₀ : 85 μ M	Kang, 2003
		Growth inhibition (82%), 200 μ M	Katsube, 2003
	LXFL529L	IC ₅₀ 73 μ M	Meiers, 2001
	A431	IC ₅₀ 42 μ M	“
	MCF-7	Growth inhibition (47%), 200 μ g/ml	Zhang, 2005

	HL60	Growth inhibition (85%), 200µM	Katsube, 2003
		↑Apoptosis, 200µM	“
Malvidin	U937	IC ₅₀ 40 µg/ml	Hyun, 2004
	LXFL529L	IC ₅₀ >100 µM	Meiers, 2001
	A431	IC ₅₀ 61 µM	“
	HT29	IC ₅₀ 35 µM	Marko, 2004
	HCT-116	Growth inhibition (76%)	Zhang, 2005
	SF-268	Growth inhibition (41%)	“
	AGS	Growth inhibition (69%)	“
	NCI H460	Growth inhibition (68%)	“
	MCF-7	Growth inhibition (75%)	“
	HL60	Growth inhibition (97%), 200 µM	Katsube, 2003
		↑Apoptosis, 200 µM	“
	HCT116	Growth inhibition (22%), 200 µM	“
Peonidin	HT29	IC ₅₀ 90 µM	Marko, 2004
	HL60	Growth inhibition (80%), 400 µM	Katsube, 2003
Pelargonidin	HT29	IC ₅₀ >100 µM	Marko, 2004
	HCT-116	Growth inhibition (63%)	Zhang, 2005
	SF-268	Growth inhibition (34%)	“
	AGS	Growth inhibition (64%)	“
	NCI H460	Growth inhibition (62%)	“
	MCF-7	Growth inhibition (63%)	“

Petunidin	MCF-7	Growth inhibition (53%), 200 µg/ml	“
Anthocyanins			
Del-3-Gal	HL60	Growth inhibition (~80%) 200 µg/ml	Katsube, 2003
	HCT116	Growth inhibition (~85%) 400 µg/ml	“
Del-3-Glu	HT29	Growth inhibition (87%) 200 µg/ml	Olsson, 2004
	MCF-7	Growth inhibition (82%) 200 µg/ml	“
	HL60	Growth inhibition (~75%) 100 µg/ml	Katsube, 2003
	HCT116	Growth inhibition (~80%) 200 µg/ml	“
Cy-3-Gal	LXFL529L	IC ₅₀ >100 µM	Meiers, 2001
	A431	IC ₅₀ >100 µM	“
Cy-3-Glu	U937	No effect	Hyun, 2004
	HT29	Growth inhibition (88%) 200 µg/ml	Olsson, 2004
	MCF-7	Growth inhibition (85%) 200 µg/ml	“
	Jurkat	IC ₅₀ 175 µg/ml	Fimognari, 2004a
	HL60	Growth inhibition (37%) 200 µg/ml	“
Mal-3-Glu	LXFL529L	IC ₅₀ >100 µM	Meiers, 2001
	A431	IC ₅₀ >100 µM	“
	U937	No effect	Hyun, 2004
	HT29	Growth inhibition (90%) 200 µg/ml	Olsson, 2004
	MCF-7	Growth inhibition (84%) 200 µg/ml	“

Anthocyanin-rich extracts

Chokeberry extract	NCM 460	25 µg/ml*	Zhao, 2004
	HT29	IC ₅₀ 10 µg/ml *	“
		Growth inhibition (37%), 5 mg/ml	Olsson, 2004
	HT29	Growth inhibition (69%)	Lala, 2006
	MCF-7	Growth inhibition (19%), 5 mg/ml	Olsson, 2004
Grape extract	HT29	IC ₅₀ 25 µg/ml*	Zhao, 2004
	NCM 460	IC ₅₀ 75 µg/ml*	“
	RBA	IC ₅₀ ~14 µg/ml	Singleton, 2003
Cherry extracts	HT29	IC ₅₀ : 780 µM	Kang, 2003
		No effect	Olsson, 2004
	HCT116	IC ₅₀ : 285 µM	Kang, 2003
	MCF-7	No effect	Olsson, 2004
Bilberry extract	NCM 460	IC ₅₀ 25 µg/ml	Zhao, 2004
	HT29	IC ₅₀ 25 µg/ml *	“
		Growth inhibition (69%)	Lala, 2006
		No effect	Olsson, 2003
	MCF-7	Growth inhibition (25%), 5 mg/ml	“
	HL60	Growth inhibition (84%), 4 mg/ml	Katsube, 2003
	HCT116	Growth inhibition (97%), 4 mg/ml	“
Black currant	HT29	No effect	Olsson, 2004
	MCF-7	Growth inhibition (45%) 5 mg/ml	“
Cranberry	CAL27	Growth inhibition (~20%)	Seeram, 2004

Anthocyanins	KB	Growth inhibition (~20%)	“
	HCT116	Growth inhibition (~15%)	“
	SW620	Growth inhibition (~15%)	Seeram, 2004
	RWPE-1	Growth inhibition (~55%)	“
	RWPE-2	Growth inhibition (~60%)	“
	22Rv1	Growth inhibition (~70%)	“

Cy, del and mal refer to cyanidin, delphinidin and malvidin, respectively. Glu and gal refer to glucoside and galactoside, respectively. H.E.F stands for human embryonic fibroblasts. HT29, HCT-116, SW620 and CaCo-2 are colon carcinoma cells. NCM460 are normal colon cells. LXFL529L and NCI H460 are lung cells originating from athymic mice. A431 cells are from vulva carcinoma. HeLa S3 is a uterine carcinoma cell line U937 Monocytic leukaemia cells. RBA are rat mammary gland adenocarcinoma cells and MCF-7 is a human breast cancer cell line. KB and CAL27 are oral cancer cells from mouth epidermis and tongue epithelium, respectively. RWPE-1 (normal), RWPE-2 (*k-ras* transfected) and 22Rv1 are prostate cancer cells lines. SF-268 and AGS are a glioblastoma cell line derived from nude mice and a stomach carcinoma cell line, respectively. HL60 are human promyelocytic leukaemia cells. *IC₅₀ estimated from published data after 72 h exposure to extracts. Growth inhibition is given as the percentage decrease in cell number compared to cells receiving no treatment.

Table 1.6: Summary of evidence of underlying mechanisms responsible for the chemopreventive efficacy of anthocyanins

Treatment	Cell Line	Effect	Reference
Anthocyanidins			
Delphinidin	JB6	↓ TPA-induced AP-1 activation	Hou, 2004b
		↓ JNK/ERK phosphorylation	"
	A431	↓ EGFR tyrosine kinase	Meiers, 2001
		↓ <i>Elk-1</i> activation	"
	HT29	↓ EGFR tyrosine kinase activity	Marko, 2004
		↑ PDE4 inhibition	"
	CaCo-2	G ₂ /M phase arrest	Lazze, 2004
		↑ Apoptosis	"
			"
	HeLa S3	G ₂ /M phase arrest	"
		↑ Apoptosis	"
			"
	H.E.F	↑ Apoptosis	"
		S-Phase arrest	"
	HL60	↑ Apoptosis	Hou, 2003
		Caspase 3 activation	"
		↑ JNK phosphorylation	"
	RAW264	↓ LPS-induced IκB degradation	Hou, 2004a

Cyanidin	RAW264	↓ LPS-induced NFκB activation	Hou, 2004a
		↓ LPS induced COX2 expression	"
	R.S.V	↓ Cox-1 activity	Seeram, 2003
	I.C.L	↓ Cox-2 activity	"
	JB6	↓ TPA-induced AP-1 activation	Hou, 2004b
	HL60	↑ Apoptosis	Hou, 2003
	CaCo-2	No effect	Lazze, 2004
	HeLa S3	No effect	"
	N.H.F	G1 phase arrest	"
	A431	↓ EGFR tyrosine kinase	Meiers, 2001
		↓ Elk-1 activation	"
	HT29	↓ EGFR tyrosine kinase activity	Marko, 2004
		↑ PDE4 inhibition	"
	U937	Arrest of G ₂ /M Phase	Hyun, 2004
		↑ Apoptosis	"
	R.S.V	↓ COX-1 activity	Seeram, 2001a
	R.S.V	↓ COX-2 activity	Seeram, 2003
	I.C.L	↓ COX-1 activity	Seeram, 2001a
	I.C.L	↓ COX-2 activity	Seeram, 2003
	R.L.M	Antioxidant	Tsuda, 1994
	Liposomes	Antioxidant	"
	R.E.M	Antioxidant	"
Malvidin	U937	Arrest of G ₂ /M Phase	Hyun, 2004
		↑ Apoptosis	"

Malvidin	A431	↓ <i>Elk-1</i> activation	Meiers, 2001
	JB6	Weak effect on AP-1	Hou, 2004b
	HT29	↓ EGFR tyrosine kinase activity ↑ PDE4 inhibition	Marko, 2004 “
	R.S.V	↓ Cox-1 activity	Seeram, 2003
	I.C.L	↓ Cox-2 activity	“
Petunidin	JB6	↓ TPA-induced AP-1 activation	Hou, 2004b
	HL60	↑ Apoptosis	Hou, 2003
Peonidin	JB6	No effect on AP-1	Hou, 2004b
	HT29	↓ EGFR tyrosine kinase activity ↑ PDE4 inhibition	Marko, 2004 “
	R.S.V	↓ Cox-1 activity	Seeram, 2003
	I.C.L	↓ Cox-2 activity	“
Pelargonidin	JB6	Weak effect on AP-1	Hou, 2004b
	HT29	↓ EGFR tyrosine kinase activity ↑ PDE4 inhibition	Marko, 2004 “
	R.S.V	↓ Cox-1 activity	Seeram, 2003
	I.C.L	↓ Cox-2 activity	“

Anthocyanins

Cy-3-Glu	Lymphocytes	↑ Apoptosis	Fimognari, 2004a
	Jurkat cells	↑ Apoptosis	"
		↑ p53	"
		↑ bax levels	"
	HL-60	↑ Apoptosis	"
		↓ c-myc	"
		↓ bcl-2	"
	R.L.M	Antioxidant	Tsuda, 1994
	Liposomes	Antioxidant	"
	R.E.M	Antioxidant	"
Cy-3-Gal	A431	↑ eNOS activity	Bub, 2001
		↑ Akt phosphorylation	"
Mal-3-Glu	A431	No effect	Meiers, 2001
			"

Anthocyan-rich extracts

Cherry extract	R.S.V	↓ Cox-1 activity	Seeram, 2001a
	I.C.L	↓ Cox-2 activity	"

Raspberry	R.S.V	↓ Cox-1 activity	“
extract	I.C.L	↓ Cox-2 activity	“
Grape colour	RBA	↓ DNA synthesis	Singletary, 2003
extract		G ₁ phase arrest	“
Bilberry extract	RAW264	↓LPS induced COX-2 expression	Hou. 2004a
	HL60	↑ Apoptosis	Katsube, 2003
	HCT116	↑ Apoptosis	“
	Plasma	Antioxidant	Mazza, 2002
Blackcurrant	Plasma	Antioxidant	Nielsen, 2003
juice			

Cy-3-Glu, Cy-3-Gal and Mal-3-Gal are cyanidin-3-glucoside, cyanidin-3-galactoside and malvidin-3-galactoside, respectively. H.E.F stands for human embryonic fibroblasts, R.S.V is rat seminal vesicle, I.C.L is insect cell lysate, N.H.F is normal human fibroblasts, R.L.M is rat liver microsomes, R.E.C is rabbit erythrocyte membranes and B.A.E.C is bovine artery endothelial cells. JB6 (mouse skin epidermal cell line), U937 are human monocytic leukaemia cells. A431 is a vulva carcinoma cell line. Jurkat cells are a T-lymphoblastoid cell line. HL-60 is a leukaemia cell line. RBA cells are from rat mammary gland adenocarcinoma. HT-29 and CaCo-2 are colon adenocarcinoma cell lines and HeLa S3 cells are from uterine carcinoma. Raw264 are mouse macrophage cells. HL60 are human promyelocytic leukaemia cells.

1.5 Aims

There is increasing evidence to suggest that anthocyanins from fruit and vegetables have a beneficial role as cancer chemopreventive agents (see sections 1.4.8 -1.4.9, Cooke *et al.*,2005). The overall aim of this project is to gather information which may help adjudge whether anthocyanins possess the potential to be considered as cancer chemopreventive agents in humans, and whether they should be advanced to the stage of clinical development.

There is evidence of cancer chemopreventive effects by anthocyanins in carcinogen-induced rodent models of colorectal cancer (see section 1.4.8). Attempts to corroborate chemopreventive activity in genetic models have been limited thus far (Kang *et al.*, 2003), and this study showed no significant effect on G.I. tract adenoma formation. Specifically the following hypotheses were tested:

- The anthocyanin C3G and the anthocyanin mixture Mirtoselect decrease gastrointestinal carcinogenesis in the Apc^{MIN} mouse.
- The adenoma-preventing efficacy of the anthocyanins is dose-dependent.
- The adenoma-preventing effect of anthocyanins is reflected by their effect on murine packed cell volume.

The metabolism and pharmacokinetics of anthocyanins either as single compounds or constituents of fruit extracts is relatively poorly understood (see sections 1.4.3 – 1.4.6), and a direct relationship between chemopreventive efficacy and systemic concentration has not been established. To better

understand anthocyanin pharmacokinetics the following hypotheses were tested:

- Anthocyanins and their metabolites can be measured in blood, urine and tissues of mice which received C3G or Mirtoselect with their diet at levels consistent with physiological activity.
- Anthocyanins are systemically bioavailable when administered to mice orally. Calculation of bioavailability involves comparison of plasma anthocyanin concentrations after oral and I.V. dosing.
- Anthocyanidins are generated from anthocyanins in the intestinal mucosa in mice.
- Administration of anthocyanins gives rise to levels of anthocyanins and anthocyanidins sufficient to exert a pharmacological effect in tissues.

To enable the above hypothesis to be tested a rapid, selective and reproducible HPLC- Visible (520 nm, in the visible region of the spectrum) method for the separation and quantitation of Mirtoselect, C3G and its metabolites from biomatrices has been developed.

Another aim of the work was to improve understanding of the mechanism of chemopreventive activity of anthocyanins. It has been suggested that anthocyanins are powerful anti-oxidants. Most experiments have been *ex vivo* and have used calculated anti-oxidant capacity (section 1.4.9) to reflect anti-oxidant potential. Therefore levels of oxidative damage were investigated in adenoma tissue from Apc^{MIN} mice by investigating malondialdehyde-deoxyguanosine (M1dG) adducts (see section 1.1.5). The hypothesis tested

was that anthocyanins decrease M1dG, and therefore oxidative damage, in adenoma tissue of mice.

2. Materials and Methods

2.1 Materials

2.1.1 Sources of Anthocyanins and Method of Purification of Anthocyanins from Berries

Cyanidin-3-glucoside (C3G) was kindly supplied by Prof. Peter Winterhalter (Technical University of Braunschweig, Germany) who purified cyanidin-3-glucoside from fresh blackberries using a counter current chromatographic method (Schwarz *et al.*, 2003). Mirtoselect, an extract of bilberry, standardized for anthocyanin content, which is used in health supplements, was obtained from Indena SpA (Milan, Italy, see <http://www.indena.it/pdf/mirtoselect.pdf>).

Mirtoselect is a standardised, highly water soluble, bilberry extract from *Vaccinium myrtillus* L. It comprises ~39% anthocyanins consisting of 15 different components, i.e. the glucose, galactose and arabinose conjugates of delphinidin, cyanidin, petunidin, peonidin and malvidin, with the residual content being plant-derived polysaccharides. Identities of anthocyanin components in Mirtoselect (as provided by the manufacturer) were confirmed by LC/MS/MS analysis (see 2.2.3 for method) using specific multiple reaction monitoring (MRM) transitions.

2.1.2 Chemicals Used

All chemicals, unless otherwise stated were purchased from Sigma Aldrich, (Poole, UK). Solvents used were obtained from Fisher Scientific,

(Loughborough, UK). All other chemicals used are listed in the body of the text. Extraction and analysis media were purchased from Waters Ltd, (Elstree, UK). Water used was purified in the laboratory by a Nanopure Diamond (Barnstead, Iowa, USA).

2.1.3 Polymerase Chain Reaction (PCR) Materials Used

Cell lysis solution	tris aminomethane, EDTA, sodium dodecyl sulphate (Gentra Systems, MN, USA)
Protein precipitation solution	water, ammonium acetate (Gentra Systems)
DNA hydration solution	10 mM Tris, 1 mM EDTA, pH 7.0 – 8.0 (Gentra Systems)
10X TBE buffer	1.0M Tris, 0.9M boric acid, 0.01M ethylenediaminetetraacetic acid (EDTA) (Invitrogen, Paisley, UK)
dNTP's	2.5 mM of dATP, dCTP, dGTP, and dTTP (Invitrogen, Paisley, UK)
Primer MAPC9	} The Protein Nucleic Acid Chemistry Laboratory, University of Leicester.
Primer MAPC15	
Primer APC JR2020	
Taq polymerase	5 Units/ μ l enzyme (Invitrogen, Paisley, UK)
Agarose, electrophoresis grade	(Invitrogen, Paisley, UK)
Ethidium bromide solution	10 mg/ml (Invitrogen, Paisley, UK)
Ready Load 100bp DNA ladder	(Invitrogen, Paisley, UK)

Bluejuice gel loading buffer 65% (w/v) sucrose, 10 mM Tris-HCl (pH 7.5),
10 mM EDTA, and 0.3% (w/v) bromophenol
blue.

2.2 Analytical Methods

2.2.1 HPLC Method for the Separation of 15 Anthocyanins Present in Mirtoselect

Aqueous Mirtoselect solutions and human biomatrices were analyzed for anthocyanin content by HPLC with UV-visible detection (520 nm). The HPLC system (Varian Analytical Instruments, Oxford, United Kingdom) comprised a Varian 230 pump, Varian 410 autosampler, and Varian 325 UV-vis detector. Separation of anthocyanins was performed using an Xterra Phenyl column (Waters; 4.6 mm x 150 mm, 5 μ m) with matching guard column (Waters, 4.6 mm x 10 mm, 5 μ m) at 40 °C with a flow rate of 1.5 ml/min. The gradient elution system comprised two solvents: A, 9:1 water:formic acid, pH = 1.6; and B, acetonitrile. The gradient employed was as follows: 99 to 97% A over 5 min, 97 to 90% A over 3 min, unchanged for 4 min, decrease of A to 70% within 1 min, and then maintained for 2 min. When using human biomatrices column integrity was maintained by injecting water every 5 runs and allowing the method to complete. Dimethyl sulphoxide (DMSO) was injected at the end of everyday to clear any insoluble matter remaining.

2.2.2 HPLC Method for the Separation of Cyanidin-3-Glucoside and its Metabolites from Biomatrices

As described in 2.2.1, samples were analyzed for anthocyanin content using a Varian HPLC with UV-visible detection (520 nm) employing the same mobile phases. Separation of cyanidin-3-glucoside and its metabolites was performed using a longer Xterra Phenyl column (Waters, 4.6 mm x 250 mm, 5 µm). Flow rate was 1 ml/min. The gradient employed started at 99% A and changed to 97% over 12 min, and to 90% over the next 7.5 min. The composition remained at 90% for 6.5 min, then dropped to 60% A over 2 min, and was held at 60% A for a further 2 min.

2.2.3 LC/MS/MS Method (Short and Long)

LC/MS/MS analysis was performed using an API2000 mass spectrometer (Applied Biosystems, Warrington) with sample delivery via a 1100 series HPLC instrument (Agilent Technologies UK Ltd., South Queensferry). The HPLC separation used was essentially as described in 2.2.1/2.2.2. The differences to the method are in the columns used for the separation. For the comparable method to 2.2.1 we used an Xterra phenyl column (2.1 mm x 150 mm, 3.5 µm, Waters). However, for the comparable method to 2.2.2 we needed an equivalent 250 mm column length, which was unavailable from the supplier (Waters). To overcome this we used an Xterra Phenyl column (2.1 mm x 150 mm, 3.5 µm) attached via a low dead-volume column connector to a second Xterra Phenyl column (2.1 mm x 100 mm, 3.5 µm, Waters) to give a total column length of 250 mm. For both methods (LC/MS/MS equivalents to 2.2.1 and 2.2.2) a guard column was used (Xterra Phenyl, 2.1 mm x 20 mm, 3.5 µm -

Waters), solvent system A was held at 90% for an additional 5 min, and the flow rate was reduced to 0.31 ml/min to allow direct injection into the mass spectrometer without the need for eluant splitting. Mass spectrometric analyses were performed in positive ion mode under the following conditions: declustering potential, 55V, focusing potential, 380 V; entrance potential, 10 V; collision energy, 50 V; collision energy exit potential, 16 V; ion spray voltage, 5000 V; and temperature, 450 °C. Anthocyanins were identified using multiple reaction monitoring (MRM) for fragments generated by the loss of the sugar moiety, anthocyanidin glucuronides by monitoring of fragments that had lost glucuronic acid (176 amu), and anthocyanin glucuronides by combined loss of sugar and glucuronic acid. Appropriate transitions for detecting methoxylated and methoxylated-glucuronidated were also used, with the transitions investigated listed in Tables 2.1 – 2.5.

Table 2.1: Transitions employed for the detection of parent anthocyanin ions present in Mirtoselect and cyanidin-3-glucoside and for their corresponding aglycons, in mouse biomatrices

Parent Transitions	<i>m/z</i>	MRM Transition
Delphinidin-3-galactoside/glucoside	465	465 → 303
Delphinidin-3-arabinoside	435	435 → 303
Cyanidin-3-galactoside/glucoside	449	449 → 287
Cyanidin-3-arabinoside	419	419 → 287
Petunidin-3-galactoside/glucoside	479	479 → 317
Petunidin-3-arabinoside	449	449 → 317
Peonidin-3-galactoside/glucoside	463	463 → 301
Peonidin-3-arabinoside	433	433 → 301
Malvidin-3-galactoside/glucoside	493	493 → 331
Malvidin-3-arabinoside	463	463 → 331
Delphinidin aglycon	303	303 → 229
Cyanidin aglycon	287	287 → 137
Petunidin aglycon	317	317 → 217
Peonidin aglycon	301	301 → 201
Malvidin aglycon	331	331 → 242

m/z = mass to charge ratio, MRM = multiple reaction monitoring.

Table 2.2: Transitions employed for the detection of the glucuronide metabolites of anthocyanins present in Mirtoselect and cyanidin-3-glucoside, in mouse biomatrices.

Glucuronide Metabolites	<i>m/z</i>	MRM Transition
Delphinidin glucuronide	479	479 → 303
Cyanidin glucuronide	463	463 → 287
Petunidin glucuronide	493	493 → 317
Peonidin glucuronide	477	477 → 301
Malvidin glucuronide	507	507 → 331
Delphinidin-3-gal/glu glucuronide	641	641 → 303
Delphinidin-3-arab glucuronide	611	611 → 303
Cyanidin-3-gal/glu glucuronide	625	625 → 287
Cyanidin-3-arab glucuronide	595	595 → 287
Petunidin-3-gal/glu glucuronide	655	655 → 317
Petunidin-3-arab glucuronide	625	625 → 317
Peonidin-3-gal/glu glucuronide	639	639 → 301
Peonidin-3-arab glucuronide	609	609 → 301
Malvidin-3-gal/glu glucuronide	669	669 → 331
Malvidin-3-arab glucuronide	639	639 → 331

m/z = mass to charge ratio, MRM = multiple reaction monitoring.

gal = galactoside, glu = glucoside and arab = arabinoside.

Table 2.3: Transitions employed for the detection of the methylated metabolites of anthocyanins present in Mirtoselect and cyanidin-3-glucoside, in mouse biomatrices.

Methylated Metabolites	<i>m/z</i>	MRM Transition
Methyl delphinidin-3-gal/glu	479	479 → 317
Methyl cyanidin-3-gal/glu	463	463 → 301
Methyl petunidin-3-gal/glu	493	493 → 331
Methyl peonidin-3-gal/glu	477	477 → 315
Methyl malvidin-3-gal/glu	507	507 → 345
Methyl cyanidin aglycon (peonidin)	301	301 → 201
Dimethyl cyanidin aglycon	315	315 → 287
Trimethyl cyanidin aglycon	329	329 → 287
Tetramethyl cyanidin	343	343 → 287
Dimethyl cyanidin-3-glucoside	477	477 → 315
Trimethyl cyanidin-3-glucoside	491	491 → 345

m/z = mass to charge ratio, MRM = multiple reaction monitoring.

gal = galactoside, glu = glucoside

Table 2.4: Transitions employed for the detection of the sulphated metabolites of anthocyanins present in Mirtoselect and cyanidin-3-glucoside in mouse biomatrices.

Sulphated Metabolites	<i>m/z</i>	MRM Transition
Cyanidin sulphate	367	367 → 287
Cyanidin disulphate	447	447 → 287
Cyanidin trisulphate	527	527 → 287
Cyanidin tetrasulphate	607	607 → 287
Cyanidin-3-glucoside sulphate	529	529 → 287
Cyanidin-3-glucoside disulphate	609	609 → 287
Cyanidin-3-glucoside trisulphate	689	689 → 287
Cyanidin-3-glucoside tetrasulphate	769	769 → 287

m/z = mass to charge ratio, MRM = multiple reaction monitoring.

Table 2.5: Transitions employed for the detection of the conjugated metabolites of anthocyanins present in Mirtoselect and cyanidin-3-glucoside, in mouse biomatrices.

Multiply Conjugated Metabolites	<i>m/z</i>	MRM Transition
Methyl cyanidin glucuronide	477	477 → 301
Dimethyl cyanidin glucuronide	491	491 → 315
Trimethyl cyanidin glucuronide	505	505 → 329
Methyl cyanidin diglucuronide	653	653 → 301
Dimethyl cyanidin diglucuronide	667	667 → 315
Methyl cyanidin-3-glu glucuronide	639	639 → 301
Dimethyl cyanidin-3-glu glucuronide	653	653 → 315
Methyl cyanidin-3-glu diglucuronide	815	815 → 301
Dimethyl cyanidin-3-glu diglucuronide	829	829 → 315
Trimethyl cyanidin-3-glu glucuronide	667	667 → 345
Methyl cyanidin-3-glu triglucuronide	829	829 → 301

m/z = mass to charge ratio, MRM = multiple reaction monitoring.

glu = glucoside.

2.3 Polymerase Chain Reaction (PCR) for Confirming Presence of APC Mutation in Tissue Samples from Apc^{MIN} Mice.

2.3.1 DNA Extraction

Ear punch discs from 2-3 week old mice were collected by the staff of Biomedical Services, and DNA extraction was carried out in accordance with the manufacturer's guidelines for the Puregene Genomic DNA Purification Kit (Gentra Systems, MN, USA). The method used involved adding 300 µl of Cell Lysis solution (Gentra Systems) to the ear disc in a 1.5 ml Eppendorf and vortexing. To this was added 1.5 µl of Proteinase K Solution (20 mg/ml). The Eppendorf was then inverted 25 times, and placed at 55 °C overnight. The sample was treated with 1.5 µl RNase A solution (4 mg/ml), inverted 25 times and incubated for 45 min at 37°C. Once cooled to room temperature, 100 µl of Protein Precipitation solution (Gentra systems - water, ammonium acetate) was added and the mixture vortexed for 20 s. The tube was centrifuged (16,060 g, 3 min) and the supernatant carefully transferred into a clean 1.5 ml Eppendorf containing 300 µl isopropanol. Mixing was facilitated by inverting gently 50 times, and the sample was then centrifuged (16,060 g for 1 min). The supernatant was removed, and the tube allowed to dry. Aqueous ethanol 70% (300 µl) was used to wash the DNA, with vortexing, followed by centrifugation (16,060 g, 1 min), and removal of the supernatant. The tubes were again allowed to dry for 10 min, before adding 50 µl of DNA hydration solution, and incubating for 1 h at 65°C. Samples were stored at either 4°C or -20°C for long term storage.

2.3.2 PCR of DNA to Detect the APC Mutation

A master mix solution for PCR was prepared as described in Table 2.4.1.

Table 2.6: Master mix composition for PCR of mouse DNA for identifying mutations of the APC gene.

Reagent	Final Concentration	Vol/Reaction (μl)
RNase/RNase Free H ₂ O	Up to 50μl	18.7
10X TBE PCR Buffer	1.29	6.5
50mM MgCl ₂	2.4mM	2.4
2.5mM dNTP's	0.24mM	4.8
MAPC9 Primer	1.48μM	5
MAPC15 Primer	1.5μM	5
APC (JR2020) Primer	1.2μM	5
Taq Polymerase	0.06 U/μl	0.6 (5 U/μl)

The master mix was vortexed and 48 μl added to a 200 μl thermocycler tube. DNA solution (2 μl, from above) was added to the same tube. Once added the tubes were sealed, and placed into the Geneamp PCR System 9700 (Applied Biosystems). The cycling conditions were as stated in Table 2.7.

Table 2.7: PCR Cycling sequence used for the amplification of the Apc^{MIN} gene sequence (* = repeat steps 2 – 4, 35 times)

Step No.	Temp (°C)	Time
1	94	3 min
2	94	30 sec *
3	55	30 sec *
4	72	1 min *
5	72	2 min
6	4	∞

A 1.5% electrophoresis gel was prepared, by adding 1.5 g agarose to 100 ml of 1X TBE buffer, and microwaving on high power for 2.5 min. Once cooled slightly, 5 µl of ethidium bromide (10 mg/ml, Invitrogen) was added and mixed into the gel, which was then poured into an assembled electrophoresis tank (BioRad Wide Mini Sub Cell GT) with casting gates in place. Once poured, a comb was inserted to create the wells. Once the gel had set the comb and gates were removed, the tank was filled to within 1 cm of the top with electrophoresis buffer (1X TBE) and 20 µl of ethidium bromide solution (10 mg/ml, Invitrogen) was added to the tank.. The outside wells were filled with 5 µl Ready Load 100bp DNA ladder, and 20 µl of PCR product was added to 4 µl of Bluejuice loading buffer, and 20 µl of this was added to each of the wells.

The power pack (BioRad Powerpac 300) was attached to the positive and negative terminals of the gel tank, and the voltage set to 80V. Once the dye front neared the end of the gel the voltage was switched off, and the gel removed and visualised by UV using the GeneGnome bioimaging apparatus. Presence of the APC mutation is observed by the appearance of a unique band. A second band (positive control) is observed that corresponds to the presence of the mouse housekeeping gene.

2.4 Animal Experiments

Two investigations were conducted into the potential efficacy of anthocyanins as chemopreventive agents, as demonstrated by adenoma formation in the Apc^{MIN} mouse. A pilot study using a single dose of anthocyanins in diet (0.1% w/w C3G, 0.1% w/w Mirtoselect (n = 12)), and a dose escalation/de-escalation study where mice were given diets with C3G or Mirtoselect at 3 different concentrations (0.03, 0.1 & 0.3 w/w %, n = 16).

2.4.1 Feeding Study Design

An Apc^{MIN} breeding colony was established in the Biomedical Services Unit, University of Leicester, UK, and the Apc^{MIN} genotype was confirmed by PCR. Four-weeks-old heterozygous Apc^{MIN} mice were randomly assigned to control and intervention groups to receive either standard AIN93G diet or AIN93G diet supplemented with Mirtoselect or C3G until they were 16 weeks old. AIN93G diet is a standardised, nutritionally complete diet for rodents, and is recommended by the American Institute of Nutrition (AIN). Group sizes were n = 12 and n = 16 in the first and second studies, respectively, with equal gender distribution. Dietary concentrations of anthocyanin preparations were 0.1% (w/w) in the first and 0.03, 0.1 or 0.3% (w/w) in the second study. These doses approximate to 0.9, 3 or 9 mg test compound per mouse per day or 45, 150 or 450 mg per kg body weight per day, which equates to 0.26, 0.87 or 2.6 g/80 kg human when extrapolated using the dose/surface area comparison between species (Freireich *et al.*, 1966). Murine body weights were checked once weekly.

2.4.2 Oral Pharmacokinetic Study

C57BL mice were purchased from Harlan (Oxon, UK), and fasted overnight prior to dosing with C3G. Animals were divided into seven groups (n = 3), and were culled 5, 10, 20, 30, 60, 90 and 120 min after receiving 500 mg/kg of cyanidin-3-glucoside by oral gavage. A control group (n = 2) receiving vehicle (water) alone were included in the study. The animals were culled as described in 2.4.4.

2.4.3 Intravenous Pharmacokinetic Study

C57BL mice were purchased from Harlan (Oxon, UK). Mice were divided into eight groups (n = 5), and were culled 5, 10, 15, 20, 30, 60, 90 and 120 min after dosing with 1000 µg/kg (10 µl of a 2 mg/ml solution to a 20 g mouse) of cyanidin-3-glucoside by intravenous injection via the tail vein. A control group (n = 2) receiving vehicle (water) alone were included in the study. The animals were culled as described in 2.4.4.

2.4.4 Sample Collection

At the end of each experiment mice were killed by exsanguination (under halothane or isoflurane-induced terminal anaesthesia) and cervical dislocation. Blood was collected by cardiac puncture using a heparinised syringe, and then transferred to a heparinised blood tube, to be stored at 4°C until centrifugation; urine was collected directly from the bladder. The small and large intestines were flushed with phosphate buffered saline (PBS) and extricated and further processed (described later). Tissues (liver, kidney, heart, lung, brain, prostate

and gall bladder) were removed and flash frozen in liquid N₂, prior to storage at -80°C. The heparinised blood was centrifuged at 16,060 g for 10 min after an aliquot was removed for measurement of packed cell volume (PCV - volume of packed red blood cells which is a direct indication of anaemia and health status, method described in 2.4.5) The plasma was removed and transferred to a fresh vial and stored at -80°C until analysis.

For adenoma counting (study described in 2.4.1), the intestine was extended on filter paper pre-soaked in PBS and then cut open longitudinally to expose the mucosal surface. The mucosal surface was rewashed with PBS, and the small intestine was subdivided into 3 equal sections: Proximal, medial and distal, approximating to the duodenal, jejuna and ileal regions, while the colon was left complete. Adenoma number for each region was counted by eye based on size (<1 mm, 1 – 3 mm and >3 mm). Adenoma tissue for each mouse was harvested and combined from each intestinal region for further analyses. Similarly, adenoma-free mucosal scrapings of all regions were taken and combined. Tissues were immediately immersed in liquid nitrogen until transfer to the -80°C freezer for storage until analysis.

After the adenomas had been harvested (study described in 2.4.1), a method was published by Goodlad *et al* which described a novel way to improve evaluation of the adenoma burden of the mice (Goodlad *et al.*, 2006). The tumour burden was calculated as the product of adenoma number and adenoma volume. For the small intestines hemispherical volume ($[\frac{4}{3} \pi r^3] / 2$) was used for the adenomas, and spherical volume in the colon. To allow retro-calculation using the method described by Goodlad *et al*, tumour volume had to

be calculated, which required the adenoma radii. To facilitate this calculation the adenoma size graduations (<1, 1 – 3 and >3 mm) were approximated to diameters of 0.5, 2 and 4 mm. The burden was then calculated as a total figure for each animal, and from this a mean was obtained.

2.4.5 Packed Cell Volume Measurement

Measurement of the packed cell volume (PCV) involves sampling a small volume (few μ l) of whole blood to determine the PCV. A narrow gauge capillary tube (Richardsons, Leicester, UK) is introduced into the whole blood, and filled by capillary action. When 80% of the tube is filled, one end is carefully sealed using a Bunsen flame, and the tube is placed into a micro haematocrit centrifuge (Hawksley, Sussex, UK), for 10 min. The cells and platelets are centrifuged to the bottom of the tube, leaving the plasma as the supernatant. To determine the PCV the tube was aligned with a scale reading from 0 – 100%, the bottom of the blood column was positioned at zero, and the top of the plasma at 100%. The PCV is then calculated by reading the % at which the packed erythrocytes and plasma meet (see Figure 2.1).

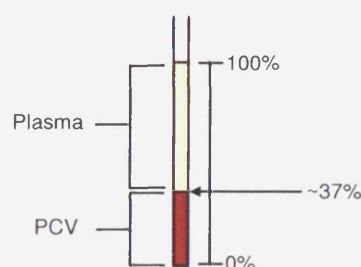


Figure 2.1: Representation of a blood sample, after centrifugation. The dark area shows the PCV. The value of 37% shown in this example is considered a normal value for a healthy C57BL mouse.

The purpose of measuring PCV is to give an indication of the health of the animal with respect to anaemia. A high number of adenomas or a high proportion of large adenomas will result in increased bleeding into the intestinal lumen, causing a loss of erythrocytes and plasma equally. However, plasma volume is replaced more quickly than the erythrocytes to maintain a constant blood volume. This results in a change in the erythrocyte to plasma ratio, and a lower PCV. A healthy animal with no tumours should have a consistent level of blood cells, and should therefore achieve a PCV rating of normal for that strain (37% for C57BL mouse).

2.4.6 Pharmacokinetic and Bioavailability Calculations

The pharmacokinetic (PK) analysis of samples following oral and I.V. dosing experiments (see section 2.4.2 and 2.4.3) was completed using a software package called WinNonlin (v2.1, Pharsight Software). All PK parameters were calculated as non-compartmental. Samples from orally dosed mice were analysed using the model 200 distribution profile for bolus extra vascular input and samples from the I.V. dosed mice were analysed using the model 201 distribution profile for Bolus I.V. input. Parameters calculated included: T_{MAX} , C_{MAX} , rate of elimination (constant, K_E), half-life ($t_{1/2}$) and area under the curve predicted to infinity (AUC_{INF}). The equation used to calculate AUC utilises the linear trapezoidal rule. AUC_{INF} is an extrapolation of the last observed concentration and the last predicted concentration, based on the terminal elimination rate (K_E). Both equations are shown in Figure 2.2. Bioavailability was calculated using the equation shown in Figure 2.2.

$$AUC \int_1^2 = \delta t * \frac{C1 + C2}{2}$$

$$AUC_{INF} = AUC_{last} + \frac{C_{last}}{K_E}$$

$$Bioavailability = \frac{AUC_{oral} * Dose_{IV}}{AUC_{IV} * Dose_{oral}} * 100$$

Figure 2.2: The equations used for calculating the AUC, AUC_{INF} and bioavailability following oral and I.V. bolus dosing. Calculations completed using WinNonlin (see section 2.4.6). AUC = area under curve, $\delta t = (t_2 - t_1)$, C = concentration, AUC_{last} = last observed AUC value.

2.5 Solid-Phase Extraction of Anthocyanins from Biological Samples

2.5.1 Plasma and Urine

Aliquots of plasma (200 µl) or urine (50 – 100 µl) were diluted to 1 ml with KCl solution (1.15% w/v) and centrifuged (16 060g, 5 min) to remove particulates prior to loading onto Oasis HLB solid-phase extraction cartridges (30 mg packing material, 1 ml cartridge; Waters, Elstree, UK), which had previously been conditioned with 1 ml of acetone:formic acid (9:1) and 1 ml of water:formic acid (9:1). Samples were loaded and 500 µl of 1.15% KCl solution was used to wash the cartridge at a flow rate of approximately 1 ml/min. Anthocyanins were eluted sequentially with 0.2, then 0.1 ml acetone:formic acid (9:1). Pooled eluants were evaporated to dryness under a stream of nitrogen (BOC, Guildford, UK) at 40°C. Residues were reconstituted in water:formic acid (9:1, 75 µl) and centrifuged (16,060g, 10 min, 4°C) prior to transferring supernatant to 150 µl inserts for HPLC vials and analysis by HPLC (50 µl injection volume).

2.5.2 Mucosa, Bile and Brain

Mucosal samples (100 – 180 mg) or brain tissue (236 – 416 mg) were vortexed with KCl (1.15% w/v, 1:1), and centrifuged (16,060g, 10 min, 4°C) to remove any surface anthocyanin contamination – this was not possible with the gall bladder (containing bile). With the supernatant removed, fresh KCl (1.15% w/v, 1:1) was added, and the sample homogenised using a blade homogeniser at full speed (X-1020 homogeniser, Ystral, Germany) for 1 min. The homogenate

was made up to 1ml with KCl (1.15%), and centrifuged (16,060g, 5 min) to remove particulates prior to loading onto Oasis HLB solid-phase extraction cartridges containing 30 mg of sorbent (1 ml; Waters, Elstree, UK), which had previously been conditioned with 1 ml of acetone:formic acid (9:1) and 1 ml of water:formic acid (9:1). Samples were loaded and 500 µl of 1.15% KCl solution was used to wash the cartridge at a flow rate of approximately 1 ml/min. Anthocyanins were eluted sequentially with 0.2, then 0.1 ml acetone:formic acid (9:1). Pooled eluants were evaporated to dryness under a stream of nitrogen (BOC, Guildford, UK) at 40°C. Residues were reconstituted in water:formic acid (9:1, 75 µl) and centrifuged (16,060g, 10 min, 4°C) prior to transferring supernatant to 150 µl inserts for HPLC vials and analysis by HPLC (50 µl injection volume).

2.6 Liquid-Liquid Extraction of Murine Tissues

This method was used for the extraction of anthocyanins from liver, heart, lung, kidney and prostate tissues. After washing with KCl (1.15%) the tissues were homogenised using a blade homogeniser (X-1020 homogeniser, Ystral, Germany) in KCl (1.15% w/v, 1:1). For liver, only 300 µl of the 1:1 (KCl to tissue) homogenate was used, for remaining tissues all of the homogenate was used, except for kidney where only one of the organs was homogenised. Homogenates were diluted with 600 µl of cold acetone (-20°C, 20 min) and vortexed thoroughly before being placed in a -20°C freezer for 20 min, and then centrifuged (16,060g, 10 min, 4°C) to remove the precipitated proteins. The supernatant was removed and evaporated to dryness under a stream of nitrogen at 40°C. Residues were reconstituted in water:formic acid (9:1, 75 µl) and centrifuged (16,060 g, 10 min, 4°C) prior to transferring the supernatant to 150 µl inserts for HPLC vials and analysis by HPLC (50 µl injection volume).

2.7 Determination of Malondialdehyde-deoxyguanosine (M1dG)

Adducts in DNA

2.7.1 DNA Extraction from Adenoma Tissue

DNA was extracted using the Qiagen Genomic DNA Kit (Qiagen GmbH, Germany) in accordance with the following manufacturers' guidelines: Combined adenomas weighing ~20 mg, obtained from an adult mouse, stored at -80°C were thawed. 9.5 ml of G2 (digestion buffer) containing 200 µg/ml RNase A was added and the tissue homogenised using a glass homogeniser. To the homogenate 0.5 ml proteinase K was added and mixed by vortexing. This mixture was then incubated at 4°C and the supernatant removed and transferred to an equilibrated (4 ml QBT equilibration buffer, gravity fed) Qiagen genomic-tip 100/G. Once the supernatant had been eluted from the genomic-tip it was washed twice with 7.5 ml QC buffer (wash buffer), and this was allowed to flow through by gravity. The DNA was eluted by adding 5 ml QF elution buffer at 50°C, and allowed to drip into 3.5 ml isopropanol at room temperature. The precipitated DNA was centrifuged (4000 g, 15 min at 4°C), supernatant discarded and the pellet washed in 1 ml 70% aqueous ethanol. The solution was transferred to a 2 ml tube, and centrifuged (16 060 g, 10 min at 4°C). The supernatant was discarded and the pellet resuspended in 200 µl distilled water. DNA solutions were stored at -80°C.

2.7.2 Determining DNA Concentration

DNA quantification was performed on a GeneQuant spectrophotometer (Biochrom, LTD, Cambridge). The spectrophotometer was zeroed at 260 nm using distilled water in a quartz cuvette. DNA extract (2 µl) was added to 98 µl of distilled water. This solution was transferred to the quartz cuvette, and the machine set to a dilution factor of 50:1 and a pathlength of 10 mm. DNA concentration was calculated assuming dsDNA 50 µg/ml has an absorbance of 1.0 at 260 nm in a 10 mm pathlength cell. This is derived from the following equation (A = absorbance at 260 nm):

$$\text{DNA concentration (}\mu\text{g/ml)} = A[260 \text{ nm}] \times 50 \times \text{Dilution factor (50)}$$

2.7.3 Immunoslot-blot for Determination of M1dG Adduct Concentration

The method originally described by Leuratti *et al* (1998) and modified by Singh *et al* (2001) was used. A series of nine standards were prepared by diluting malondialdehyde (MDA)-treated calf thymus DNA (10 fmol adduct per µg DNA) with control calf thymus (both kindly supplied by Dr Raj Singh, University of Leicester). The standards, each containing 3.5 µg DNA contained 0, 0.4, 1, 2, 3, 5, 6, 8 and 10 fmol/µg M1dG, respectively. Experimental samples were pipetted into 3.5 µg DNA aliquots. All samples (standards and experimental) were adjusted to a final volume of 100 µl with potassium phosphate buffer to which 150 µl of PBS was added, and the solution sonicated for 20 min in an ultrasonic bath. DNA was then denatured using a heating block set to 100°C for

5 min, before cooling on ice for 10 min. 250 µl of 2M ammonium acetate was added before vortexing and centrifugation at 16 060 g for 30 s.

Two blotting paper sheets were soaked in 1M ammonium acetate and then placed in a Minifold II slot blotting apparatus (Schleicher and Schuell, Middlesex, UK). A nitrocellulose membrane (Schleicher and Schuell, Middlesex, UK) was soaked in water followed by 1M ammonium acetate before being added to the blotting apparatus, and the top layer containing 24 wells (in triplicate) was then assembled. Suction was applied to the apparatus and the DNA solutions loaded in triplicate, 143 µl (1 µg) per slot. The wells were allowed to run dry before 200 µl of 1M ammonium acetate was added and also allowed to run dry. After removing the filter from the apparatus it was baked dry at 80°C for 90 min. The filter was washed in PBS containing 0.1% (v/v) Tween-20 (Sigma) (PBS-T), 5% milk powder (Marvel, Spalding, UK) for 1h, at room temperature and washed twice in PBS-T for 1 min. After washing, the filter was incubated with 0.25 µg M1dG primary antibody (kindly supplied by Prof. Marnett, Dept of Biochemistry, Vanderbilt University, USA) in 40 ml PBS-T, 0.5% milk powder for 2 h at room temperature, followed by overnight at 4°C. After overnight incubation the filter was washed with 50 ml PBS-T for 1 min, and then twice more for 5 min, it was then incubated with 8.8 µg polyclonal goat anti-mouse HRP antibody (Dako, Ely, UK) in 32 ml PBS-T, at room temperature for two hours. The filter was washed in PBS-T for 15 min followed twice more in fresh PBS-T for 5 min. Finally, the filter was incubated in 8 ml Supersignal® West Dura HRP Detection Kit (Pierce Biotechnology, Rockford, USA) extended duration substrate for 5 min. All washes and incubations were performed with gentle rocking (Heidolph Unimax 1010) except for incubation at 80°C.

The chemiluminescence image was captured using a GeneGnome bioimaging system (Syngene, Cambridge). The intensity of the signal from each slot blot was recorded using GeneSnap and GeneTools image analysis software.

The filter was washed on a rocker at room temperature for 1h in PBS and incubated in 50ml PBS solution containing – 50 µl of propidium iodide solution (5 mg/ml) at room temperature for 2h. The filter was then washed in PBS for 1h before being transilluminated with UV light and the image captured with GeneGenius imaging system. The intensity of each slot blot was recorded using GeneSnap and GeneTools image analysis, to compare the degree of loading at each site

2.7.4 Calculation of M1dG Concentrations

To simplify the calculation of M1dG adduct levels an Excel spreadsheet template was designed by Dr Raj Singh (Biocentre, University of Leicester).

1. The values obtained for the chemiluminescence and propidium iodide (PI) imaging are entered into the template
2. The Mean PI value is calculated, and each PI value is divided by the mean to determine the PI to Mean PI ratio, for each slot
3. The GeneGnome chemiluminescence value for each slot is then divided by the PI to Mean PI ratio, to account for equal loading.
4. The concentration of M1dG adducts is then calculated using the calibration curve

Initial investigations using this method showed that the 0 fmol/ μ g standard generates a measurable reading suggesting that the calf thymus DNA used contains substances reacting with the anti-M1dG antibody. The value for the 0 fmol/ μ g standard was subtracted from all samples.

Due to the limited space on each blot it was not possible to analyse all samples simultaneously. To overcome inter-assay variation the mean value for DNA from control animals was set as 100%, and the values for each treatment were standardised by expression as a percentage of control the value from the same blot, in this way data from multiple runs could be combined.

2.8 Statistics

All statistical analyses used the SPSS v12 computer software package (SPSS Inc).

The data was first confirmed as being normally distributed using the Kolomogorov-Smirnov test, in which normally distributed data is not significant. For normally distributed data parametric statistical analysis could be performed. Potential parametric tests which could be utilised include: students t-test and analysis of variance (ANOVA). It was decided that ANOVA would accurately describe the data, simplify the calculation procedure by reducing the number of comparisons required and minimise type 1 errors which may occur through multiple comparisons through the t-test, a type 1 error being a false positive.

Statistical significance was acknowledged when a p-value of < 0.05 was observed for a given analysis.

Students t-test was used in the determining the statistical significance of M1dG adduct levels.

3. Development and Optimisation of Methods for the Extraction and Analysis of Anthocyanins in Biological Samples

3.1 Method Development for Separation of Anthocyanins in Mirtoselect

3.1.1 Aims

A rapid, reliable and reproducible method for the analysis of anthocyanins in plasma, urine and tissues using HPLC-Vis spectroscopy was required. This HPLC method was also to be used to determine the best method of extraction of anthocyanins from a range of biomatrices. The method should be validated and improve on those previously published, for speed and/or resolution. Of the HPLC methods published previously for constituents of bilberry and other *Vaccinium spp* (Nyman *et al.*, 2001, Mazza *et al.*, 2002, Wu *et al.*, 2002, Afaq *et al.*, 2005 and Wu *et al.*, 2005), only one report shows separation (not to baseline) of 25 anthocyanins (Mazza *et al.*, 2002), and this employed a 60 min run time, typical for most published methods. A second method required the deconjugation of the anthocyanins to anthocyanidins (Nyman *et al.*, 2001), and so would not be suitable for analysis of individual anthocyanins. Limited validation of some of these methods has been performed, but not for Mirtoselect in plasma and urine.

3.1.2 Literature Methods for the Separation of Anthocyanins by HPLC

At the commencement of this project, published HPLC techniques for the separation of anthocyanins from *Vaccinium spp* were to the best of our knowledge, limited. A preliminary method was based on that described by Nielsen *et al* (2003a), Figure 3.1, used for the separation of anthocyanins from commercial blackcurrant juices. This method was chosen because it had the desirable characteristics of being validated, with good separation of 9 anthocyanins and possessing a short run time (13 min). This HPLC method employed an Agilent Zorbax SB-C18 (4.6 x 150 mm, 5 μ m) column.

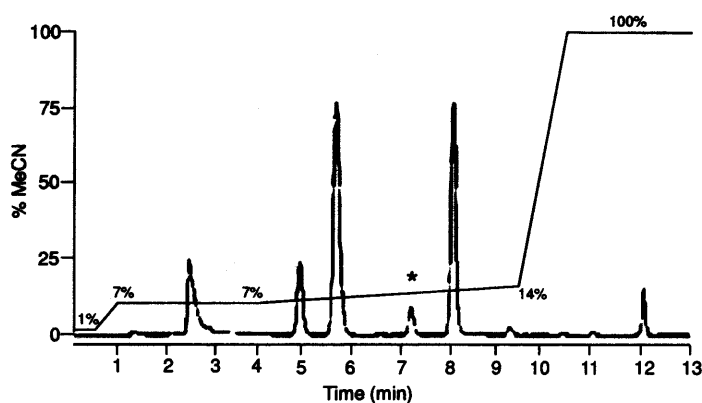


Figure 3.1: HPLC method employed by Nielsen *et al* (2003a) the separation of anthocyanins from commercial blackcurrant juices.

* signifies C3G. A: Water:formic acid (9:1, v/v). B: Acetonitrile (MeCN). % MeCN overlaid on the trace. Flow rate: 1 ml/min, 520 nm UV). Figure adapted from that of Nielsen *et al* (2003a).

The composition of blackcurrant juice is different to Mirtoselect, so some modification was necessary. Indena SpA, the manufacturer of Mirtoselect, supplied an example chromatogram identifying the 15 components of Mirtoselect (Figure 3.2) over a 50 min run time; the HPLC conditions were not made available however. From this chromatogram the order of retention for the constituents of Mirtoselect and their relative peak heights and shapes could be established.

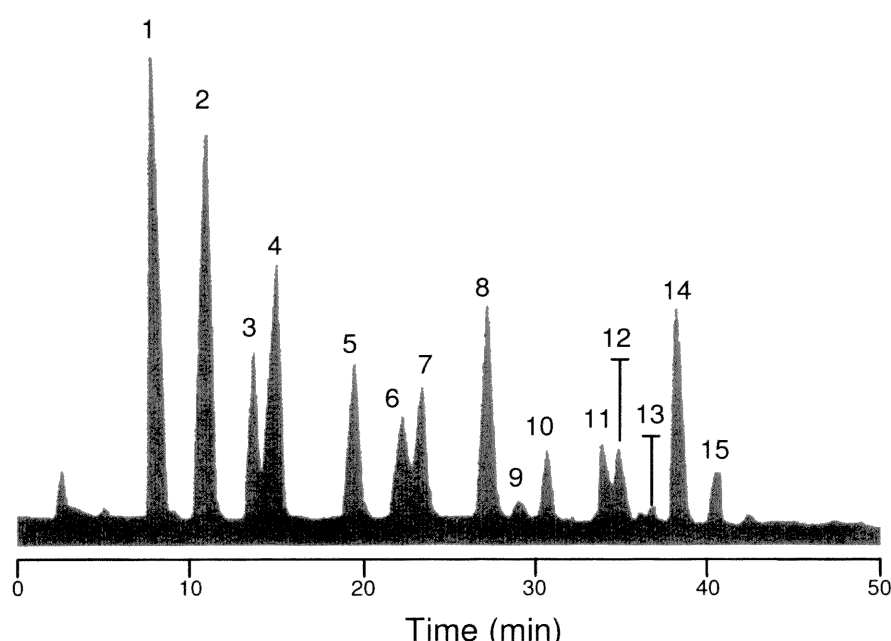


Figure 3.2: Example chromatogram for the separation of the anthocyanin components of Mirtoselect (Indena SpA). 1 = delphinidin-3-galactoside, 2 = delphinidin-3-glucoside, 3 = cyanidin-3-galactoside, 4 = delphinidin-3-arabinoside, 5 = cyanidin-3-glucoside, 6 = petunidin-3-galactoside, 7 = cyanidin-3-arabinoside, 8 = petunidin-3-glucoside, 9 = peonidin-3-galactoside, 10 = petunidin-3-arabinoside, 11 = peonidin-3-glucoside, 12 = malvidin-3-galactoside, 13 = peonidin-3-arabinoside, 14 = malvidin-3-glucoside and 15 = malvidin-3-arabinoside. HPLC conditions not supplied.

3.1.3 Selection of Stationary Phase

Three stationary phases were tested based on the manufacturers proposed suitability. Columns were assessed using the elution gradient described in Figure 3.1. The columns tested were: a Zorbax SB-C18 (4.6 mm x 150 mm), as used by Nielsen *et al* (2003a), but with smaller pore size (3.5 μ m), an Atlantis dC18 (4.6 mm x 150 mm, 3.5 μ m, Waters) for its ability to separate very polar compounds at low pH whilst retaining lipophilic compounds, and Xterra Phenyl (4.6 mm x 150 mm, 5 μ m, Waters) for its ability to retain and separate aromatic/polycyclic hydrophilic compounds at extremes of pH. Figure 3.3 shows the separations achieved with each stationary phase, and the solvent conditions used (3.3i).

Comparing the results presented in Figure 3.3 with the chromatogram supplied by Indena (fig. 3.2), it is clear that the Xterra column represents the best starting point for optimisation of the method. The peak shape and resolution is much better than with either the Zorbax or Atlantis columns. For this study Xterra Phenyl was thought to provide the best base for optimisation.

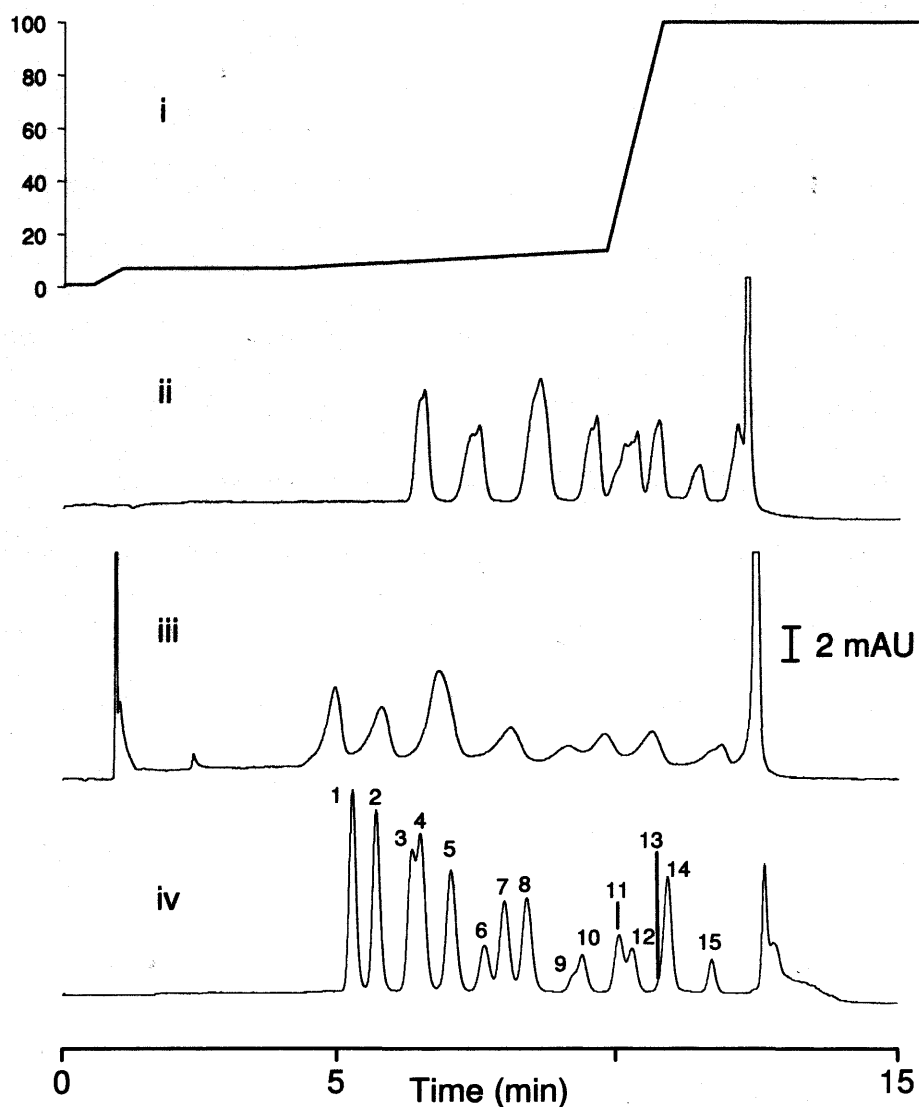


Figure 3.3: The ability of different stationary phases to separate 15 anthocyanins from Mirtoselect, using the method described in Figure 3.1. i – Composition (%) of acetonitrile. ii – Zorbax SB-C18 3.5 μm column. iii – Atlantis dC18 3.5 μm column. i.v. – Xterra Phenyl 3.5 μm column. Detection was carried out at 520 nm, using a 50 μl injection volume of a 10 $\mu\text{g}/\text{ml}$ stock solution of Mirtoselect. Numbered peaks are as detailed in fig 3.2.

3.1.4 Optimisation of Mobile Phase Compositions and Elution

Gradient

The method described by Nielsen *et al* (2003a) incorporated the use of 10% formic acid (natural pH of 1.7). The Xterra Phenyl column is designed to operate at pH 1 – 12, but was not designed to cope with a formic acid content exceeding > 1%. A lower formic acid concentration would reduce exposure to large amounts of a strong acid and so provide safer handling whilst prolonging column life. Anthocyanins are more stable at low pH, and their chromophore is regulated through pH (see Figure 1.9). Initially, 1% formic acid:water (v/v, natural pH 2.5) was tested, but this significantly reduced the quality of the chromatography, increased retention times, gave poor peak resolution and reduced separation (Figure 3.4).

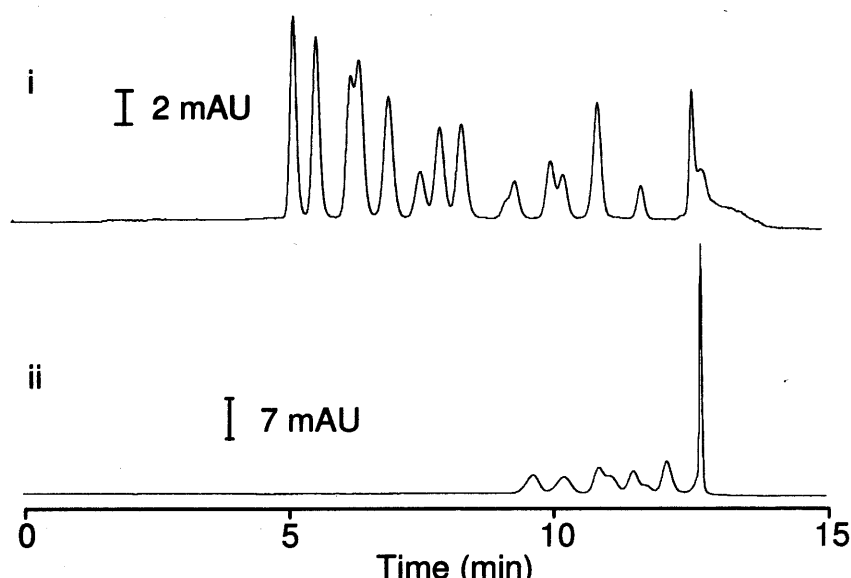


Figure 3.4: Effect of formic acid concentration of mobile phase A on the separation of anthocyanins from Mirtoselect. Chromatogram i is with 10% formic acid, chromatogram ii is with 1% formic acid.

It was decided to keep the formic acid at 10% and optimise the method further by changing the gradient. It was clear in Figure 3.3 that most (12) of the anthocyanins in Mirtoselect are being eluted under primarily aqueous conditions (up to 86% aqueous), with the later peaks (3) being washed off by increased organic solvent (acetonitrile). To achieve better separation it was decided that the gradient should be held at 1% acetonitrile for 4.5 min at the beginning of the run. The resulting chromatogram is shown in Figure 3.5i with gradient profile overlaid. The separation here was better for peaks 3, 4, 11 and 12, and peak 13 was also resolved, but the run time had, as a result, been extended to 20 min. Next a 1% B (acetonitrile) isocratic system was tested. Initially a 1 ml/min 99% A (aqueous):1% B (organic) isocratic system was investigated with the result shown in Figure 3.5ii. Separation was good when analysed in detail, but the total run time was 40 min, which though an improvement to previously published methods, was a significant increase compared with the gradient elution methods. To counter this prolonged retention time, the flow rate was increased to 1.5 ml/min (Figure 3.5iii), with little loss of resolution and a total runtime of 30 min. .

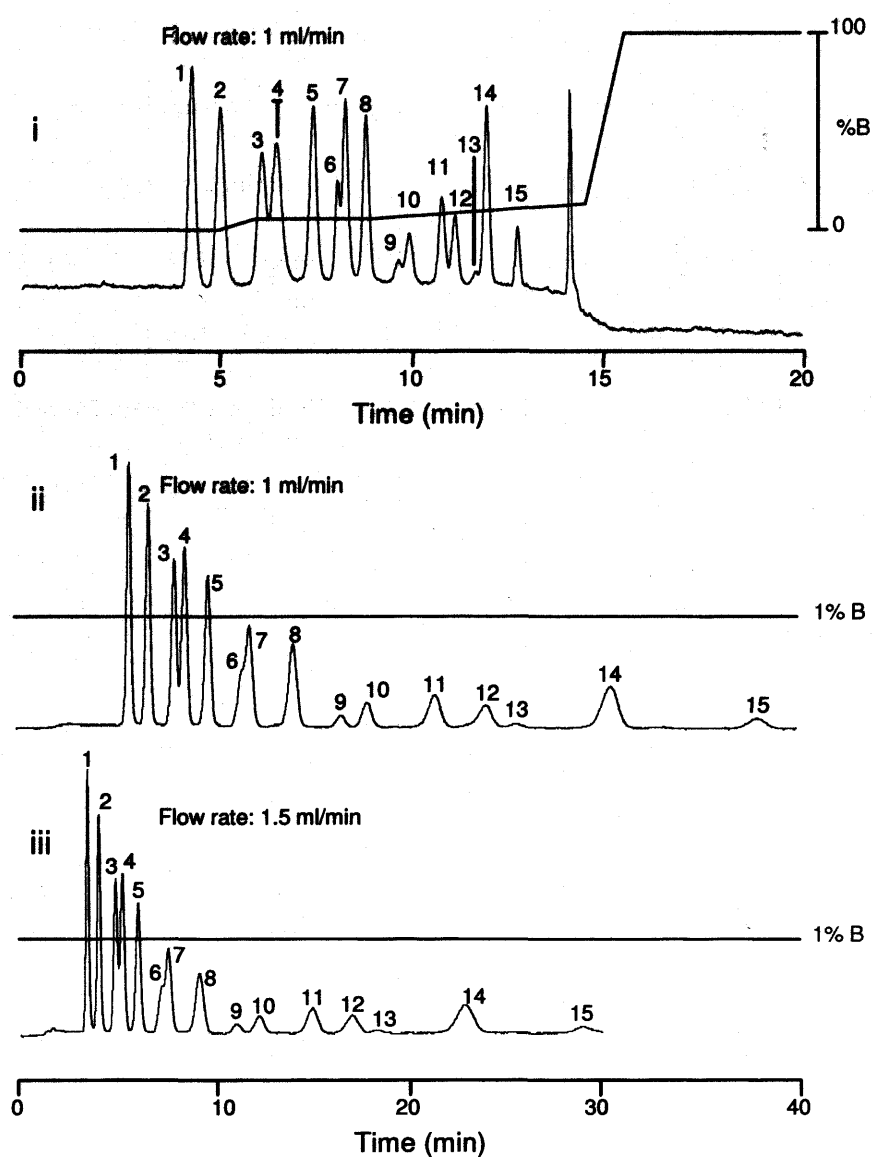


Figure 3.5: Chromatograms showing the separation of anthocyanins in Mirtoselect under varying HPLC conditions. Overlaid line represents %B (organic) in the mobile phase. Legend (i, ii & iii) detailed in the text, peak numbers detailed in fig 3.2.

Using this method I analysed the effect of changes in the composition of the mobile phase. With the intention of reducing the amount of formic acid in the

system again, the effectiveness of the free acid with its ammonium formate salt in mobile phase A was compared. An investigation into whether acetonitrile or methanol was the better solvent for mobile phase B was also conducted. Methanol is a weaker eluent than acetonitrile, and as such, may provide better separation of the early hydrophilic components of Mirtoselect. The result (Figure 3.6) was better separation of peaks 3 and 4 but co-elution of others, as well as an increase in run time and pressure. Therefore changing to methanol gave no net gain.

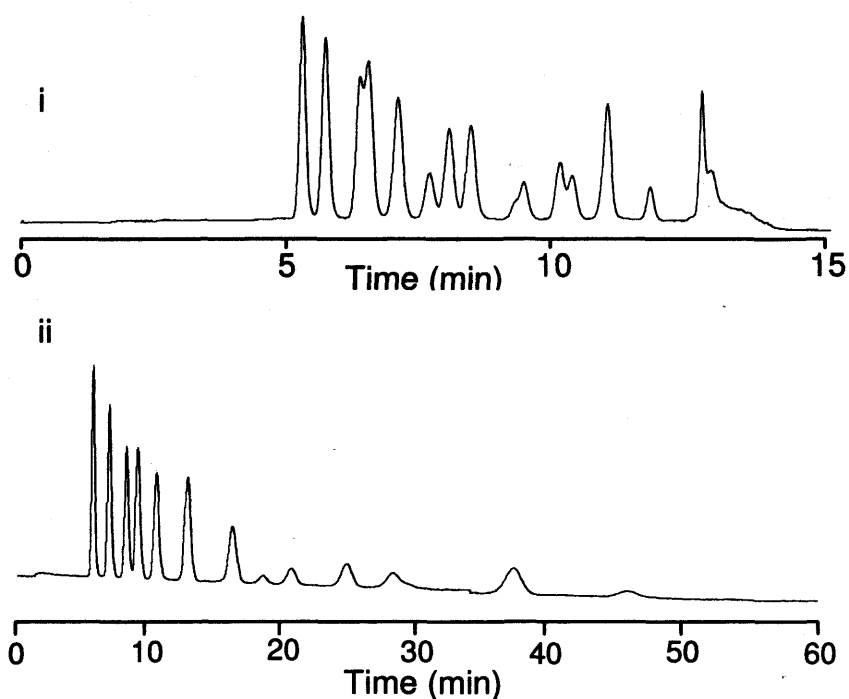


Figure 3.6: Chromatograms showing the effect of changing channel B from acetonitrile (chromatogram i) to methanol (chromatogram ii) for the separation of anthocyanins in Mirtoselect. Channel A remained as 10% formic acid in water, gradient as described in Figure 3.5iii. Flow rate of 1.5 ml/min.

Whilst the separation of the first 5 peaks had been improved, the later peaks were broad with base widths as long as 4 min. This as well as the long run time was reason to stay with acetonitrile as mobile phase B and to attempt improvements to the isocratic method. The reason for the broadening of the peaks at the end of the run was most likely due to the low organic composition of the isocratic method. Altering this to 97 and 96% A (3 and 4% acetonitrile) was attempted, but no marked improvement was seen. It was decided that a gradient system would have to be re-employed to solve the peak width issue. After many subtle changes to the gradient system the best compromise between peak resolution and short run time (Figure 3.7), in conjunction with a flow rate of 1.5 ml/min, was used for separating Mirtoselect. This method uses a 3.5 μm pore size Xterra Phenyl (4.6 x 150 mm) column. The 5 μm column was also tested with a negligible change to the elution profile, but greater column integrity over multiple (~50) injections. Peak resolution remained constant with the 5 μm column. With this in mind it was decided to use the 5 μm column routinely for experimental samples. It was also apparent that, contrary to manufacturers' recommendation, the high formic acid content did not seem to adversely affect the columns' lifetime.

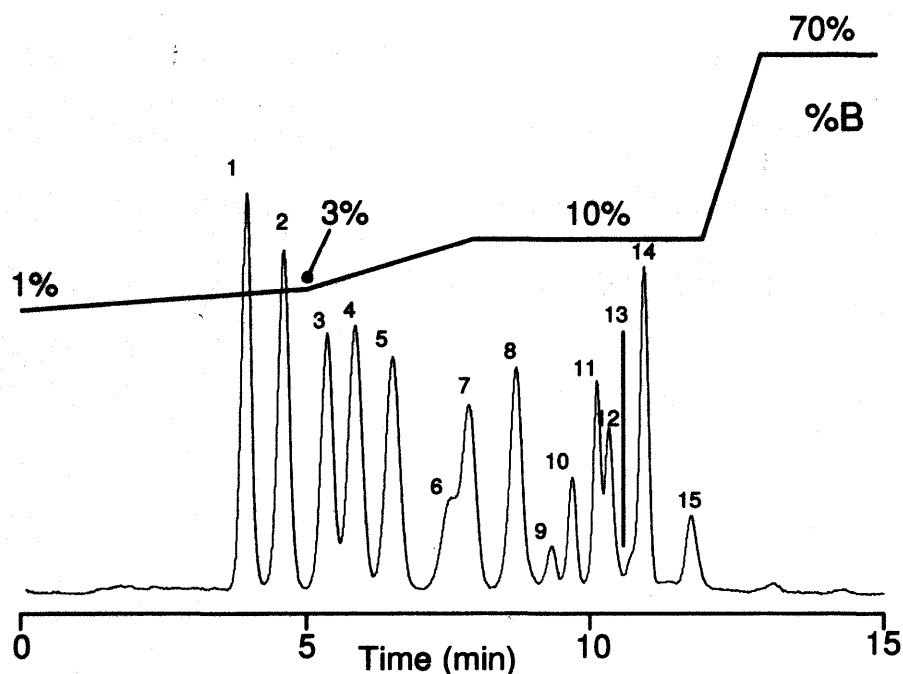


Figure 3.7: Representative HPLC chromatogram of optimal Mirtoselect separation. This method (acetonitrile - %B, overlaid) achieved the best balance between peak resolution and run time, and would provide the basis for future HPLC conditions for the analysis of Mirtoselect and C3G. Analysis carried out at 520 nm, with a flow rate of 1.5 ml/min and at a column oven temperature of 40°C. Solvent used for A channel was 10% formic acid in water.

The shoulders observed in Figure 3.7 could not be resolved further with gradient change, and so a narrow bore, low flow rate Xterra Phenyl column (2.1 mm x 150 mm, 3.5 μ m, Waters) was tested. The low flow rate (0.31 ml/min) meant injection volumes needed to be drastically reduced, which the Varian HPLC autosampler could not achieve reliably. Dead volume in the system became a problem, and the Varian HPLC was not ideally suited to this type of chromatography, so we reverted to the method shown in Figure 3.7.

To compliment the optimised HPLC system a number of reconstitution buffers were tested. It was decided to continue using 10% aqueous formic acid, as this minimised solvent mixing upon injection, enabled dissolution of the extracted samples and maintained the stability of the anthocyanins and their chromophore.

3.2 Method Development for the Separation of Cyanidin-3-Glucoside and Its Metabolites

With a rapid and efficient method developed for the analysis of Mirtoselect anthocyanins in place, attention shifted to the analysis of C3G metabolites. C3G metabolite analysis is important for the analysis of biomatrices from the pharmacokinetic studies. Whilst the method outlined in Figure 3.7 was a good starting point it was required that the C3G metabolite method be able to differentiate and separate constitutional (structural) isomers of each metabolite type, and multiple conjugated metabolites. Initial experiments using an extract of urine from mice fed C3G, indicated that it was not possible to achieve efficient separation of C3G metabolites using the Mirtoselect HPLC-Vis method. Using the method developed in Figure 3.7 as a starting point it was decided extra column length would be key to improving separation of the metabolites. Two of the Xterra Phenyl columns (4.6 mm x 150 mm, Waters) were connected with a low dead-volume connector. The gradient profile from Figure 3.7 was also used as the basis for the two-column method, but the time of each gradient change was doubled resulting in a total run time of 30 min. This experiment showed separation as expected, and spread the elution over 30 min, effectively increasing the peak capacity of the method. The elution profile was improved and simplified further using a (4.6 x 250 mm, Waters) column to allow better separation, and the flow rate reduced to 1 ml/min to reduce back pressure, a result of increased column length. The column oven on the Varian 410 autosampler could not accommodate columns longer than 150 mm, so the column was used at room temperature (20°C), in an air-conditioned laboratory.

Lowering the column temperature had the effect of lengthening the run time.

The finalised method is overlaid on the C3G standard shown in Figure 3.8A.

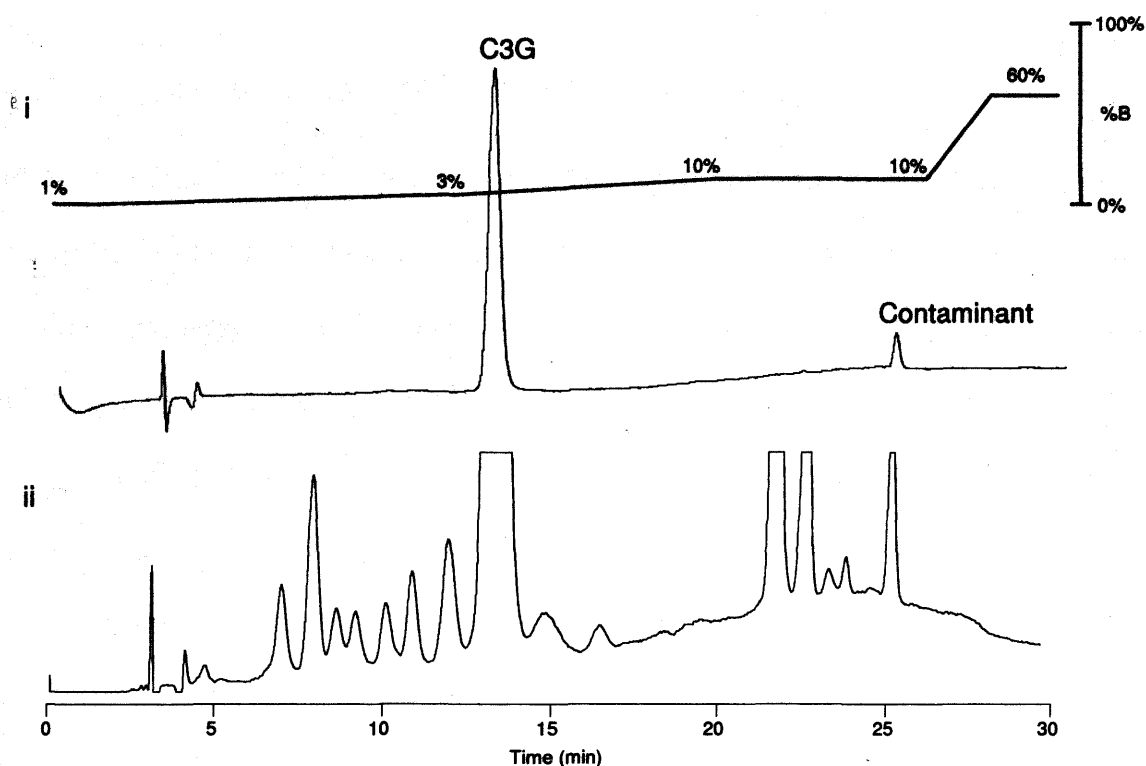


Figure 3.8: Representative HPLC chromatograms of C3G and its metabolites in urine. Channel A in both cases is 10% formic acid in water. Chromatogram i – C3G standard (RT ~13 min) showing associated contaminant peak (RT ~25.5 min). Gradient (%B, acetonitrile) overlaid. Chromatogram ii – example chromatogram from an extract of plasma from mice dosed orally with C3G (500 mg/kg). Chromatogram magnified to show the metabolite distribution. A long stationary phase afforded better separation of metabolites, and their constitutional (structural) isomers. Detection carried out at 520 nm, with a flow rate of 1 ml/min at room temperature. This method was used in the analysis of C3G metabolites as described in chapter 5, sections 5.3 and 5.4.

3.3 Development of Techniques for the Extraction of Anthocyanins from Biological Samples

3.3.1 Liquid-liquid Extraction of Anthocyanins

With an HPLC system in place a reliable, reproducible and efficient method for the extraction of anthocyanins from biomatrices was developed. It was decided to first investigate liquid-liquid extraction techniques. The candidate organic solvents investigated were ethyl acetate, methanol, acidified acetone (10% formic acid) and acetonitrile. A suitable solvent for extraction needs to provide high extraction efficiency, with good reproducibility and high throughput. To simplify method development a single compound, cyanidin-3-glucoside, was used for quantitative assessment of extraction methodologies. The assumption was made that its chemical properties are similar to those of the other components of Mirtoselect. C3G was extracted in triplicate for each solvent, from spiked human plasma supplied by healthy volunteers. The method comprised the addition of 600 μ l of solvent to 100 μ l of plasma, previously spiked with 40 ng C3G. The sample was then vortexed (1 min), and placed in a -20°C freezer for 20 min. The samples were centrifuged (16,060 g, 10 mins at 4°C), and the supernatant reduced to dryness under a stream of N₂ at 40°C. The samples were reconstituted in 70 μ l 10% aqueous formic acid and analysed using the HPLC method described in Figure 3.7. The results are shown in Table 3.1.

Table 3.1: Assessment of liquid-liquid methods for the extraction of C3G from human plasma. Efficiency is calculated based upon the HPLC peak area (PA) of a non-extracted standard of same-mass (40 ng) to the spiked plasma ([PA sample/PA standard] x 100).

Solvent	Extraction Efficiency	Comments
Ethyl Acetate	0% (n = 3)	C3G remains in aqueous phase
Methanol	40.1% (n = 3)	Poor efficiency and chromatography. Long evaporation time.
Acetonitrile	66.4% (n = 3)	Good efficiency and poor chromatography. Long evaporation time.
Acidified acetone (10% formic acid)	66.7% (n = 3)	Good efficiency and chromatography. Shorter evaporation time.

Acidified acetone (10% formic acid) offered the best combination of speed and extraction efficiency, and was considered the best solvent method for liquid-liquid extraction of anthocyanins.

3.3.2 Solid-Phase Extraction of Anthocyanins

Although protein precipitation with acidified acetone offers a rapid and efficient mode of anthocyanin extraction, clean up of samples is minimal. An alternative to solvent extraction is solid-phase extraction (SPE). SPE has the potential to be a cleaner, more selective method of extraction. It was decided to investigate SPE using Oasis HLB 1cc 30 mg cartridges (Waters) to assess their suitability for the extraction of C3G and its aglycon cyanidin. Initially, a pilot experiment with aqueous solutions of C3G was conducted to determine the best eluent for retrieving C3G from the Oasis HLB stationary phase. A range of aqueous MeOH solutions (10 – 90% MeOH) containing 2% formic acid was used, and all elutions were completed at a flow rate of ~1 ml/min using a vacuum manifold (Waters). The following steps were the same for all samples:

1. Cartridge was conditioned with 1 ml MeOH then 1 ml H₂O.
2. 10 µg of C3G or cyanidin in 500 µl of aqueous standard solution was loaded onto the cartridge
3. Cartridge washed with 1 ml water
4. Sample eluted with 1 ml of a range of aqueous methanol solutions (Figure 3.9)

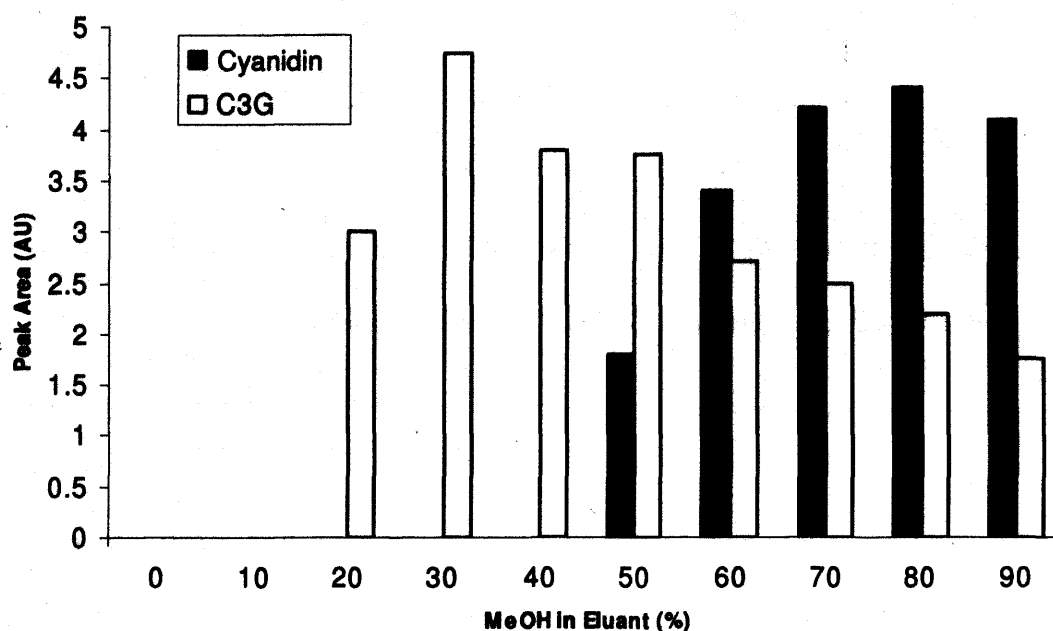


Figure 3.4: Effect of increasing Methanol concentration on the elution of cyanidin and C3G from Oasis HLB 1cc, 30 mg SPE cartridges.

It is clear from Figure 3.9 that cyanidin and C3G were eluted over a broad range of MeOH concentrations. Maximum C3G elution was attained with 30% MeOH, but significant elution was still occurring at up to 90% MeOH. The maximum cyanidin elution was achieved with 80% MeOH, but as with C3G the range was broad, from 50 – 90% MeOH. The best compromise for C3G and cyanidin elution was achieved with 60% MeOH. Therefore using aqueous MeOH for elution may not be optimal, as it possesses a broad elution range and containing a large proportion of water in the eluent, making evaporation time lengthy. Acidified acetone (10% formic acid) was tested as an eluent. Using spiked plasma samples, the method was designed as follows:

1. Cartridge was conditioned with 1 ml acetone (10% formic acid) and then 1 ml H₂O (10% formic acid).
2. 300 µl of spiked (C3G) plasma (diluted to 1 ml with 1.15% KCl) was loaded onto the cartridge
3. cartridge washed with 1 ml 1.15% KCl
4. anthocyanins eluted with 1 x 200 µl acetone (10% formic acid) and then 1 x 100 µl acetone (10% formic acid) into the same vial

This method produced an extraction efficiency of 71% for C3G, with an elution volume of 300 µl acidified acetone. The benefits of this method are its simplicity, high throughput, inclusion of a wash step, good extraction efficiency and quick workup. It was decided to adopt this SPE method for the extraction of anthocyanins from plasma, urine and soft tissues (mucosa, bile and brain with a prior homogenisation step). However, the remaining tissues were found not to be suitable for SPE extraction because the cartridges often become blocked, even after prior multiple centrifugation and clean-up steps. For these tissues the liquid-liquid method outlined in 3.3.1 was used.

3.4 Validation of Methods

3.4.1 Validation of Acetone Precipitation Extraction Method Using Cyanidin-3-Glucoside

Table 3.2 summarises the data obtained in validating the acetone precipitation method for extraction of anthocyanins from plasma. Three standards of the same concentration were analysed, and mean peak area determined, which was considered to be 100% for extraction efficiency. Same-mass amounts were added to control plasma, and extracted using the acetone precipitation method described in section 3.3.1. Samples were evaporated to dryness and reconstituted in 70 µl (10% aqueous formic acid), the same as for the standards. Peak areas for extracted samples were calculated as a percentage of the mean unextracted standards, and the extraction efficiency was determined. The mean extraction efficiency for days 1, 2 and 3 was 63, 62 and 63%, respectively. Intra and interday variability was deemed acceptable if the standard deviations were less than 15% (ICH Guidelines, 1996), and actual values achieved were 9.2% and 8.6% for intra and inter day variability, respectively. Peak drift for C3G over all runs was less than 12 seconds.

Limit of detection (LOD) and limit of quantitation (LOQ) were determined for unextracted C3G standards, based on the ratio between peak height and baseline noise. A peak height ratio of 2:1 (peak area:noise) was used to determine limit of detection and 10 times the baseline noise was used for the limit of quantitation in accordance with good clinical laboratory practise (GCLP) guidelines (ICH Guidelines, 1996); these were 12 and 20 ng (mass on column, or 0.03 and 0.04 nM), respectively.

Table 3.2: Validation of the acidified acetone extraction method. Validation conducted using C3G-spiked human plasma, three times on day 1 (n=5 for each), and once more on two consecutive days (n = 5 for each). Values shown are percentage of mean standard (n=3).

Extraction Number	Day 1 (n = 5 x 3)			Day 2 (n= 5)	Day 3 (n = 5)
	Ext 1 (% of std)	Ext 2 (% of std)	Ext 3 (% of std)	Ext (% of std)	Ext (% of std)
1	60.3	63.0	65.6	59.5	59.4
2	54.7	67.5	53.1	60.3	75.5
3	69.6	65.4	65.5	50.4	67.8
4	74.5	66.8	54.3	58.7	68.9
5	63.8	62.5	59.7	60.8	63.2
Mean (±SD)	64.6 ±7.7	65.0 ±2.2	59.6 ±5.9	62.0 ±4.3	63.2 ±6.1
Day 1 mean (±SD)		63.1 ±5.8			

The observed drift in retention time was < 12 s.

Intraday (Day 1) Variability: 3 extractions (n = 5) of same concentration completed independently on day 1. SD of peak area less than 15% is within limits set out for good clinical laboratory practise (GCLP); actual value = (9.4%).

Interday Variability (between day 1, 2 and 3): Mean of day 1 extractions compared to 1 extraction (n = 5) on day 2 and 3. SD of peak area less than 15% is within limits set out for GCLP; actual value = 11.0%.

3.4.2 Validation of Solid-Phase Extraction Method Using Cyanidin-3-Glucoside

A validation similar to that described for the acetone precipitation extraction was completed for the SPE extraction method over 3 days. The validation consisted of preparing a range of C3G standards (50, 100, 200, 400 and 800 ng) for injection via HPLC-Vis spectroscopy. The mean peak area for the unextracted standards was assigned as 100% extraction efficiency, and the extracted sample peak areas were compared to these and reported as a percentage. Human plasma was spiked with same-mass amounts as the standards and the 5-point standard curve from spiked plasma was completed using the finalised SPE method described in section 3.3.2. These extractions were completed over 1 day and results of this validation are shown in Table 3.3. Linearity for each run was determined by the R^2 value for each run and is shown in Figure 3.10. The mean extraction efficiency for all samples was 70.7%, and the retention time drift was < 6s over all injections.

Table 3.3: Validation of the SPE method for C3G extraction from human plasma. Values shown are extraction efficiencies (%). Standards are unextracted, with peak area assigned as 100% extraction efficiency. 5 concentrations completed in triplicate (Ext 1, 2 and 3) on separate occasions. The symbols (Δ , \times , \diamond , \square) represent the standard curve derived R^2 values as seen in Figure 3.10.

Mass C3G (ng)	Standard (\diamond) (% of standard)	Ext 1 (\square) (% of standard)	Ext 2 (Δ) (% of standard)	Ext 3 (\times) (% of standard)	Mean Extraction Efficiency
50	100	66.0	72.4	66.2	68.2
100	100	75.0	81.6	69.7	75.4
200	100	74.5	74.6	53.4	67.5
400	100	74.4	72.4	68.1	71.6
800	100	69.6	77.4	64.2	70.4

Mean extraction efficiency 70.7%.

HPLC retention time drift < 6 s over 15 injections.

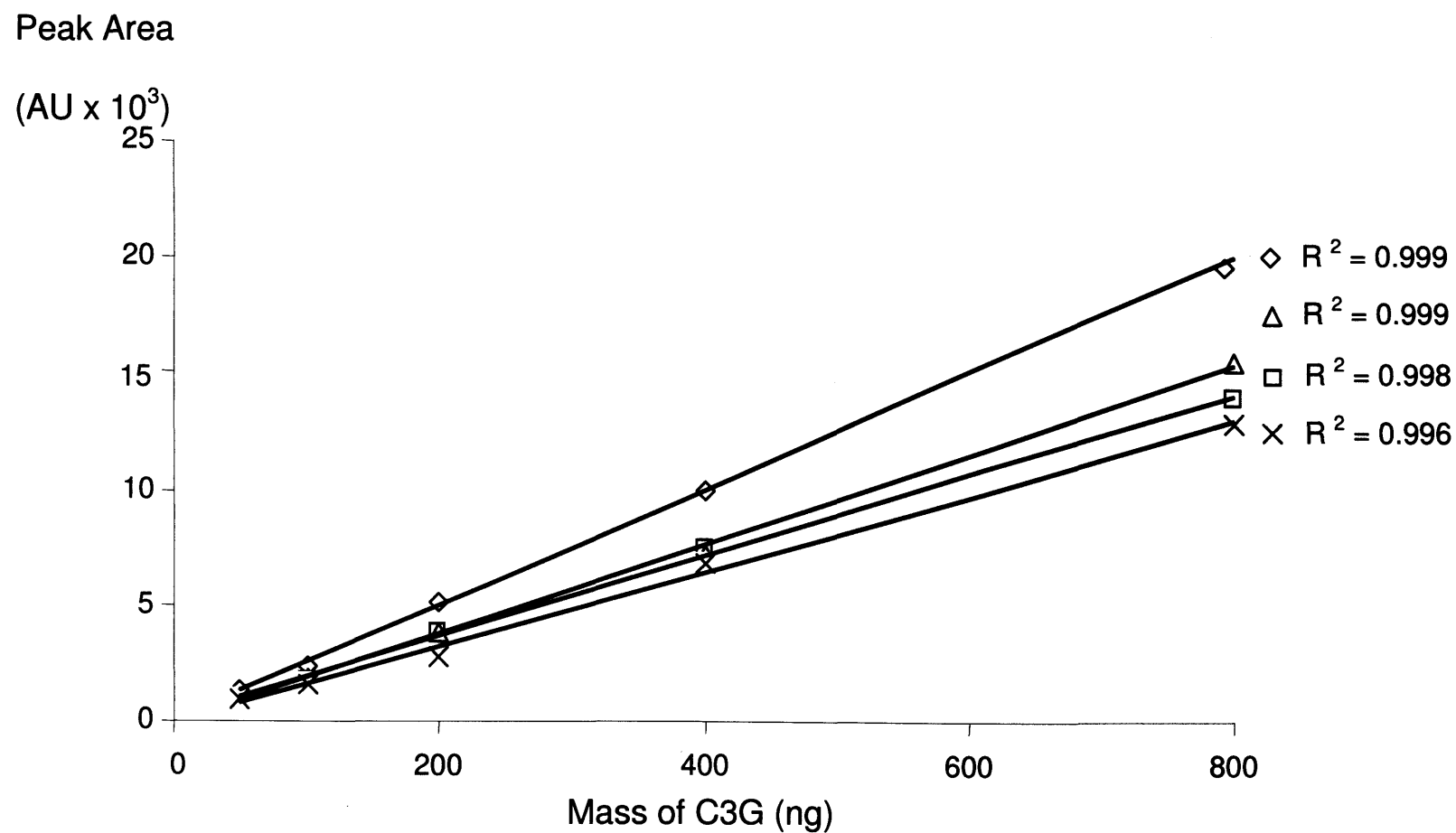


Figure 3.5: Standard curve of - ◇ Unextracted standards, △ Ext 2, □ Ext 1 and × Ext 3 from Table 3.3 . R² values shown in legend as a measure of linearity.

3.4.3 Validation of SPE and HPLC-Vis Methods for Extraction and Measurement of Mirtoselect

Utilising the SPE method described above, with spiked human plasma samples, afforded extraction efficiencies for bilberry anthocyanins averaging 91%. The range of extraction efficiencies was calculated for each Mirtoselect component and varied from 65% for peonidin-3-glucoside to 102% for malvidin-3-glycosides. These recoveries are in agreement with previously published data (Mazza *et al.*, 2003). Mazza *et al.*, using a SPE method, retrieved 70-84% of blueberry anthocyanins from human serum (1.5 ml). Although the method described here has no advantage over the earlier method (Mazza *et al.*, 2003) with respect to recovery, it is considerably more rapid, when comparing the evaporation of 7 ml of methanol used to elute anthocyanins in the earlier paper, with the evaporation of 300 μ L of acetone in the SPE method. When the anthocyanins from Mirtoselect were extracted by SPE and reconstituted for analysis by HPLC, the resultant chromatograms showed no discernible differences in terms of anthocyanin peaks between the Mirtoselect standard and the SPE eluent. Hence, the SPE method did not introduce any significant bias in terms of extraction efficiency for any individual anthocyanins.

The HPLC method employed here for the separation of Mirtoselect was capable of resolving 15 anthocyanins within a run time of 15 min (Figure 3.7). The retention time of C3G (4.6 min) was characterized by a coefficient of variation of 1.23% (based on 10 injections; Table 3.4). In 10 repeated injections of Mirtoselect, the retention times of the individual anthocyanins had coefficients of

variation between 0.33 and 1.68%, and their retention indices, as compared with C3G, displayed coefficients of variation between 0.19 and 1.15% (Table 3.4). Analysis of spiked human plasma (1 ml) furnished limits of detection and quantitation of 0.5 and 1.5 ng/ml (1 and 3 nM), respectively, assuming equal absorbance to C3G. Extraction from spiked urine or aqueous solution gave LOD and LOQ values of 0.25 and 1.0 ng/ml (0.5 and 2 nM), respectively. These numbers suggest good sensitivity when compared to previously published methods for the extraction of anthocyanins from bilberry (Nyman *et al.*, 2001). The LOD and LOQ values determined here for urinary anthocyanins are comparable to those described before for anthocyanins ingested with foodstuffs other than bilberries (Frank *et al.*, 2003 and Talavéra *et al.*, 2005).

Table 3.4: Repeatability of Retention Time (t_R) and Retention Index (i_R) relative to C3G for anthocyanins in the standardized bilberry extract Mirtoselect.

Peak No	Anthocyanin	$t_R \pm SD$ (min)	C_V %	$i_R \pm SD$	C_V %
Single Compound					
5	cyanidin-3-glucoside	4.64±0.06	1.23	n/a	n/a
Bilberry Extract					
1	delphinidin-3-galactoside	3.01±0.04	1.30	0.65±0.00	0.68
2	delphinidin-3-glucoside	3.40±0.05	1.34	0.74±0.00	0.52
3	cyanidin-3-galactoside	3.94±0.05	1.28	0.86±0.00	0.22
4	delphinidin-3-arabinoside	4.20±0.06	1.39	0.91±0.00	0.19
5	cyanidin-3-glucoside	4.60±0.06	1.28	1.00±0.00	0.00
6	petunidin-3-galactoside	5.29±0.06	1.08	1.15±0.01	0.78
7	cyanidin-3-arabinoside	5.47±0.06	1.04	1.19±0.01	0.38
8	petunidin-3-glucoside	6.09±0.07	1.19	1.32±0.01	0.53
9	peonidin-3-galactoside	6.89±0.12	1.68	1.50±0.02	1.14
10	petunidin-3-arabinoside	7.42±0.08	1.06	1.61±0.01	0.78
11	peonidin-3-glucoside	8.21±0.06	0.74	1.78±0.02	0.97
12	malvidin-3-galactoside	8.60±0.05	0.57	1.78±0.02	1.02
13	peonidin-3-arabinoside	9.02±0.04	0.45	1.96±0.02	1.07
14	malvidin-3-glucoside	9.34±0.04	0.38	2.03±0.02	1.09
15	malvidin-3-arabinoside	10.0±0.03	0.33	2.18±0.03	1.15

Number of samples (n) = 10; SD, standard deviation; C_V , coefficient of variation (SD/mean) x 100.

4. Effect of Anthocyanins on Colorectal Carcinogenesis in the Apc^{MIN} Mouse

4.1 Introduction

Anthocyanins have been hypothesised to be chemopreventive agents (see 1.4.6 – 1.4.8, Cooke *et al.*, 2005). Work thus far has been limited to *in vitro* experiments with only a few *in vivo* experiments completed (see 1.4.7, Cooke *et al.*, 2005). One study in the Apc^{MIN} mouse model showed no significant effect of anthocyanins on intestinal adenoma formation (Kang *et al.*, 2003). One reason Kang *et al* (2003) may not have seen a significant effect of anthocyanins could be due to the way the mice were dosed. Mice consumed anthocyanins in their drinking water; however, anthocyanins have been shown to be unstable in aqueous solution, especially in the pH range of 3.8 – 8 (Cabrita *et al.*, 2000 and Nielsen *et al.*, 2003a) (Section 1.4.2). Kang *et al* (2003) tried to limit any breakdown by incorporating ascorbic acid (50 mg/l) into the drinking water of all treatments including control. Ascorbic acid is an anti-oxidant, and may have affected adenoma formation thereby masking any decrease caused by anthocyanins. Furthermore, in an orientation experiment conducted here, ascorbic acid at a concentration of 50 mg/l elicited a pH of 3.9, which suggests that the pH in the drinking water containing ascorbic acid might be detrimental for anthocyanin stability. Kang *et al* (2003) did not provide analytical evidence that ascorbic acid helped stabilise anthocyanins, nor did they mention how frequently the water was changed; an important factor in determining what proportion of intact anthocyanin would be available to the mice.

A second study conducted in Apc^{MIN} mice by Bobe *et al* (2006) tried to determine the effect of increasing concentrations of tart cherry extracts on the chemopreventive efficacy of sulindac. The anthocyanin preparation was an extract from the same species of tart cherry used by Kang *et al* (2003). All groups received sulindac in the diet (100 mg/kg) (including controls). Sulindac has previously been shown to inhibit tumorigenesis in the Apc^{MIN} mouse (Bobe *et al.*, 2006). Co-administration of sulindac with increasing doses of tart cherry extracts was used to determine if there was a greater decrease in adenoma number with anthocyanin co-intervention than with sulindac alone. Bobe *et al* observed significant decreases in adenoma number with anthocyanin intervention, although this effect was not dose-dependent. Also with each group (including control) receiving sulindac, it is unclear to what extent the anthocyanins contributed to the overall inhibition of tumorigenesis.

In the two studies in Apc^{MIN} mice described above there has been a lack of clarity as to the role anthocyanins may have played in preventing tumorigenesis. To improve understanding, an efficacy study was undertaken to determine the effect of anthocyanins administered with the diet. In this experiment, the hypothesis was tested that either Mirtoselect, a standardised blueberry extract containing a mixture of 15 anthocyanins, or C3G alone affect gastrointestinal carcinogenesis in Apc^{MIN} mice. Initially, in a preliminary experiment at a single dose level, 0.1% (w/w) Mirtoselect (containing ~39% anthocyanins) or C3G were tested. Subsequently, the study was extended to include a range of doses – 0.03, 0.1 and 0.3% (w/w) in AIN93G diet.

A further hypothesis tested was whether PCV measurement can reflect any effect of anthocyanins on adenoma formation within the G.I. tract of Apc^{MIN} mice (see section 2.4.5).

Anthocyanins are strong antioxidants (see section 1.4.8). Therefore, the hypothesis was tested that administration of Mirtoselect or C3G causes a decrease in oxidative DNA adduct levels in gastrointestinal tissue as reflected by immunoslot blot measurement of M1dG.

4.2 Effect of a 0.1% Dietary Dose of Anthocyanins on Adenoma Development in Apc^{MIN} Mice

Four-week-old weanling Apc^{MIN} mice were randomly assigned to control and intervention groups to receive either standard AIN93G diet or AIN93G diet supplemented with Mirtoselect or C3G (0.1%) from weaning until animals were 16 weeks old. Group size was n = 12, with equal gender distribution. At the end of the experiment mice were exsanguinated, the small intestine and colon were removed, and the small intestine divided into 3 approximate sections – proximal, medial and distal. Adenomas were counted and graded on the basis of their diameter. The groupings used were < 1 mm, 1 – 3 mm and > 3 mm. Figure 4.1 shows the mean adenoma number for all mice in each group (n = 12). The mean adenoma number for control, Mirtoselect and C3G groups were 62, 42 and 51, respectively. The effect of Mirtoselect was statistically significant.

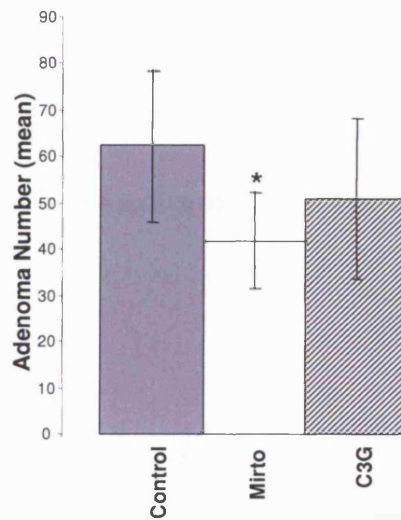


Figure 4.1: Effect of Mirtoselect or C3G (0.1% in the diet) on total numbers of intestinal adenomas in Apc^{MIN} mice, male and female data combined. Control mice received standard AIN 93G diet. Values are the mean \pm SD (n = 12 per group). Star indicates value is significantly different from control, * = $p < 0.001$.

PCV, was used to determine the extent of intestinal bleeding. The PCV (Figure 4.2) showed no significant differences.

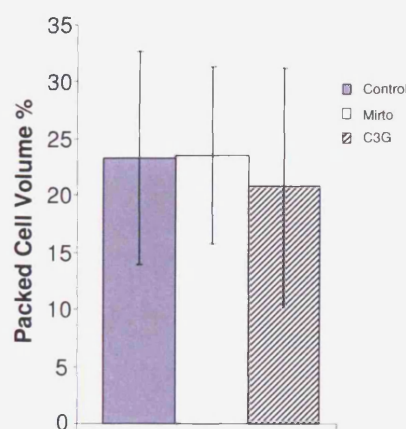


Figure 4.2: Lack of effect of Mirtoselect or C3G (0.1% in the diet) on mean packed cell volume. Control mice received standard AIN93G diet. Values are the mean \pm SD (n = 12 per group).

When analysing the intestinal tract as a whole (Figure 4.3) it is clear that adenomas < 1 mm in diameter showed the biggest decrease with intervention. Mirtoselect and C3G significantly decreased adenoma formation with a value of $p < 0.002$ and 0.01 , respectively. Adenomas with a diameter of 1 – 3 mm showed a decrease with Mirtoselect treatment, but this was not significant ($p < 0.066$).

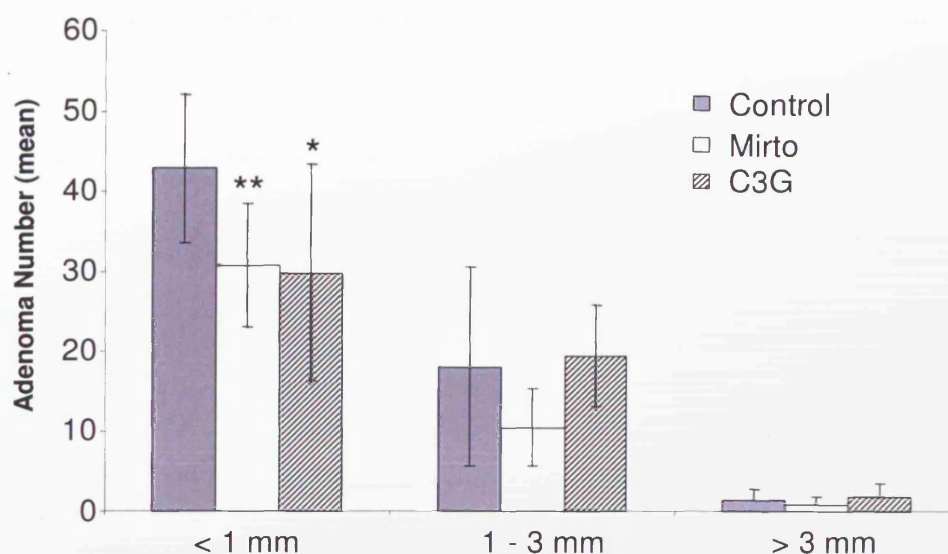


Figure 4.3: Effect of Mirtoselect and C3G (0.1% in the diet) on number and size of adenomas. Values shown are the mean \pm SD ($n = 12$ per group) of all intestinal sections combined (proximal, medial and distal small intestines and colon). Significant differences to control are highlighted with a star, $* = p < 0.011$, $** = p < 0.002$. Mirtoselect had an approaching significance effect on the growth of adenomas in the 1 - 3

Figure 4.4 shows the number; size and distribution of adenomas in the intestinal tract of the Apc^{MIN} mice fed either control diet, Mirtoselect or C3G. The colon had the lowest number of adenomas, consistent with what is known about the

Apc^{MIN} mouse model (see section 1.2.2). The largest effect of intervention was observed for the < 1mm size adenomas, which is the most abundant size of adenoma throughout the small intestine. C3G significantly reduced adenoma formation in the proximal region for < 1 mm adenomas ($p < 0.002$), with Mirtoselect approaching significance with $p < 0.066$. There was no other significant decrease in adenoma number within the proximal region of the intestine. Adenoma number in the medial region was decreased the most with a significant decrease in number of adenomas of < 1 mm size number for Mirtoselect and C3G. For Mirtoselect a significant difference within the medial region was also observed for the 1 – 3 mm adenoma size.

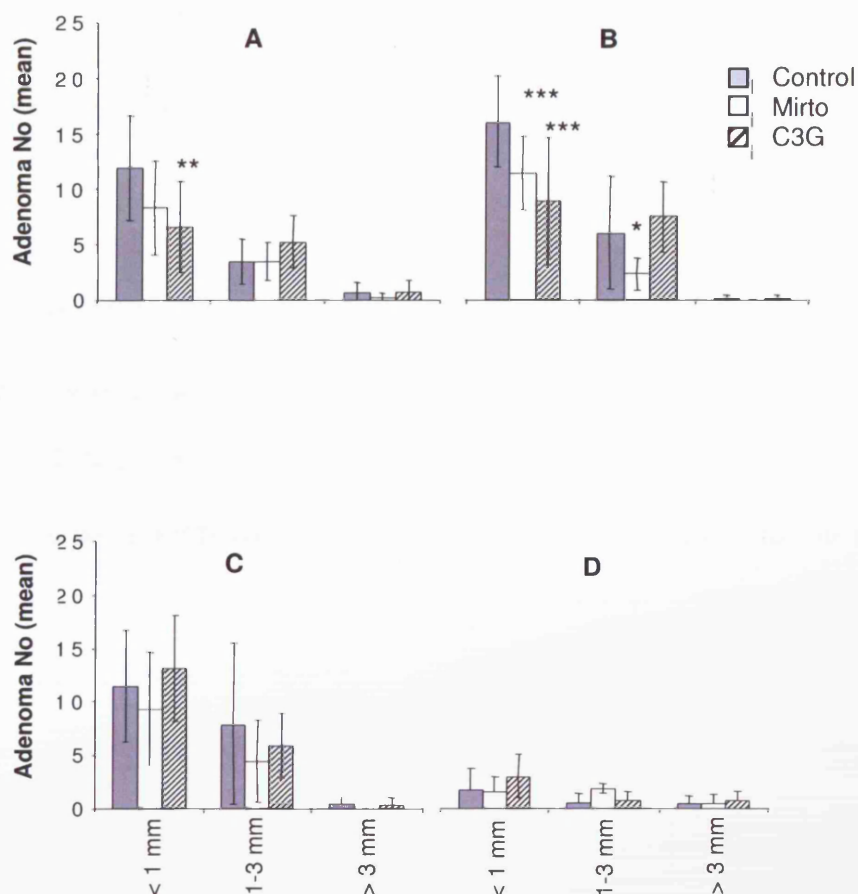


Figure 4.4: Effect of Mirtoselect and C3G at a dietary concentration of 0.1% on number and size of adenomas compared with control animals. The proximal (A), medial (B) and distal (C) are equal divisions trisecting the small intestine. The colon (D) is the remaining part of the gut, below the caecum. Adenomas from Apc^{MIN} mice were counted and graded by size. Values are mean \pm SD (n = 12 per group). Significant differences to control are highlighted with a star, * p < 0.03, ** p < 0.007 and *** p < 0.001.

4.3 Effect of Different Doses of Anthocyanins on Adenoma Development in Apc^{MIN} Mice

4.3.1 Mirtoselect

Since Mirtoselect when given in the diet at 0.1% had resulted in a significant decrease in adenoma number, a repeat study was conducted in which three dietary doses were employed: 0.03, 0.1 and 0.3% to investigate the possibility of a dose response. A dose-dependent decrease in adenoma number was observed with increasing dietary anthocyanins (Figure 4.5). The mean adenoma number per mouse for the control, 0.03, 0.1 and 0.3% Mirtoselect groups were 61, 56, 47 and 40, respectively.

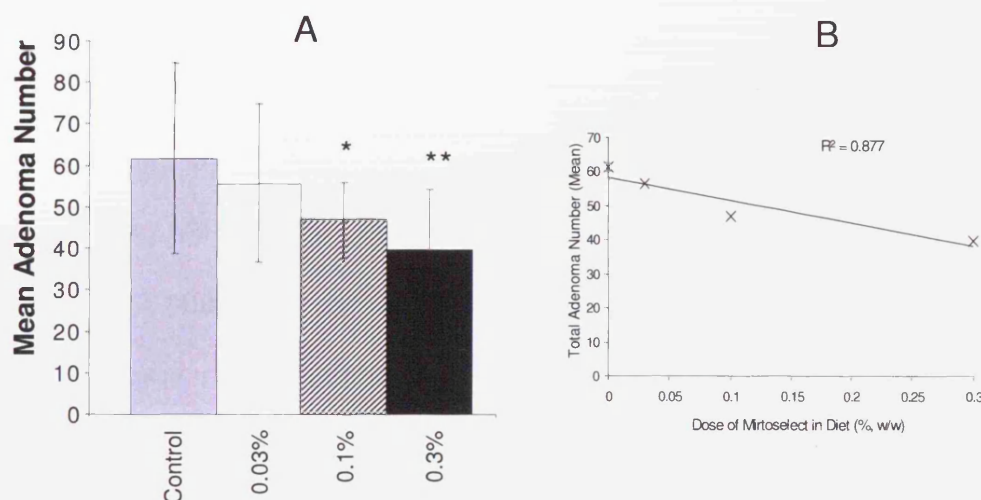


Figure 4.5: (A) Effect of Mirtoselect at three dietary concentrations (0.03, 0.1 and 0.3%) on total numbers of intestinal adenomas in Apc^{MIN} mice. Control mice received standard AIN93G diet. Values are mean \pm SD ($n = 16$ per group). Significant differences to control are marked with a star, $* = p < 0.029$ and $** = 0.003$. (B) An inverse correlation between adenoma number and dose was demonstrated by least mean square analyses – $R^2 = 0.877$.

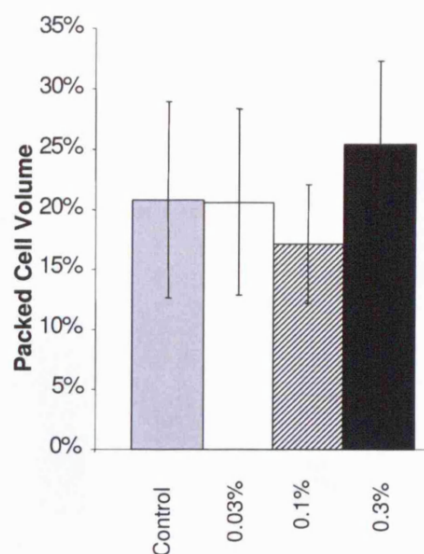


Figure 4.6: Lack of effect of Mirtoselect at three dietary concentrations (0.03, 0.1 and 0.3%) on mean PCV. Control mice received standard AIN93G diet. Values are mean \pm SD (n = 16 per group).

PCV showed no significant difference for any concentration of Mirtoselect.

Figure 4.7 shows the number and size of adenomas in the intestinal tract of mice consuming Mirtoselect. Significant differences compared to control were observed for 0.1 and 0.3%, with adenomas less than 1 mm in diameter. As with the previous study, most adenomas were in the smaller than 1 mm category. A minor increase in adenoma number was observed at 0.03% in the 1 – 3 mm size range, but this was not significant.

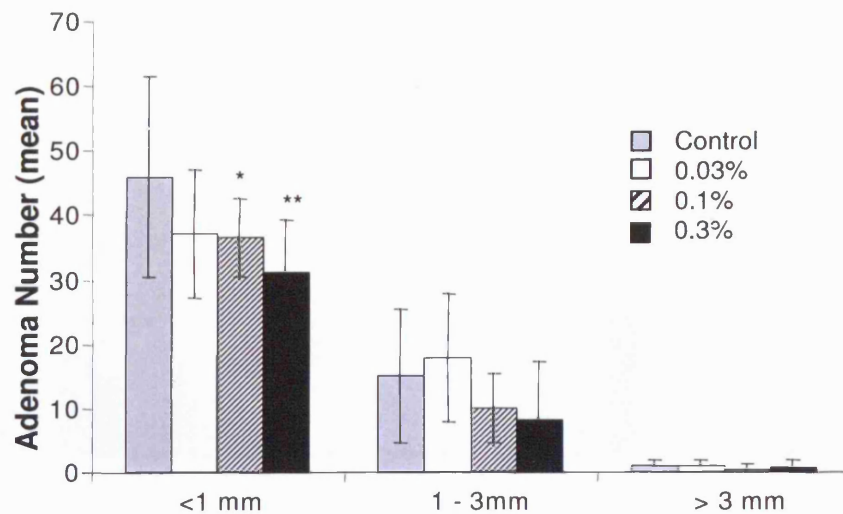


Figure 4.7: Effect of Mirtoselect at three dietary concentrations (0.03, 0.1 and 0.3%) on number and size of adenomas throughout the entire intestine (proximal, medial and distal small intestine and colon combined). Data shown is the mean \pm SD ($n = 16$ per group). Significant differences to control are marked with a star, * = $p < 0.035$ and ** = $p < 0.002$. Mirtoselect had an almost significant dose response on the growth of adenomas in the < 1 mm range, with $p < 0.063$ for 0.03% Mirtoselect.

Figure 4.8 shows the effect of Mirtoselect intervention on adenoma numbers and size in the four regions of the gastrointestinal tract. The proximal region (Figure 4.8A) showed a dose-dependent decrease at all adenoma sizes. Significant differences were observed for adenomas of < 1 mm diameter for the 0.1 and 0.3% doses and in the 0.3% intervention group for adenomas of 1 – 3 mm diameter. In the medial section of the intestine the 0.3% dose was the only intervention that showed a significant decrease ($p < 0.036$, Figure 4.8B). No other significant reduction in adenoma number was observed for any Mirtoselect treatment.

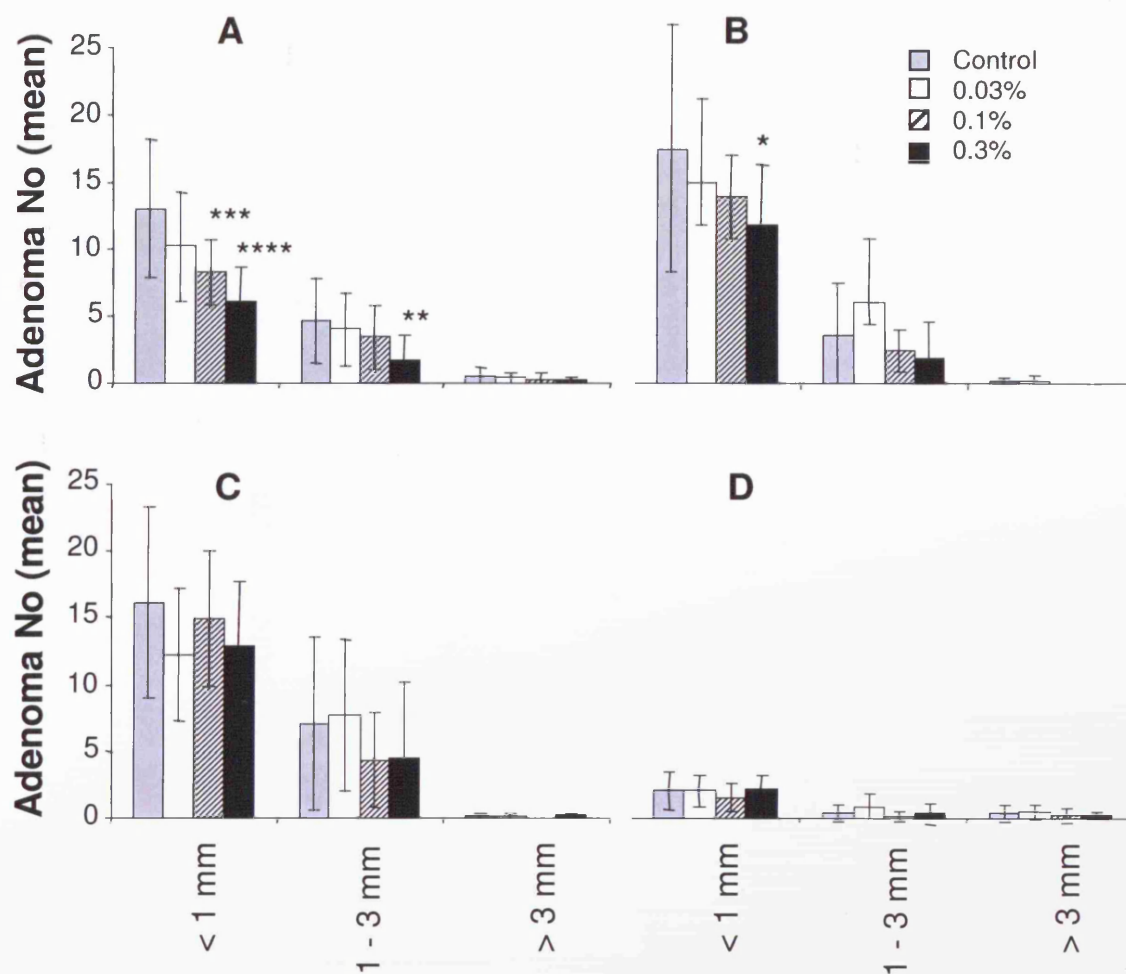


Figure 4.8: Effect of Mirtoselect at three dietary concentrations (0.03, 0.1 and 0.3%) on number and size of adenomas in the Apc^{MIN} mouse compared with control animals. The proximal (A), medial (B) and distal (C) are equal divisions trisecting the small intestine. The colon (D) is the remaining part of the gut, below the caecum. Adenomas were counted and graded by size. Values are mean \pm SD ($n = 16$ per group). Significant differences to control are highlighted by a star, * = $p < 0.036$, ** $p = < 0.004$, *** $p = < 0.002$ and **** = $p < 0.001$.

Figure 4.9 shows the effect of Mirtoselect on tumour burden (see section 2.4.4 for calculation) in the Apc^{MIN} mouse. Significant decreases were observed for both 0.1 and 0.3% dosage groups ($p < 0.05$).

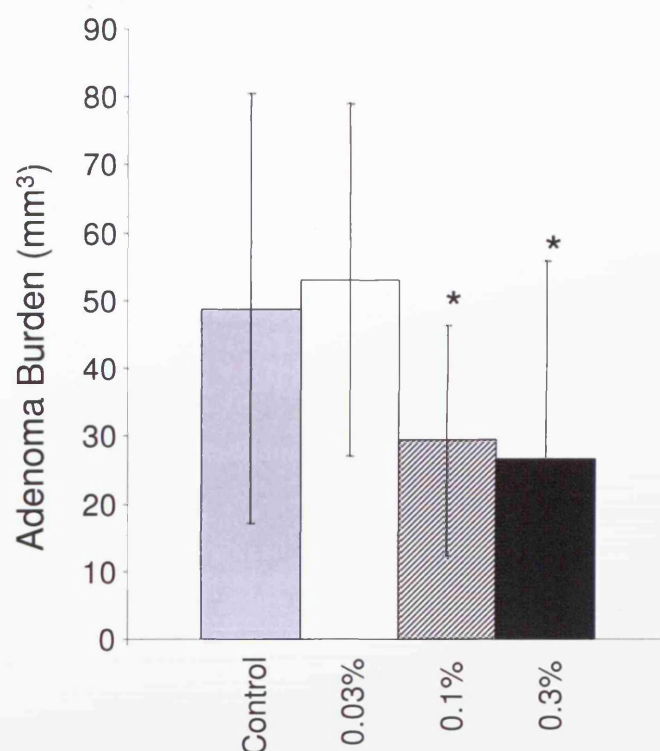


Figure 4.9: Effect of Mirtoselect at three dietary concentrations (0.03, 0.1 and 0.3%) on tumour burden in the Apc^{MIN} mouse intestine. Tumour burden is a function of hemi-spherical adenoma volume (intestinal adenomas) or spherical adenoma volume (colonic adenomas) and number (see section 2.4.4 for method of calculation). Values are the mean \pm SD of $n = 16$. Significant differences to control are marked with a star, * = $p < 0.05$.

4.3.2 Cyanidin-3-Glucoside (C3G)

In the second part of the multiple dose study C3G was tested as an intervention at the same range of doses as those used with Mirtoselect. Figure 4.10 shows the dose response observed with C3G treatment. Significant decreases were observed at both 0.1 and 0.3%. This data closely resemble that seen for Mirtoselect.

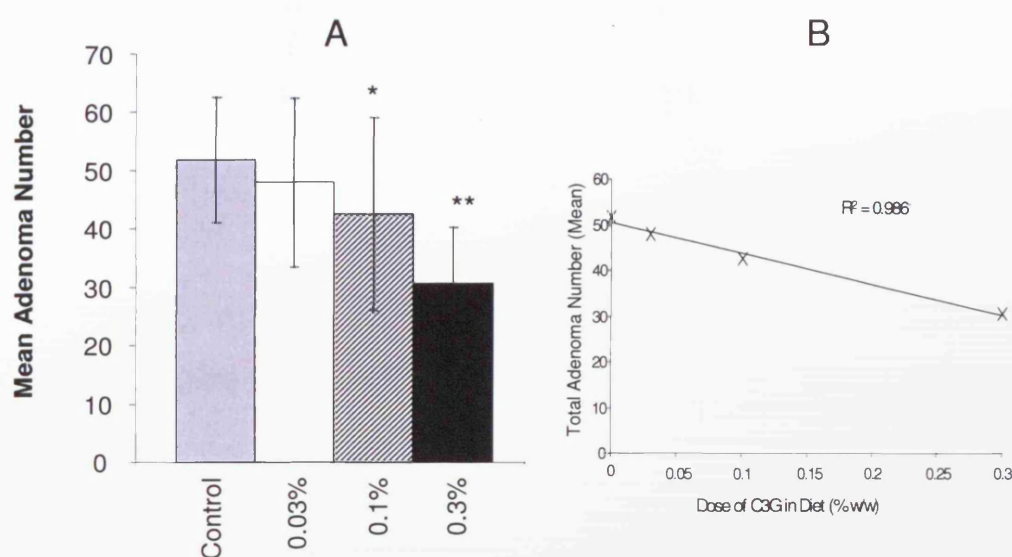


Figure 4.10: (A) Effect of C3G at three dietary concentrations (0.03, 0.1 and 0.3%) on total numbers of intestinal adenomas in Apc^{MIN} mice. Control mice received standard AIN93G diet. Values are mean \pm SD ($n = 16$ per group). Significant differences to control are marked with a star, * = $p < 0.017$ and ** = $p < 0.001$. (B) An inverse correlation between adenoma decrease and dose was demonstrated by least mean square analyses – $R^2 = 0.986$.

PCV data (Figure 4.11) did not show an effect of intervention.

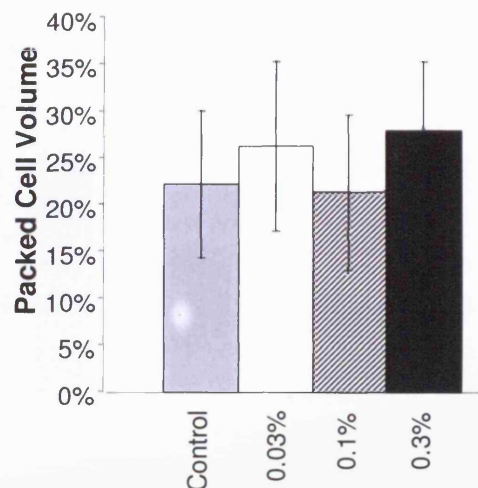


Figure 4.11: Lack of effect of C3G at three dietary concentrations (0.03, 0.1 and 0.3%) on mean PCV. Control mice received standard AIN93G diet. Values are mean \pm SD (n = 16 per group).

Figure 4.12 shows the effect of C3G intervention on adenoma number and size in the gastrointestinal tract of the Apc^{MIN} mouse. A dose-dependent decrease was observed for all adenoma sizes. Significant decreases were observed for < 1 mm adenomas with the 0.1% and 0.3% dose. For the adenomas which were > 3 mm in size there is an almost significant decrease in the 0.3% intervention group ($p < 0.058$).

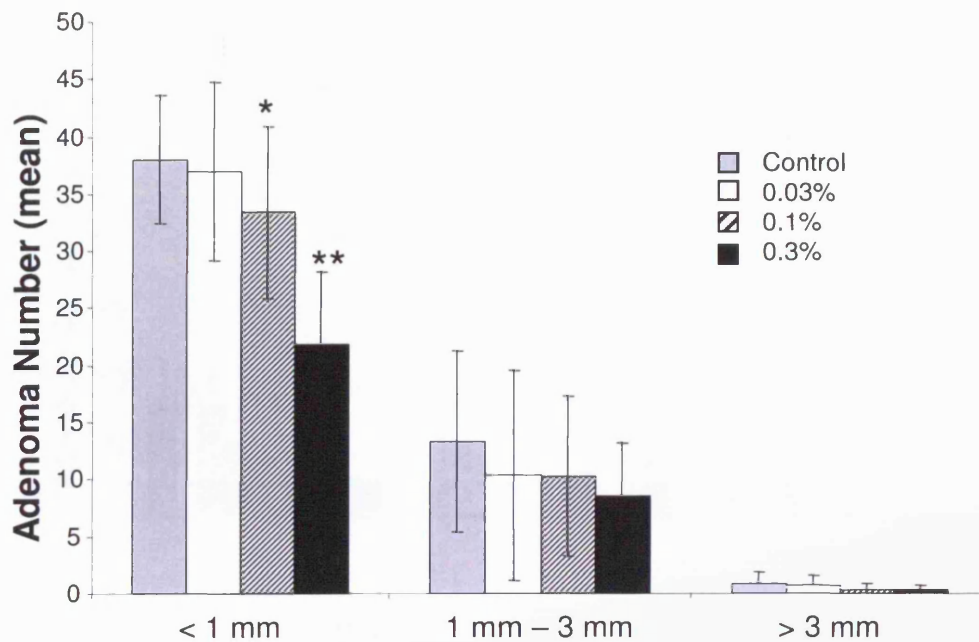


Figure 4.13: Effect of C3G at three dietary concentrations (0.03, 0.1 and 0.3%) on number and size of adenomas throughout the entire intestine (proximal, medial and distal small intestine and colon combined). Data shown are the mean \pm SD ($n = 16$ per group). Significant differences to control are marked with a star, * = $p < 0.035$ and ** = $p < 0.001$. For adenomas > 3 mm in diameter the difference in adenoma number between the 0.3% dose group and the control group approached significance with $p = < 0.058$.

In the individual sections of the intestinal tract (Figure 4.13) 0.3% C3G was the only dose to elicit a significant difference in all areas of the small intestine, with respect to the control group – most notably in the medial section of the intestine, in the adenoma size group < 1 mm (Figure 4.13B). The dose of 0.1% did show a significant decrease to control, but only in the distal region (Figure 4.13C).

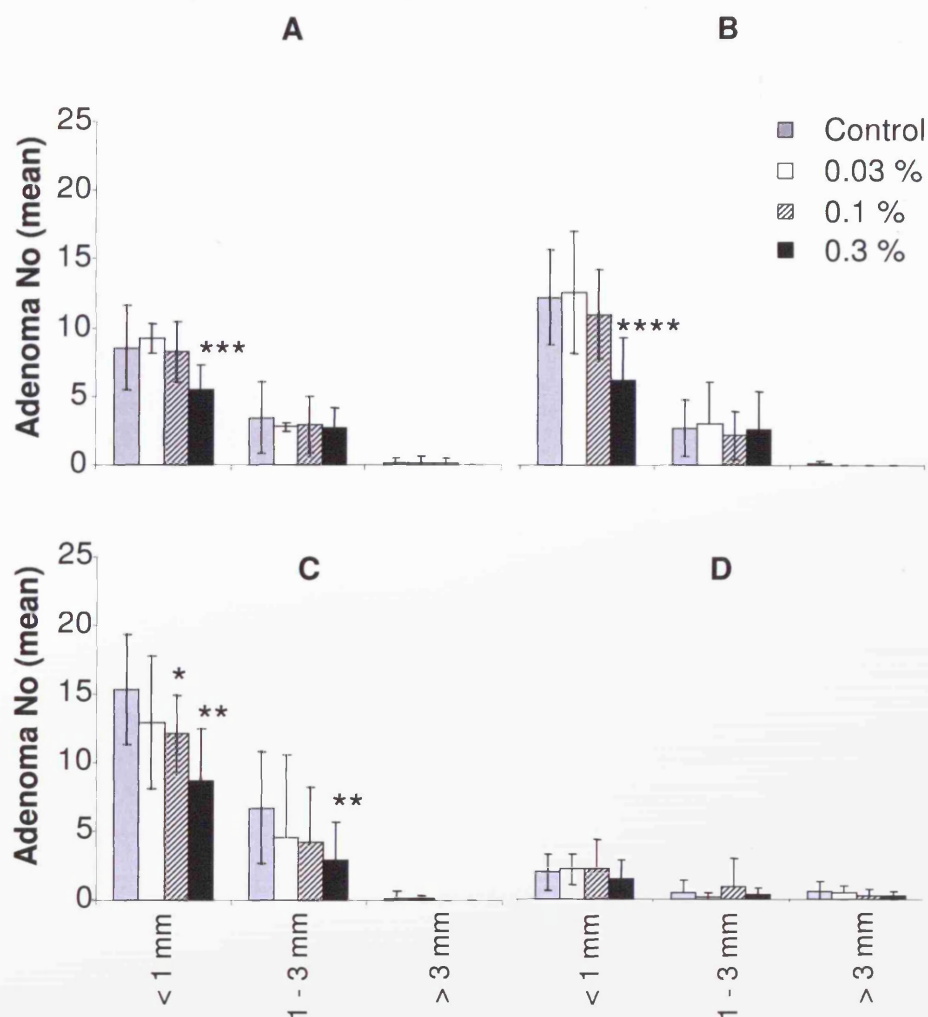


Figure 4.14: Effect of C3G at three dietary concentrations (0.03, 0.1 and 0.3%) on number and size of adenomas in the Apc^{MIN} mouse compared with control animals. The proximal (A), medial (B) and distal (C) are equal divisions trisecting the small intestine. The colon (D) is the remaining part of the gut, below the cecum. Adenomas were counted and graded by size. Values are mean \pm SD ($n = 16$ per group). Significant differences to control are marked with a star, * = $p < 0.017$, ** $p = < 0.006$, *** $p = < 0.003$ and **** = $p < 0.001$.

Figure 4.14 shows the effect of C3G on tumour burden (see 2.4.4 for calculation) in the Apc^{MIN} mouse. A significant decrease was observed for both the 0.1 and 0.3% dosage groups ($p < 0.042$ and < 0.016 , respectively).

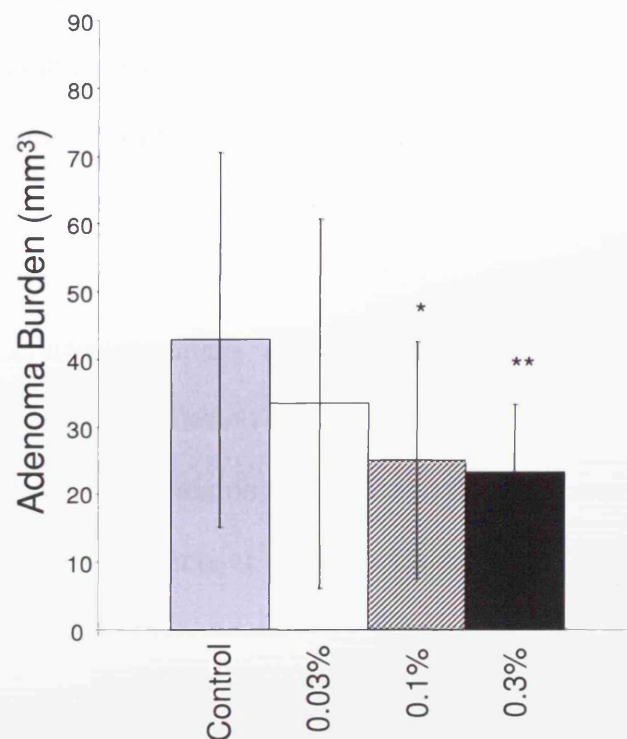


Figure 4.15: Effect of C3G at three dietary concentrations (0.03, 0.1 and 0.3%) on tumour burden in the Apc^{MIN} mouse intestine. Tumour burden is a function of hemi-spherical adenoma volume (intestinal adenomas) or spherical adenoma volume (colonic adenomas) and number (see section 2.4.4 for method of calculation). Significant differences to control are marked with a star, * = $p < 0.042$ and ** = $p < 0.016$. Values shown are mean \pm SD of $n = 16$.

4.4 Modulation of M1dG Adduct Levels in Colorectal Adenomas by Anthocyanins

Assessment of M1dG adduct levels was achieved by immunoslot blot of adenoma DNA as described in section 2.7. The first reading taken of the blot utilises chemiluminescence. Chemiluminescence is generated by enzymatic catalysis of the reaction between luminol, its enhancer, and hydrogen peroxide by horseradish peroxidase. The horseradish peroxidase is conjugated to the secondary antibody bound to the blot. The reaction emits light in proportion to the M1dG concentration, which is measured by an imaging system. To determine whether equal loading has taken place the blot is washed with propidium iodide (PI), which stains all DNA equally. UV light illuminates the PI, and the resultant fluorescence is used to determine total amounts of bound DNA. The mean of all PI-stained sites is determined, and a ratio calculated for each individual slot blot. The ratio obtained for each slot is then divided by its equivalent chemiluminescent reading to account for variations in the amount of DNA bound.

For each blot a standard curve was completed to allow quantitation of adduct levels in the experimental samples. Figure 4.15 shows an example blot for standards, before and after equal loading with PI (see section 2.7.3). Note in Figure 4.15 the 0 fmol/ μ g concentration generates a measurable reading. This means that the calf thymus DNA used contains measurable levels of substances reacting with the anti-M1dG antibody.

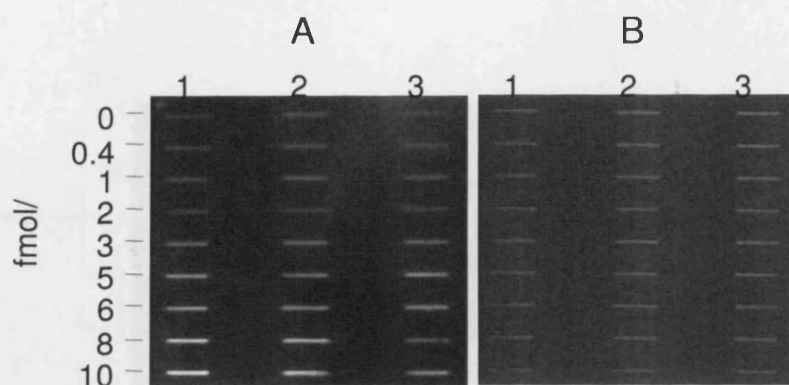


Figure 4.16: M1dG immunoslot blot standard curve completed as described in 2.7.3. Adduct concentrations shown per μg of loaded DNA, in triplicate. (A) is the chemiluminescence image captured after loading the secondary antibody and (B) is a transilluminated blot loaded so as to equalise PI concentration

On the same blot as the standard curve, DNA from control mice and DNA from mice on intervention (C3G or Mirtoselect) were included, an example is shown in Figure 4.16.

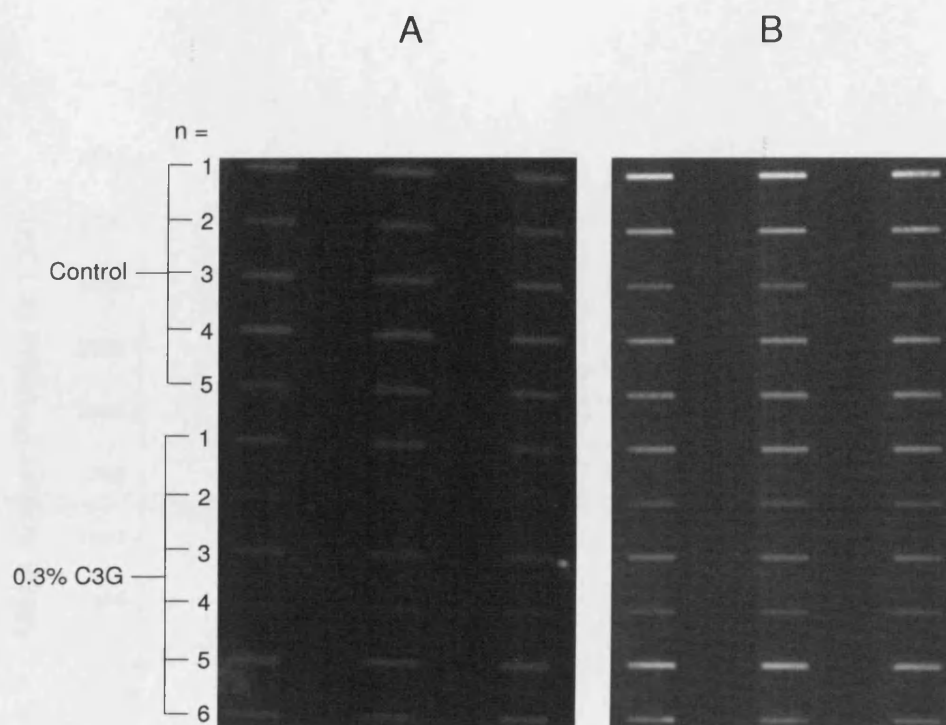


Figure 4.17: An example of an immuno-slot blot of DNA extracted from adenoma tissue from the small intestine of Apc^{MIN} mice. M1dG adduct levels in DNA from mice receiving control diet and 0.3% C3G diet are shown. (A) is the chemiluminescence image captured after loading the secondary antibody and (B) is a transilluminated blot loaded so as to equalise PI concentration. Numbers denote individual mice.

Utilising methods described in 2.7.3 standard curves were calculated and used to determine M1dG concentration in experimental samples. Figure 4.17 shows an example of a standard curve, with the proportional amounts for zero subtracted from each point (see 2.7.3).

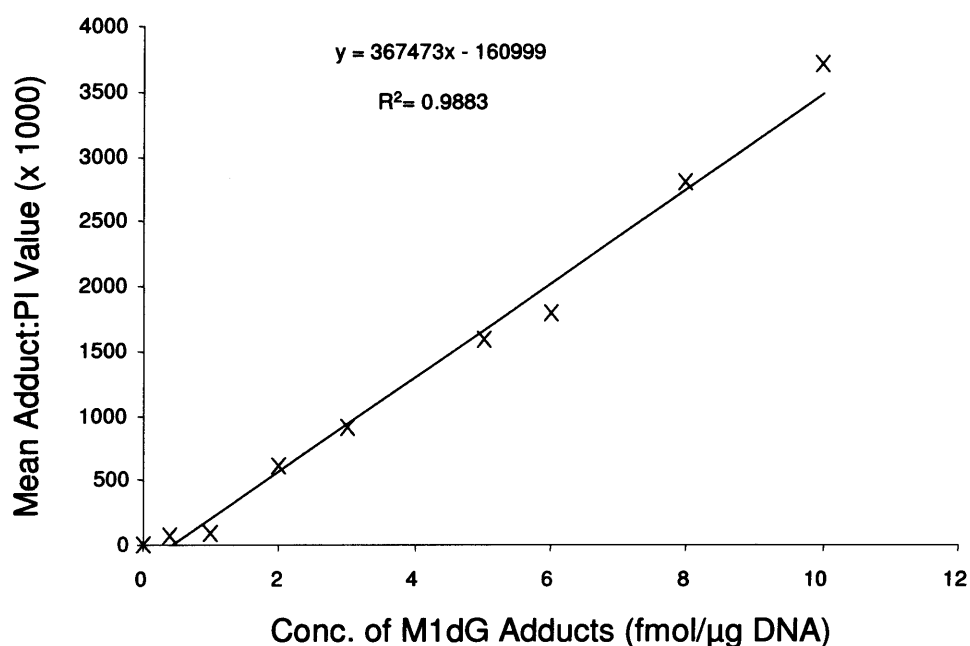


Figure 4.18: An example of a standard curve for the quantitation of M1dG adduct levels. Standard curve derived using methods described in 2.7.3 with malondialdehyde (MDA)-treated calf thymus DNA (10 fmol adduct per μg DNA) and control calf thymus DNA.

Due to limitations of the experimental technique it was not possible to complete the analysis of all samples simultaneously. As a result, variation in recorded values was observed between runs for the same tissue. To minimise this variation the data was calculated as a percentage of the control value for the same blot. Figure 4.18 shows the effect of treatment on M1dG adduct formation as a percentage of control.

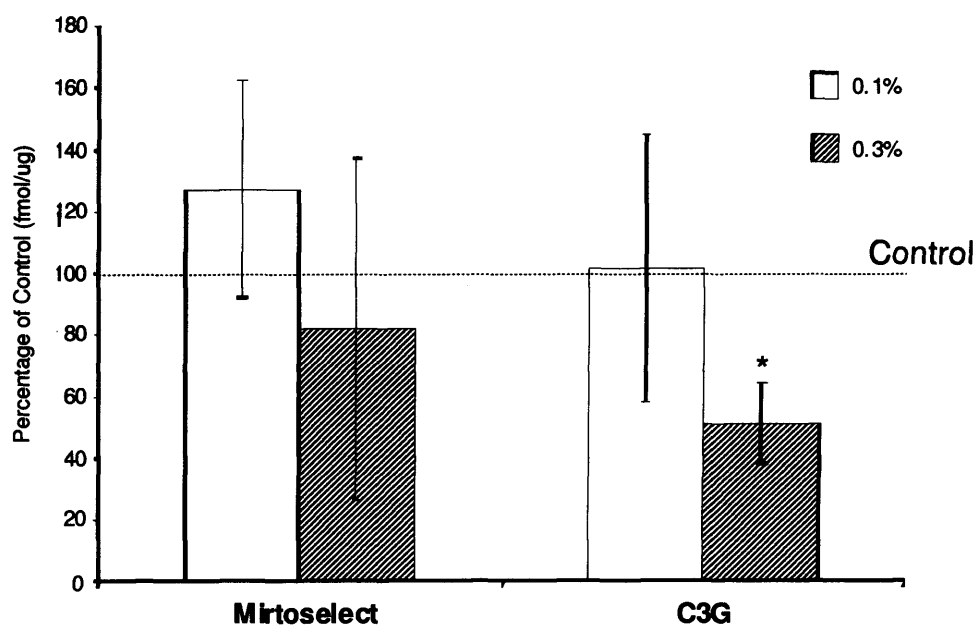


Figure 4.19: Effect of Mirtoselect or C3G at 0.1 and 0.3% in the diet, on M1dG adduct formation in adenoma tissue of the Apc^{MIN} mouse. Values are calculated as a percentage of the mean of a same-blot control value. Significant differences are marked with a star (* = $p < 0.036$). The dotted line signifies the mean concentration of M1dG adduct levels observed in control tissue (100%). For Mirtoselect at the 0.1 and 0.3% doses $n = 13$ and 6 , respectively, for C3G 0.1 and 0.3% $n = 13$ and 11 , respectively. The lower number of animals is due to rejection of the DNA in some cases because of low purity as measured by UV spectroscopy (see 2.7.2).

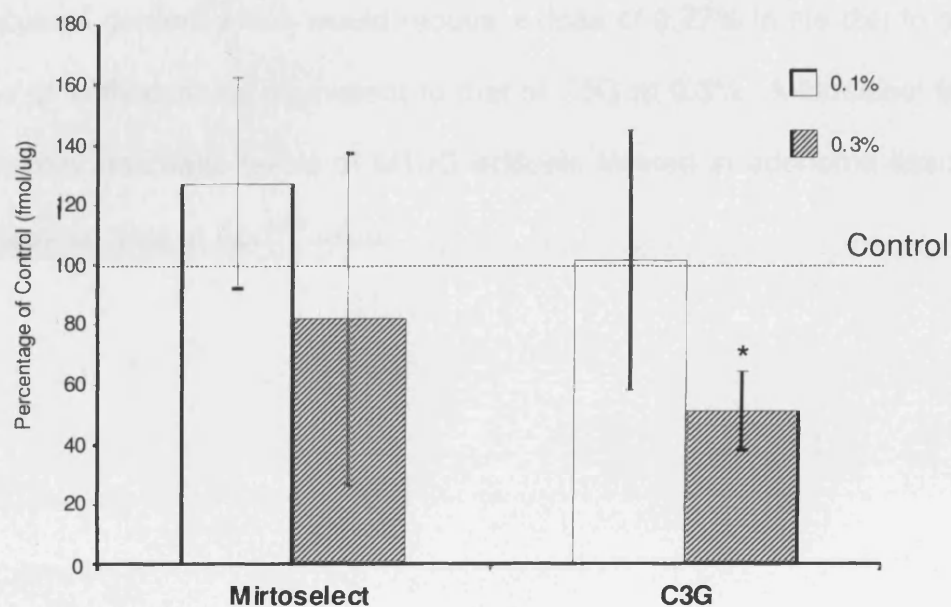


Figure 4.19: Effect of Mirtoselect or C3G at 0.1 and 0.3% in the diet, on M1dG adduct formation in adenoma tissue of the Apc^{MIN} mouse. Values are calculated as a percentage of the mean of a same-blot control value. Significant differences are marked with a star (* = $p < 0.036$). The dotted line signifies the mean concentration of M1dG adduct levels observed in control tissue (100%). For Mirtoselect at the 0.1 and 0.3% doses $n = 13$ and 6 , respectively, for C3G 0.1 and 0.3% $n = 13$ and 11 , respectively. The lower number of animals is due to rejection of the DNA in some cases because of low purity as measured by UV spectroscopy (see 2.7.2).

C3G at 0.3% elicited a significant decrease in M1dG adduct formation in adenoma tissue of Apc^{MIN} mice. Mirtoselect at 0.3% also showed a decrease of M1dG from control, but values were compromised by a much larger standard deviation. It must be remembered that the Mirtoselect mixture used is ~39% anthocyanin content which would require a dose of 0.77% in the diet to achieve a dose of anthocyanins equivalent to that of C3G at 0.3%. Mirtoselect failed to significantly decrease levels of M1dG adducts formed in adenoma tissue from the intestinal tract of Apc^{MIN} mice.

4.5 Discussion

The results described above show that both Mirtoselect and C3G significantly decrease adenoma formation in the small intestine of Apc^{MIN} mice. Significant decreases in total adenoma number and tumour burden were observed for the 0.1 and 0.3% treatments, but 0.03% in the diet was too low to elicit a significant effect. A dose-dependent decrease was observed.

These results are the first to directly relate anthocyanins, as either a single compound or a mixture, with a significant decrease in adenoma formation in the Apc^{MIN} mouse. Previously, Kang *et al* have studied anthocyanins and their effect on intestinal carcinogenesis in the Apc^{MIN} mouse. Although their study (Kang *et al.*, 2003) showed a significant decrease on caecal adenoma number with anthocyanin intervention, intestinal adenoma formation was unaltered. Kang *et al* used doses of 2.4, 0.6 and 600 mg/mouse/day for anthocyanins, cyanidin aglycon and tart cherry extracts, respectively (assuming a 20g mouse eats 3 g/day and drinks 3 ml/day). As mentioned in the introduction (section 4.1) Kang *et al* administered anthocyanins in the drinking water, and attempted to limit decomposition by using ascorbic acid. As a result consumed doses may be lower than those calculated. In contrast with the doses used by Kang *et al* the dietary doses of C3G used in our studies were 1, 3 and 9 mg/mouse/day for the 0.03, 0.1 and 0.3% doses, respectively. Therefore, C3G given at 0.1% would give a similar dose of anthocyanins compared to that used by Kang *et al*, and in our experiments resulted in a significant decrease in both adenoma number and burden. The doses of anthocyanins fed to mice with Mirtoselect were 0.4, 1.1 and 3.5 mg/mouse/day. Although in terms of anthocyanin content

the anthocyanin dose in our 0.1% Mirtoselect group was lower than those used by Kang *et al*, it still resulted in a significant decrease in adenoma number. Caecal adenoma levels were not investigated.

Another study conducted by Bobe *et al* (2006) compared the effect of anthocyanins on sulindac-assisted prevention of tumorigenesis. Whilst these data do not give a clear indication of what effect anthocyanins themselves elicited on adenoma formation, it does make clear that anthocyanins extracted from tart cherries improved the chemopreventive ability of sulindac. The doses of tart cherry extract used in this study (1.125, 2.25, 4.5 and 9 mg/mouse/day) constituted 50% anthocyanins, giving a daily anthocyanin dose of 0.57, 1.13, 2.25 and 4.5 mg anthocyanin/mouse/day, similar to the dose used here. There seemed to be no significant dose-dependent effect, and the largest decrease in adenoma number was ~26% achieved by both the lowest and highest dose. In contrast to this result, we observed both a dose-dependent decrease and a ~42% reduction in adenoma number for the 0.3% C3G treated group. Similar to our results, Bobe *et al* (2006) also noted that anthocyanin treatment resulted in a decrease in adenoma number throughout the small intestine, rather than being confined to discrete areas of the intestine.

The PCV data presented here did not mirror the trend of decreased adenoma burden with increasing anthocyanin dose. PCV has previously been shown to be a reliable indicator of intestinal bleeding both with in-house work and as published data (Verschoyle *et al*, 2007) resulting from increasing adenoma burden in the Apc^{MIN} mouse. In this study however an inverse correlation between increasing adenoma burden and PCV was not evident. The reason for

the lack of correlation between PCV and anthocyanin chemoprevention should be investigated further. Potentially, anthocyanins may be interfering with the mechanism of intestinal bleeding associated with tumour burden, and thus skewing the PCV data, or may be preventing or inhibiting tumour angiogenesis. There is also the possibility that we did not see any changes in PCV in relation to adenoma burden because the decrease in larger adenomas, those more likely to bleed, was not as large as the decrease in small adenomas (figures 4.7 and 4.12).

The effect of anthocyanins on oxidative DNA damage, as reflected by levels of M1dG adduct, has not previously been determined *in vivo*. The data presented here suggests that anthocyanins may reduce oxidative DNA damage in Apc^{MIN} mice. Adenoma tissue tested for M1dG adduct formation showed lower levels after Mirtoselect high-dose treatment, and significantly lower levels with high-dose C3G treatment. There were fewer samples tested in the Mirtoselect experiment due to the low purity of some of the extracted DNA samples. Had all samples been available for analysis the end result may have shown a greater reduction in M1dG adduct levels than that shown in Figure 4.18, but this is speculation. When compared as a percentage of same-blot control, both treatments at 0.1% increased the levels of adduct formation, but not in a significant manner, and only marginally for C3G. A study completed by Ramirez-Tortosa *et al* (2001) has related anthocyanins with both increased plasma anti-oxidant capacity and vitamin E deficiency-induced elevations in DNA damage in rats. Other literature reports of the oxidative capacity of anthocyanins mainly consist of *in vitro* experiments (Rice-Evans *et al.*, 1996, Mazza *et al.*, 2002, Nielsen *et al.*, 2003a, Zheng *et al.*, 2003, Olsson *et al.*,

2004, Galvano *et al.*, 2004 and Heo *et al.*, 2005). These studies (see section 1.4.9) compared the anti-oxidative potential of anthocyanins with respect to other anti-oxidants such as ascorbic acid. Examples of such experiments using techniques such as ORAC (Mazza *et al.*, 2002), FRAP (Nielsen *et al.*, 2003a) and TEAC (Nielsen *et al.*, 2003a, Bao *et al.*, 2005, and Borkowski *et al.*, 2005) – have shown that anthocyanins have 2 - 2.5 times the anti-oxidant potential of ascorbic acid (Garcia-Alonso *et al.*, 2004). It is difficult to apply conclusions from these *in vitro* experiments to *in vivo* models. Studies conducted in cells do not take into consideration metabolites formed in the intact organism. Further, the concentrations of anti-oxidant used in most *in vitro* experiments bear little relation to the concentrations which can be achieved in the host organism. With anthocyanins the problem is compounded by the different molecular forms existing at varying pH (see Figure 1.8) (Borkowski *et al.*, 2005). Compartments in the host organism contain regions of differing pH and inter-conversion of anthocyanins due to pH changes may not be rapid. To assess a more complete overview of the *in vivo* oxidative potential of anthocyanins we would need to determine the relative anti-oxidant potential of all conformations of anthocyanins.

Antioxidation may contribute towards a proportion of the mechanisms by which anthocyanins exert chemoprevention, although it is more likely there are other more relevant mechanisms involved (see section 1.4.9). The reduction in M1dG may contribute to a decrease in COX-2 activity, which in turn can reduce the level of oxidative damage. For example, the significant decreases in adenoma number observed for both treatments at 0.1% do not translate into a reduction in M1dG adduct levels at the same dose. Were the levels of

anthocyanins equal between interventions, we might have seen a significant decrease for Mirtoselect at 0.3%, to mimic that seen with C3G.

5. Metabolism and Pharmacokinetics of Anthocyanins in Mice.

5.1 Introduction

The metabolism and kinetics of anthocyanins have been studied mainly in rats (sections 1.4.3 - 1.4.6) with no work conducted in mice to date. The experiments described here were designed to improve on understanding anthocyanin absorption, distribution, metabolism and elimination. The hypothesis was tested that anthocyanins and their metabolites can be measured in blood, urine and tissues of mice that receive C3G or Mirtoselect over an extended period of time. We also tested the hypothesis that anthocyanins are systemically bioavailable when administered orally to mice. The comparison between oral and I.V. routes of dosing was designed to indicate whether anthocyanidins, the aglycons, were generated from anthocyanins in the intestinal mucosa in mice. Finally, we intended to test the hypothesis that administration of anthocyanins gives rise to levels sufficient to exert pharmacological effects, which would then help to predict suitable dosing regimes.

Initially Apc^{MIN} mice received either C3G or Mirtoselect with their diet at a range of dietary doses (0.03, 0.1 and 0.3%, w/w) for 12 weeks (see 5.2). A control group received unaltered AIN93G diet. Each treatment group consisted of 16 mice, with an equal division of gender. This experiment was intended to enable

identification and measurement, by HPLC-Vis, of the steady-state concentration of anthocyanins in plasma, urine, mucosa, liver and kidney.

Further to the feeding study, a comparison of pharmacokinetics following oral and I.V. dosing was performed using male C57BL mice, the background for the Apc^{MIN} strain (see 5.3). Animals were divided into seven groups (n = 3), and were culled 5, 10, 20, 30, 60, 90 and 120 min after receiving 500 mg/kg of C3G by oral gavage. A control group (n = 2) receiving vehicle (water) alone were included in the study. The second part to the experiment involved dosing with 1 mg/kg of C3G by intravenous injection via the tail vein (see 5.4). For this experiment the mice were divided into eight groups (n = 5), and were culled 5, 10, 15, 20, 30, 60, 90 and 120 min after dosing. A control group (n = 2) was also used. For both experiments the same biomatrices were collected: plasma, urine, mucosa, liver, bile, kidney, lung, heart, brain and prostate. Samples were extracted and analysed via HPLC-Vis spectroscopy (see 2.2) and where possible via LC/MS/MS (see 2.2.3).

5.2 Steady State Levels of Anthocyanins in Tissues of Apc^{MIN} Mice Following Intervention with Anthocyanins

Initial analysis of plasma samples was only able to identify low levels of anthocyanins in the 0.3% treatment group when samples were combined. Analysis of the 0.1% treatment showed that even fewer anthocyanins were detectable. Therefore, only tissues obtained from the 0.3% treatment groups for both Mirtoselect and C3G were analysed in depth. The experiment was completed as described in section 2.4.1 for Mirtoselect (see Figure 5.1) and C3G (see Figure 5.2).

5.2.1 Mirtoselect

Figure 5.1 shows the HPLC traces obtained from plasma, urine, mucosa, kidney and liver from Apc^{MIN} mice fed 0.3% Mirtoselect in the diet for 12 weeks. Each sample gave peaks which were not present in the control tissues. Four molecules were found in the plasma of mice receiving Mirtoselect (Fig. 5.1). They were tentatively identified as malvidin glucoside and the galactosides of delphinidin, cyanidin and malvidin on the basis of their retention times, when compared with those of the constituents of authentic Mirtoselect. The highest total anthocyanin plasma content observed in 1 mouse, calculated on the basis of the calibration curve established for C3G was 46 ng/ml, assuming equal absorbance with C3G and all other anthocyanin entities.

In urine and mucosal samples malvidin glycosides were most prominent. The concentrations of malvidin-3-glucoside in the mucosa and urine were 1.8 ± 1.6 $\mu\text{g/g}$ (3.7 ± 3.3 nmol, $n = 3$) and 1.6 $\mu\text{g/ml}$ (3.2 μM), respectively. Mean levels of total anthocyanins were 8.1 $\mu\text{g/g}$ in mucosa tissue and 12.3 $\mu\text{g/ml}$ in urine. Glucosides of delphinidin and cyanidin were present in the urine of mice receiving Mirtoselect at concentrations near the limit of detection, considerably below those of their respective galactosides, which occurred at 0.6 ± 0.7 and 0.6 ± 0.6 $\mu\text{g/g}$ (1.4 ± 1.5 , $n = 3$ and 1.2 ± 1.2 nmol, $n = 3$), respectively. LC/MS/MS analysis of urine samples from mice receiving Mirtoselect yielded evidence of parent anthocyanins from Mirtoselect and a range of metabolic conjugates (see Table 5.1). Mass spectrometric analyses of intestinal mucosa samples afforded peaks, which hinted at the presence of the aglycons; delphinidin (transition $303 > 229$), petunidin (transition $317 > 217$) and peonidin (transition $301 > 201$), but these species were not unequivocally identified.

Liver and kidney samples from mice on Mirtoselect contained unchanged parent anthocyanins and the same glucuronide metabolites which had been characterized in intestinal mucosa, shown in table 5.1.

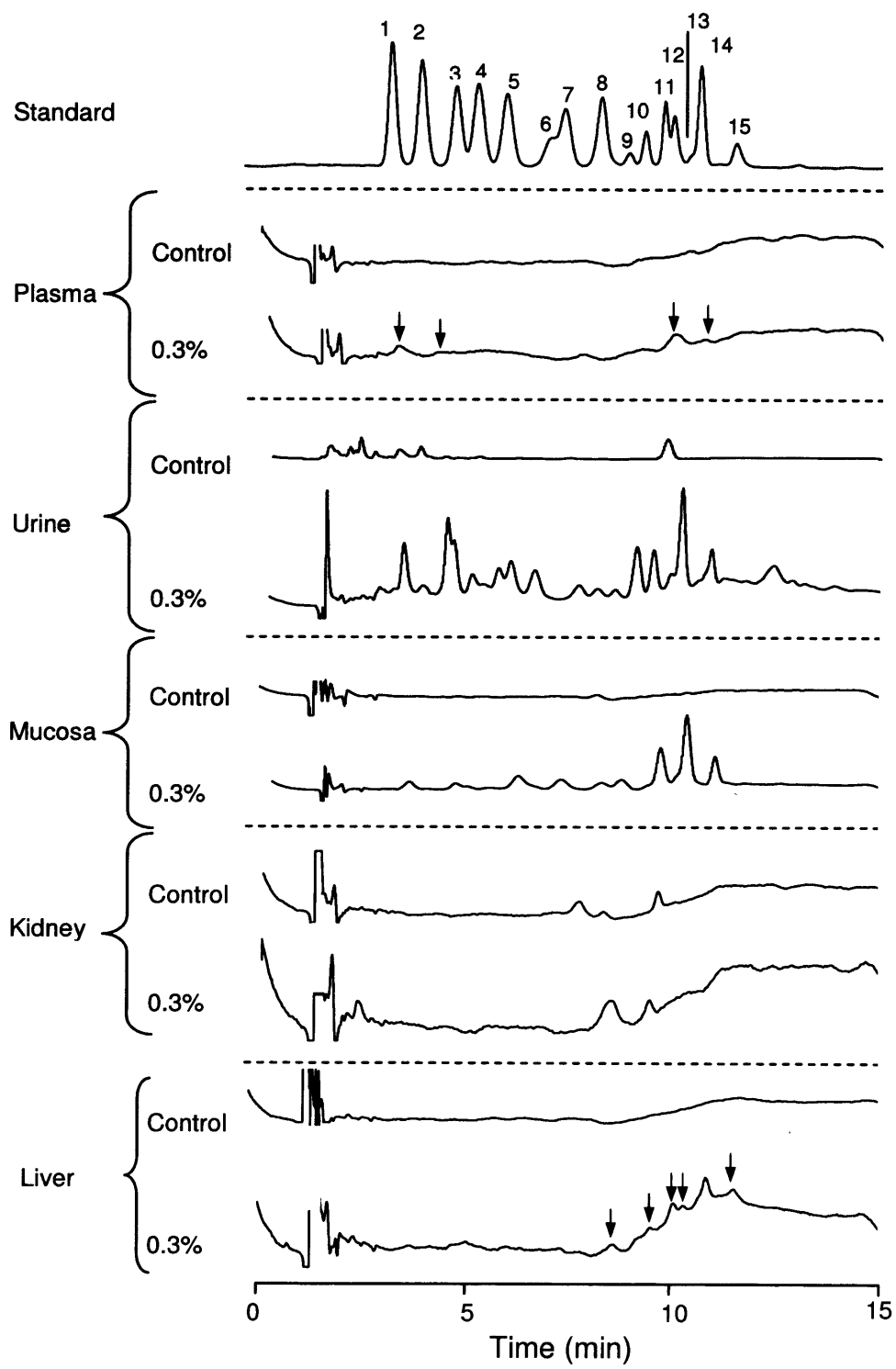


Figure 5.1: HPLC chromatograms of Mirtoselect extracts from various tissues of the Apc^{MIN} mouse which received 0.3% Mirtoselect over 12 weeks (0.3% w/w in diet). A standard of Mirtoselect is the first chromatogram with peaks labelled - 1 = delphinidin-3-galactoside, 2 = delphinidin-3-glucoside, 3 = cyanidin-3-galactoside, 4 = delphinidin-3-arabinoside, 5 = cyanidin-3-glucoside, 6 = petunidin-3-galactoside, 7 = cyanidin-3-arabinoside, 8 = petunidin-3-glucoside, 9 = peonidin-3-galactoside, 10 = petunidin-3-arabinoside, 11 = peonidin-3-glucoside, 12 = malvidin-3-galactoside, 13 = peonidin-3-arabinoside, 14 = malvidin-3-glucoside and 15 = malvidin-3-arabinoside. Chromatograms for extracted plasma, urine, mucosa, kidney and liver are shown below, from control and treated mice. Small, novel peaks are highlighted for clarity with arrows. Each chromatogram is representative of 3–6 separate animals. Y-axis scale is different between HPLC traces.

Table 5.1: Anthocyanins identified by LC/MS/MS analysis of urine and mucosa samples from Apc^{MIN} mice which received Mirtoselect (0.3%) with their diet. Parent anthocyanins from Mirtoselect were detected, but are not shown for sake of clarity.

Anthocyanin Species	RT (mins)	MRM Transition <i>m/z</i>
Delphinidin glucuronide	11.3	479 → 303
Cyanidin glucuronide	13.1	463 → 287
Peonidin glucuronide ¹	10.5, 8.1, 11.7 ²	477 → 301
Malvidin glucuronide ³	11.8, 9.9, 12.6 ²	507 → 331
Cyanidin glycoside glucuronide ⁴	2.6, 3.0 ²	625 → 287
Peonidin glycoside glucuronide ¹	3.3, 5.6, 6.4 ²	639 → 301
Peonidin arabinoside glucuronide ¹	5.3	609 → 301
Methyl delphinidin arabinoside ²	8.7	449 → 317
Methyl delphinidin glycoside ^{2, 5}	5.9	479 → 317

¹Some of the peonidin may be formed by methylation of C3G; ²Several positional isomers; ³Malvidin can be formed through dimethylation of delphinidin or methylation of petunidin; ⁴Not detected in urine; ⁵In the absence of authentic standards, species may represent either glucoside or galactoside.

5.2.2 Cyanidin-3-Glucoside

Figure 5.2 shows the HPLC traces obtained from analysing plasma, urine, mucosa, kidney and liver from Apc^{MIN} mice fed 0.3% C3G in the diet for 12 weeks. Each sample gave peaks which were not present in control tissues. Amounts of C3G in the plasma from 4 (of 16) mice on C3G were between the limits of detection and quantitation (2.5 – 7.5 ng/ml, 5 – 15 nmol, n = 4), 1 mouse contained 12.4 ng/ml (28 nmol) C3G while C3G levels in the remaining 11 mice were below the detection limit.

In the urine, metabolites of C3G were observed by HPLC-Vis (Figure 5.2), while MS analysis afforded evidence for the following C3G metabolites: methyl C3G (transition 463 > 301, 2 peaks), C3G glucuronide (transition 625 > 287, 2 peaks), methyl C3G glucuronide (transition 639 > 301, 3 or 4 peaks), cyanidin glucuronide (transition 463 > 287, 3 peaks) and methyl cyanidin glucuronide (transition 477 > 301, 2 or 3 peaks). One of the 2 peaks consistent with methyl C3G was the most abundant urinary metabolite of C3G (Figure 5.2 – urine, marked with a star, *). The retention time of this species, when compared with those of the anthocyanin components of Mirtoselect (Figure 5.1 - standard), characterizes it tentatively as peonidin-3-glucoside. Total anthocyanin levels in the urine were 7.2 ± 7.7 µg/ml (n = 3).

Mucosal levels of C3G and total anthocyanins were 16 ± 22 ng/g (37 ± 51 pmol, n = 5) and 43 ng/g tissue, respectively, and the analogous urine levels were 3.9 ± 4.2 µg/ml (8.7 ± 9.4 µM n = 4) and 7.2 µg/ml. Metabolites of C3G in the mucosa of mice were identified by LC/MS/MS as methyl C3G (transition 463 >

301, 2 or more peaks), C3G glucuronide (transition 625 > 287, one peak) and cyanidin glucuronide (transition 463 > 287, 3 peaks), consistent with retention times of peaks observed by HPLC–Vis analysis (Figure 5.2).

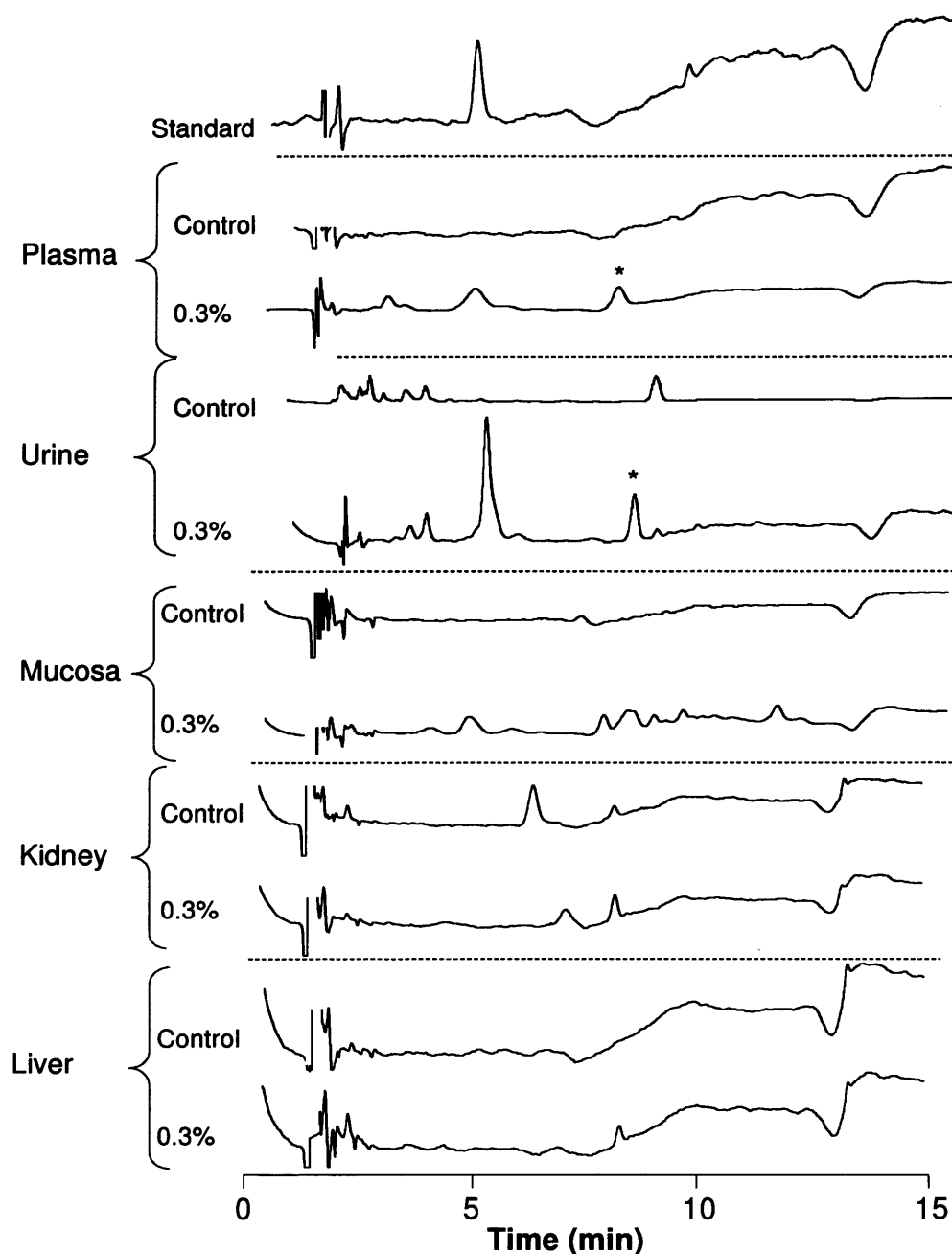


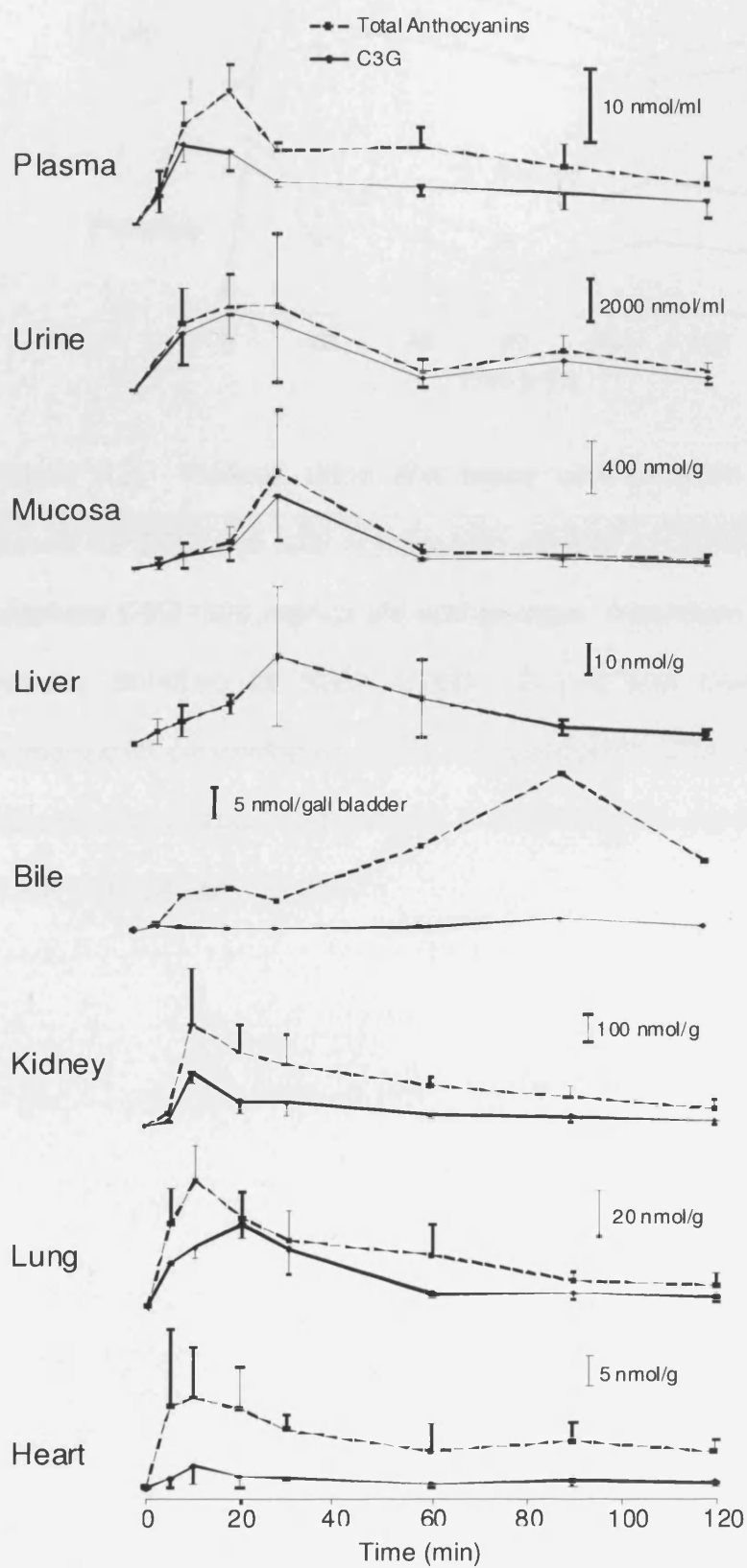
Figure 5.2: HPLC–Vis chromatograms of C3G extracts from various tissues of *Apc^{MIN}* mice. A standard of C3G is the first chromatogram with the prominent peak being C3G. Chromatograms of extracted plasma, urine, mucosa, kidney and liver are shown below, with control and treated (0.3% w/w C3G in the diet) for each. Each chromatogram is representative of 3–6 separate animals. Star denotes position of peonidin-3-glucoside/methyl C3G. Y-axis scale is different between HPLC traces.

The mass spectrometric search in the mucosa for cyanidin using the MRM transition transition 287 > 137 or selected ion monitoring (transition 287), yielded 2 peaks, neither of which could be unequivocally identified by coelution with authentic compound.

Kidney and liver tissue extracts revealed the presence of cyanidin glucuronide and methylated derivatives of C3G and C3G glucuronide.

5.3 Tissue Distribution and Pharmacokinetics of Cyanidin-3-Glucoside and its Metabolites in Mice Following Oral Bolus

Figure 5.3 shows the time versus concentration curves for the oral bolus experiment. Total anthocyanins refers to the sum concentration of all anthocyanin-related peaks, including C3G. C3G refers to the parent anthocyanin C3G. Pharmacokinetic calculations were completed as described in section 2.4.6. Table 5.2 shows T_{MAX} and C_{MAX} values for each tissue for both C3G and total anthocyanins. Most matrices show a T_{MAX} of 30 min or less, except bile which peaked at 90 min. Urine possessed the highest C_{MAX} for C3G with 3560 nmol/ml ($n = 2$, SD not calculated), with mucosa tissue concentrations being the second highest with 548.4 ± 338.1 nmol/g ($n = 3$). The lowest levels observed were in brain tissue, 0.57 ± 0.1 nmol/g ($n = 3$) for C3G. The difference between C3G values and total anthocyanin values is an approximate marker for the extent of metabolism, with a large difference between the two values suggesting a high degree of metabolism. In bile, for example, a route of excretion for anthocyanins, the majority of anthocyanin content is the result of C3G metabolism (92.1%).



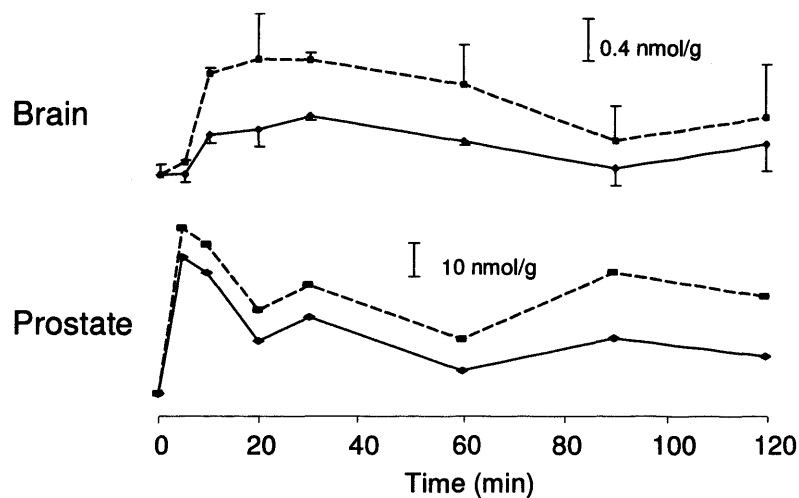


Figure 5.3: Plasma, urine and tissue concentration versus time curves for C3G and total anthocyanin content in C57BL mice which received C3G (500 mg/kg) via oral gavage. Individual biofluids and tissues identified for each graph. Dotted line represents total anthocyanin concentration, solid line represents C3G concentration. Values are the mean \pm SD, except in tissues which were pooled, with $n = 3$ animals per time point.

Table 5.2: Total anthocyanin and C3G T_{MAX} and C_{MAX} values for a range of biomatrices from mice orally dosed with 500 mg/kg C3G. C_{MAX} concentrations in nmol/ml or nmol/g depending on biomatrix.

Biomatrix	Total Anthocyanins		C3G	
	T_{MAX} (min)	C_{MAX} (n = 3, \pm SD) nmol/ml or g	T_{MAX} (min)	C_{MAX} (n = 3, \pm SD) nmol/ml or g
Plasma	20	25.1 (\pm 3.6)	10	14.9 (\pm 3.1)
Urine	30	3927.4	20	3560.2
Mucosa	30	723.8 (\pm 463.3)	30	548.4 (\pm 338.1)
Liver	30	29.2 (\pm 23.1)	30	28.9 (\pm 23.0)
Bile	90	25.4 (pooled)	90	2.0 (pooled)
Kidney	10	364.7 (\pm 199.4)	10	191 (\pm 39.4)
Lung	10	55.2 (\pm 15.2)	20	35.6 (\pm 5.6)
Heart	10	14.5 (\pm 8.1)	10	3.5 (\pm 2.9)
Brain	20	1.1 (\pm 0.4)	30	0.57 (\pm 0.1)
Prostate	5	50.5 (pooled)	5	41.8 (pooled)
Urine, in both cases, n = 2, therefore calculation of SD was not possible				

Table 5.3 shows other calculated pharmacokinetic parameters. The range of coefficients of variation (C_V) for each set of tissue concentrations is shown as a footnote to Table 5.3. The range of C_V s is included to allow assessment of the reproducibility of the data used for the pharmacokinetic analysis.

Table 5.3: Pharmacokinetic data derived from a range of biomatrices from mice dosed C3G by oral gavage. Data derived from biomatrix concentrations of C3G, with PK analysis as described in section 2.4.6

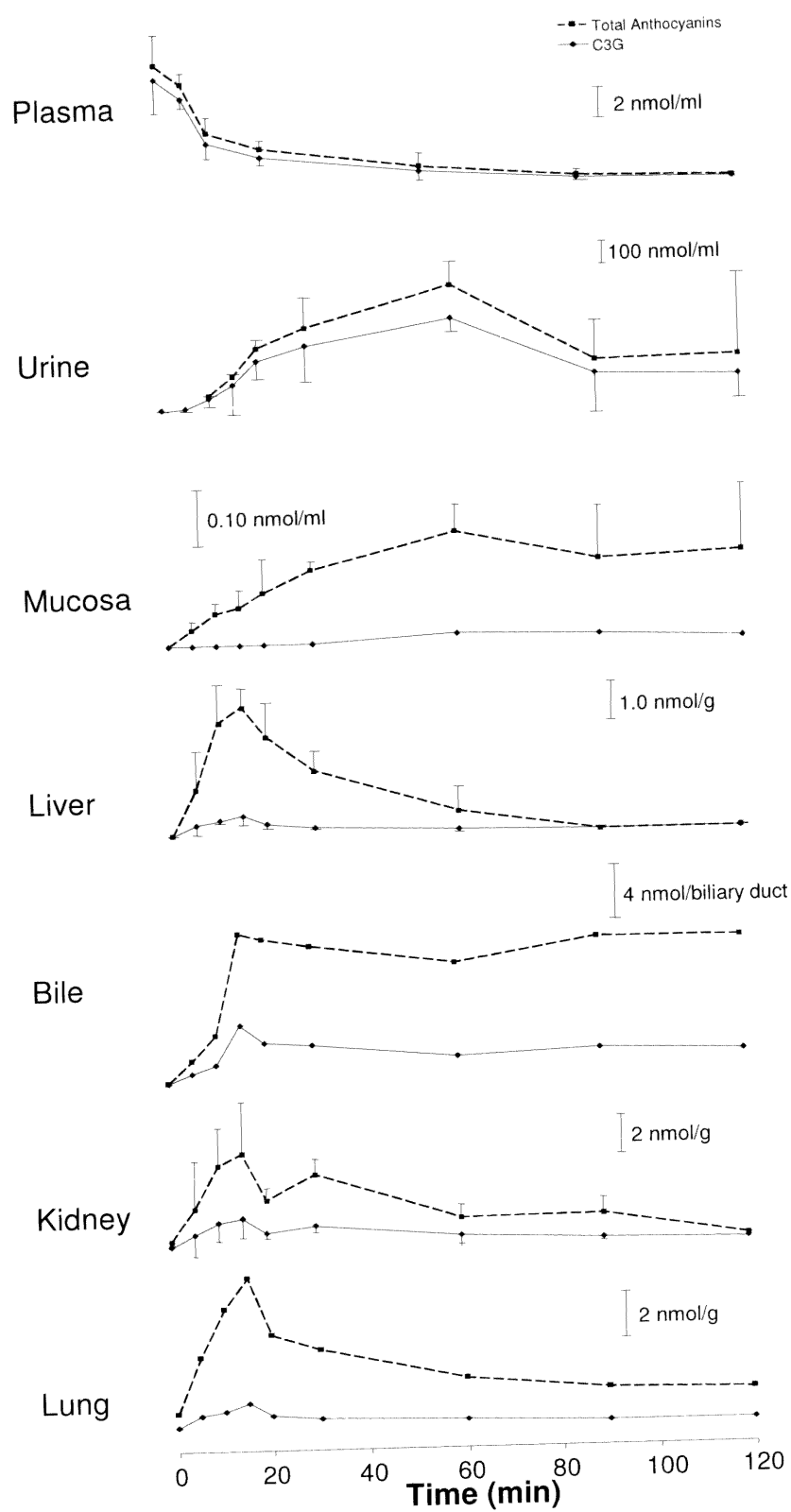
Biomatrix	Rate of Elimination (K_E) h^{-1}	Half-life (h)	AUC_{INF} (nmol.h/ml)
Plasma	0.431	1.6	25.05
Urine	0.992	0.7	3655
Mucosa	0.394	1.8	448.2
Liver	0.447	1.6	35.34
Kidney	0.601	1.2	216.8
Lung	1.084	0.6	28.34
Heart	0.563	1.2	3.634
Prostate	0.580	1.2	49.59

Range of coefficient of variations for tissue concentrations (with relevant time points) used to calculate AUC: Plasma 9% (0.5 h) to 78% (2 h), urine 48% (2 h) to 88% (0.5 h), mucosa 27% (1 h) to 86% (1.5 h) and liver 24% (0.3 h) to 86% (1 h). Of the remaining tissues, lung had the lowest C_v with 5% at 0.08 h, and heart had the highest C_v with 103% at 0.33 h.

The elimination rate constant (K_E) described in Table 5.3 ranges from 0.394 to 1.084 h^{-1} for mucosa and lung, respectively. The measured half-life ranges from 0.7 h to 1.8 h for lung and mucosa, respectively. Therefore, with the exception of lung, the half-life of the tissues closely matches that of plasma. Values for bile and brain are omitted because their time-concentration profile did not fit the pharmacokinetic profile in WinNonlin, as described in 2.4.6. It should be noted that the data in Table 5.3 relate only to C3G, and do not include total anthocyanin content.

5.4 Tissue Distribution and Pharmacokinetics of Cyanidin-3-Glucoside in Mice Following I.V. Injection

Figure 5.4 shows the time versus concentration curves for the I.V. experiment. Total anthocyanin content refers to the total concentration of all anthocyanin-related peaks, including C3G. Table 5.4 shows T_{MAX} and C_{MAX} values for each tissue for both C3G and for total anthocyanin content. The I.V. dose was 1 mg/kg, 500 times lower than the oral dose used in 5.3. Urine had the highest levels of C3G with levels of the remaining tissues being considerably less than this value. Extracted brain tissue showed the presence of anthocyanin metabolites, but C3G levels were below the limit of detection. Mucosa levels were also low. The actual concentration of C3G observed was 0.026 nmol/g, showing little elimination of anthocyanins back into the intestinal tract via biliary excretion. However, the total anthocyanin concentration in mucosa was 0.34 ± 0.08 nmol/g ($n = 5$), over ten times higher. This finding suggests that the biliary and mucosal anthocyanin contents are mostly metabolites of C3G; this is also mirrored in the liver, where C3G and total anthocyanin C_{MAX} were 0.51 ± 0.2 and 3.37 ± 0.5 nmol/g ($n = 5$), respectively, and is in agreement with the high ratio of metabolites to C3G observed in bile following oral bolus dosing.



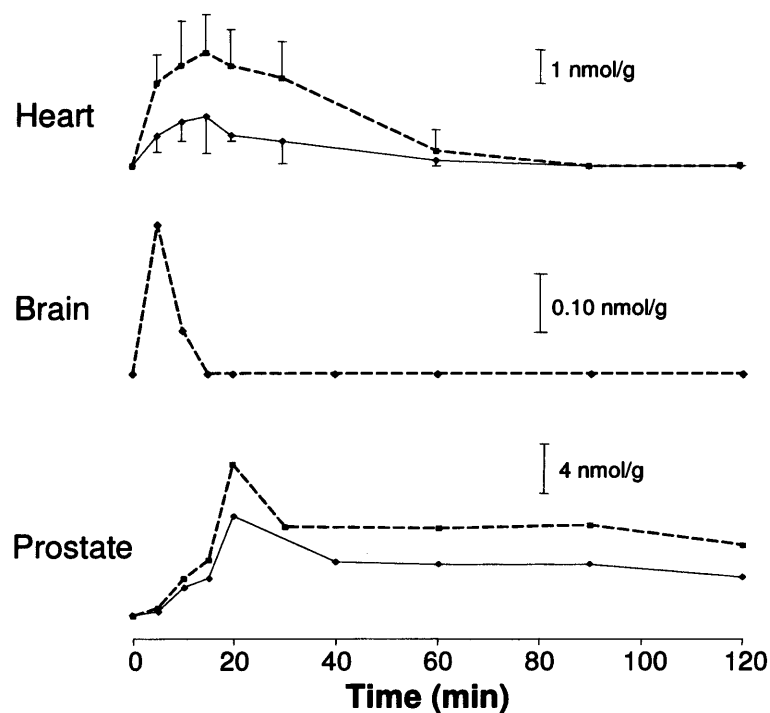


Figure 5.4: Plasma, urine and tissue concentration versus time curves for C3G and total anthocyanin content in C57BL mice which received C3G (1 mg/kg) via I.V. injection. Individual biofluids and tissues identified for each graph. Dotted line represents total anthocyanin concentration and solid line represents C3G concentration. Values are the mean \pm SD, except in tissues which were pooled, with $n = 5$ animals per time point. The measurement of C3G in mucosal samples was below LOQ in too many samples to make calculation of SD possible.

Table 5.4: Total anthocyanin and C3G T_{MAX} and C_{MAX} values for a range of biomatrices from mice dosed intravenously through the tail vein with 1 mg/kg C3G. C_{MAX} concentrations in nmol/ml or nmol/g depending on tissue type.

Biomatrix	Total Anthocyanins		C3G	
	T _{MAX} (min)	C _{MAX} (n = 5, ±SD) nmol/ml or g	T _{MAX} (min)	C _{MAX} (n = 5, ±SD) nmol/ml or g
Plasma	10	8.3 (±2.0)	10	7.4 (±2.2)
Urine	60	539.2 (±359.5)	60	387.6 (±58.1)
Mucosa	60	0.3 (±0.08)	60	0.026 (n = 1)
Liver	15	3.4 (±0.5)	15	0.5 (± 0.2)
Bile	15	11.2 (pooled)	15	4.3 (pooled)
Kidney	15	5.0 (±2.8)	15	1.5 (±1.1)
Lung	15	6.6 (pooled)	15	1.0 (pooled)
Heart	15	3.4 (±1.1)	15	1.5 (±1.1)
Brain	5	0.3 (pooled)	N/A	N/A
Prostate	20	12.2 (pooled)	20	8.1 (pooled)

Further pharmacokinetic data are shown in Table 5.5. Footnotes to Table 5.5 show the range of coefficient of variations for biomatrix concentrations used in the pharmacokinetic analysis. The ranges of C_{vs} are included to allow assessment of the reproducibility of the data used for the pharmacokinetic analysis.

Table 5.5: Pharmacokinetic data derived from a range of tissues for mice dosed by I.V. injection. Data derived from biomatrix concentrations of C3G, with Pk methods described in section 2.4.6.

Biomatrix	Rate of Elimination (K_E)	Half-life	AUC_{INF}
	h^{-1}	(h)	(nmol.h/ml)
Plasma	1.844	0.4	3.01
Mucosa	0.971	0.7	0.027
Liver	1.918	0.4	0.083
Kidney	1.538	0.5	0.969
Lung	1.786	0.4	0.428
Heart	2.281	0.3	0.716

Range of coefficient of variations for tissue concentrations used to calculate AUC: Plasma 11% (0.25 h) to 80% (1.5 h), urine 15% (1 h) to 135% (1.5 h), mucosal levels were too low to give a C_v and liver 14% (0.25 h) to 112% (1 h). Of the remaining tissues lung had the lowest C_v with 20% at 0.33 h, and heart had the highest C_v with 169% at 0.17 h

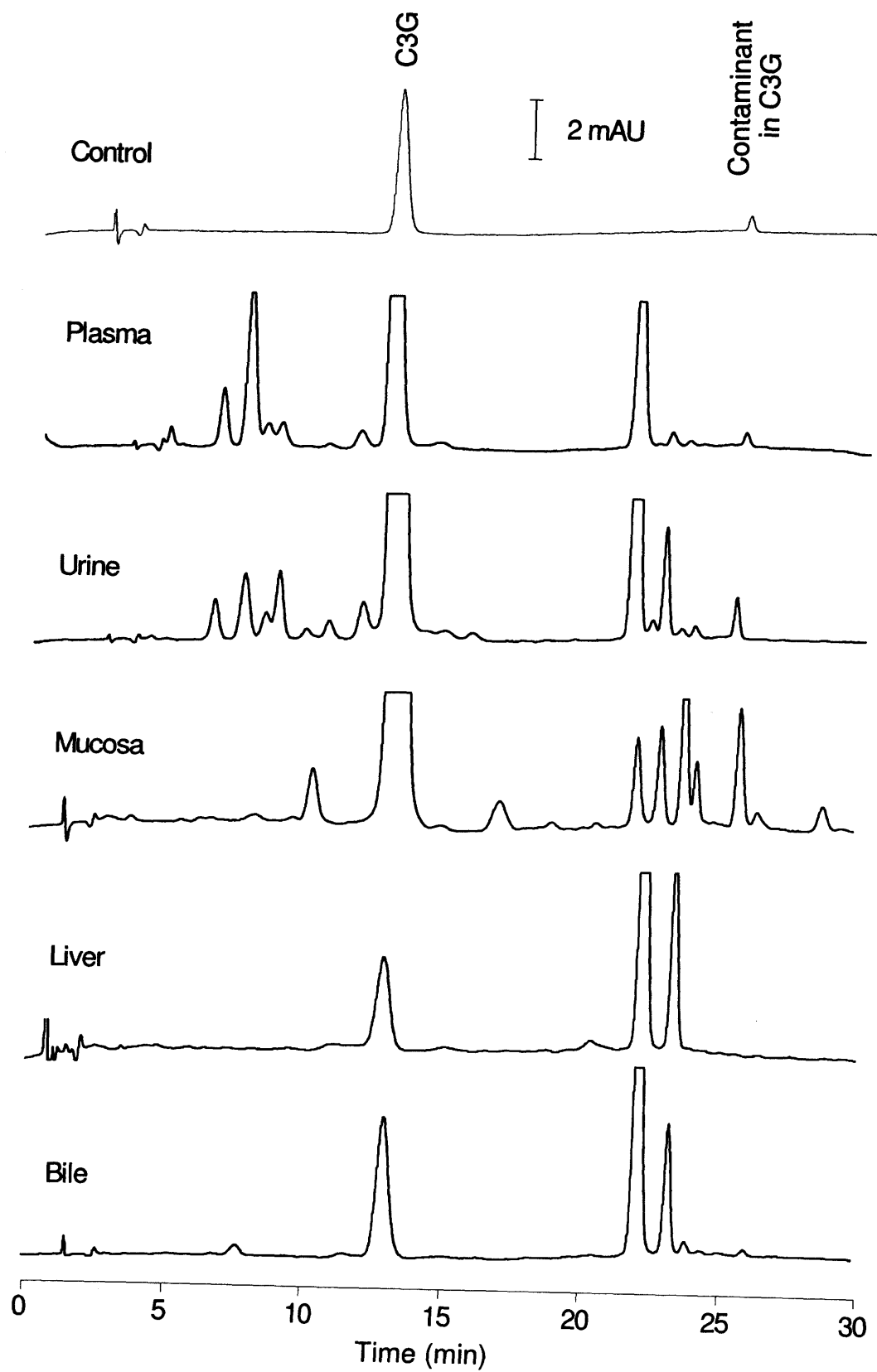
The elimination rate constant (K_E) described in Table 5.5 ranges from 0.971 to 2.281 h^{-1} for mucosa and heart, respectively. The measured half-life ranges from 0.3 h to 0.7 h for heart and mucosa, respectively. Values for urine, bile, brain and prostate are omitted because their time-concentration profile did not fit the pharmacokinetic profile in WinNonlin, as described in section 2.4.6. It should be noted that the data in Table 5.5 relates only to C3G, and does not include total anthocyanin content.

5.5 Metabolite Identification of Anthocyanins by LC/MS/MS Administered via Oral Bolus

5.5.1 Anthocyanins from Tissues of Mice Dosed with Cyanidin-3-Glucoside

Figure 5.5 shows the complete HPLC analysis of every tissue analysed from the oral bolus study (see chapter 5.3). Time points shown are not the same for each tissue (see Figure legend), and the peak area (and concentration) cannot be compared directly as they are derived from different amounts of sample. C3G is present in all tissues, and the contaminant in the standard (~ 26 mins) should not be interpreted as a metabolite. Limited metabolite identification is possible using co-elution experiments, but individual metabolite reference standards were not available. Groups of metabolites can be identified; more polar metabolites than C3G elute sooner (glucuronides) and less polar metabolites elute later than C3G (methylated metabolites). The order of elution is determined based on the order of elution of C3G and peonidin-3-glucoside in Mirtoselect (Figure 5.1) where peonidin-3-glucoside, effectively methylated C3G, elutes later than C3G. Also the more polar delphinidin-3-glucoside elutes earlier than C3G. There are multiple peaks of each metabolite type due to the multiple sites of metabolism in C3G (see 1.4.2 for structure). As well as the multiple sites for metabolism, it is also possible that more than one site may be metabolised – further complicating the identification of individual species. Aside from plasma, urine and kidney the most abundant of the metabolites visible in the analysed tissues are the two, less polar methylated metabolites. For

complete identification of metabolites each tissue was analysed via LC/MS/MS (see section 5.5.2).



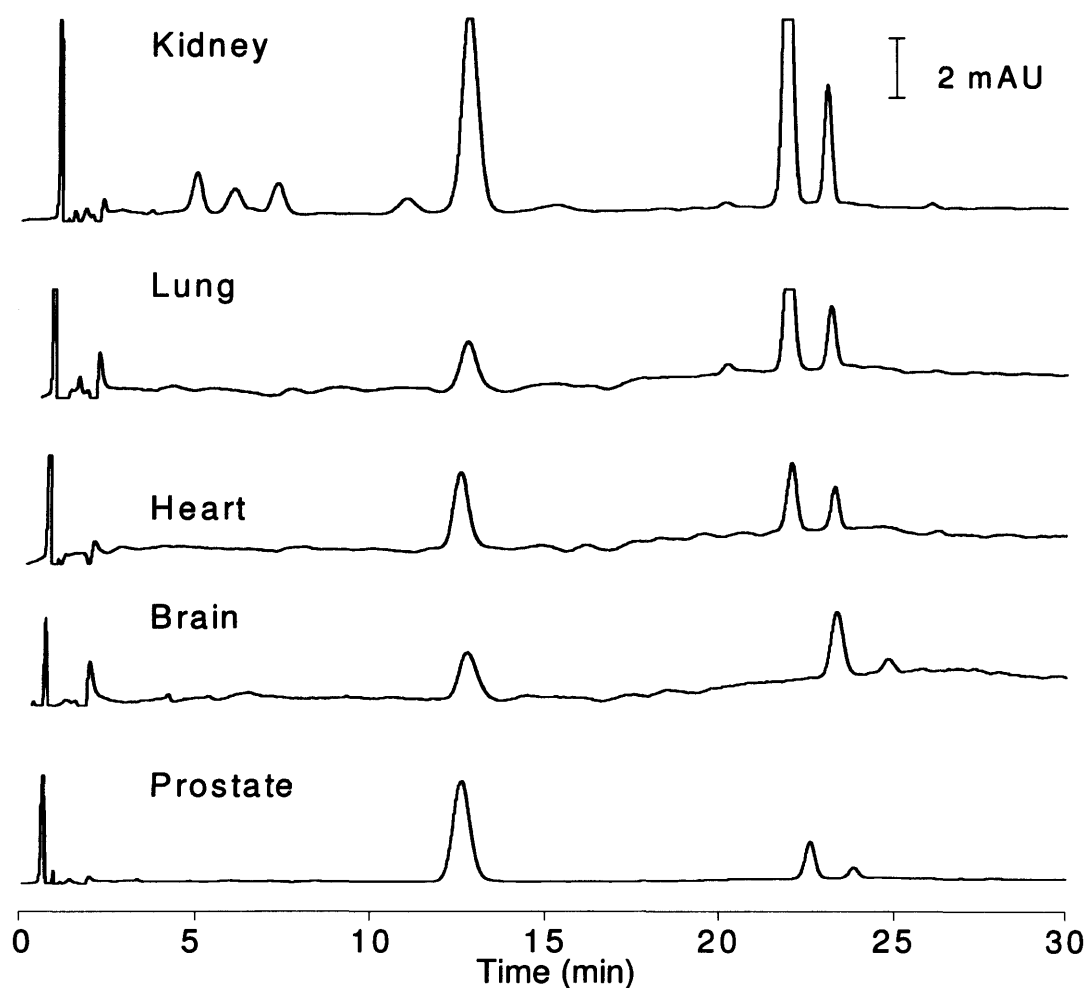


Figure 5.5: Example chromatograms of various biomatrices from male C57BL mice dosed orally with C3G via gavage (see 5.3). C3G standard is shown at the top. The contaminant observed at ~25 min is contained in the authentic C3G material. Spectra from the analysis of murine tissues are shown below the spiked control. The time points used represent T_{MAX} for individual tissues, which were: 20, 20, 30, 30, 90, 10, 10, 10, 20 and 5 min, respectively for plasma, urine, mucosa, liver, bile, kidney, lung, heart, brain and prostate. C3G is observed at ~13.8 min in all samples. Chromatograms, and amounts of anthocyanins, cannot be compared directly as differently sized aliquots were used in each example. The method used was that described in 2.2.2.

5.5.2 LC/MS/MS Identification of Metabolites

To accurately identify each metabolite in the tissues, LC/MS/MS was employed. When using LC/MS/MS in multiple reaction monitoring (MRM) mode, for a component to be identified its mass to charge ratio (m/z) and the m/z for its fragment ion have to be entered into the software, so only transitions entered will be identified. The lists of transitions investigated are shown in Tables 2.2.3 – 2.2.7, and represent the known metabolites from previous metabolism studies (see sections 1.4.3 – 1.4.5), sulphate conjugates and combinations of the two. These transitions were investigated in every tissue obtained from the oral bolus study (see section 5.3). Shown here are a urine sample (Figure 5.6) and a mucosal sample (Figure 5.7), and they represent the total range of metabolites observed across all tissues. Table 5.6 shows the distribution of metabolites in all tissues and their respective m/z ratios. Individual spectra are not shown. Figure 5.6, 1 and 2, are HPLC traces of control tissue and of tissue taken 30 minutes after dosing with C3G. A – G represent the transitions detected in the urine sample (mass to charge ratios in Figure legend). As expected the glucuronidated metabolites are eluted earlier than C3G, and the less polar methylated metabolites later. C3G sulphate was also detected.

Presented in Figure 5.7 are the HPLC and LC/MS/MS chromatograms for mucosal tissue from the oral bolus of C3G. Chromatograms 1 and 2 show control and treated mucosa, respectively, 30 minutes after the oral dose of C3G. Spectrograms A – E show the transitions observed for anthocyanins in the mucosal sample. The metabolites observed are shown in the Figure legend and Table 5.6. Of interest in the mucosa is the presence of the aglycone cyanidin.

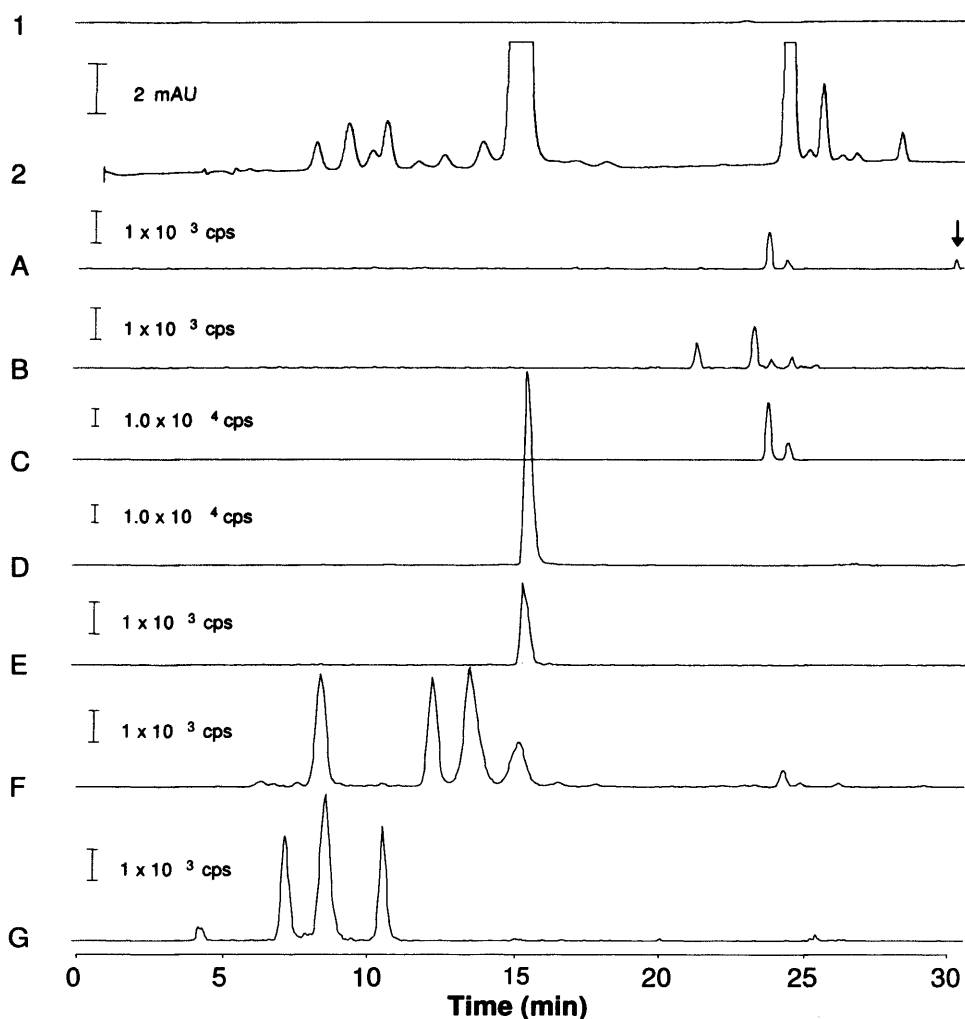


Figure 5.6: HPLC and LC/MS/MS chromatograms of urine from the oral bolus study (see section 5.3). 1 and 2 are HPLC chromatograms of control urine and urine 30 min (T_{MAX} for total anthocyanin content) after an oral dose of C3G, respectively. Traces A - G represent individual transitions (units m/z) for particular species: A - methyl-cyanidin (peonidin, marked with arrow, $301 \rightarrow 201$), B – methyl cyanidin glucuronide ($477 \rightarrow 301$, 4 isomers), C – methyl C3G ($463 \rightarrow 301$, 2 isomers), D – C3G ($449 \rightarrow 287$), E - C3G sulphate ($529 \rightarrow 287$), F – methyl C3G glucuronide ($639 \rightarrow 301$, 4 isomers) and G – C3G glucuronide ($625 \rightarrow 287$, 4 isomers). Cyanidin glucuronide was also detected, but at very low levels (not shown). Note the differing scale in C and D, cps = cycles per second.

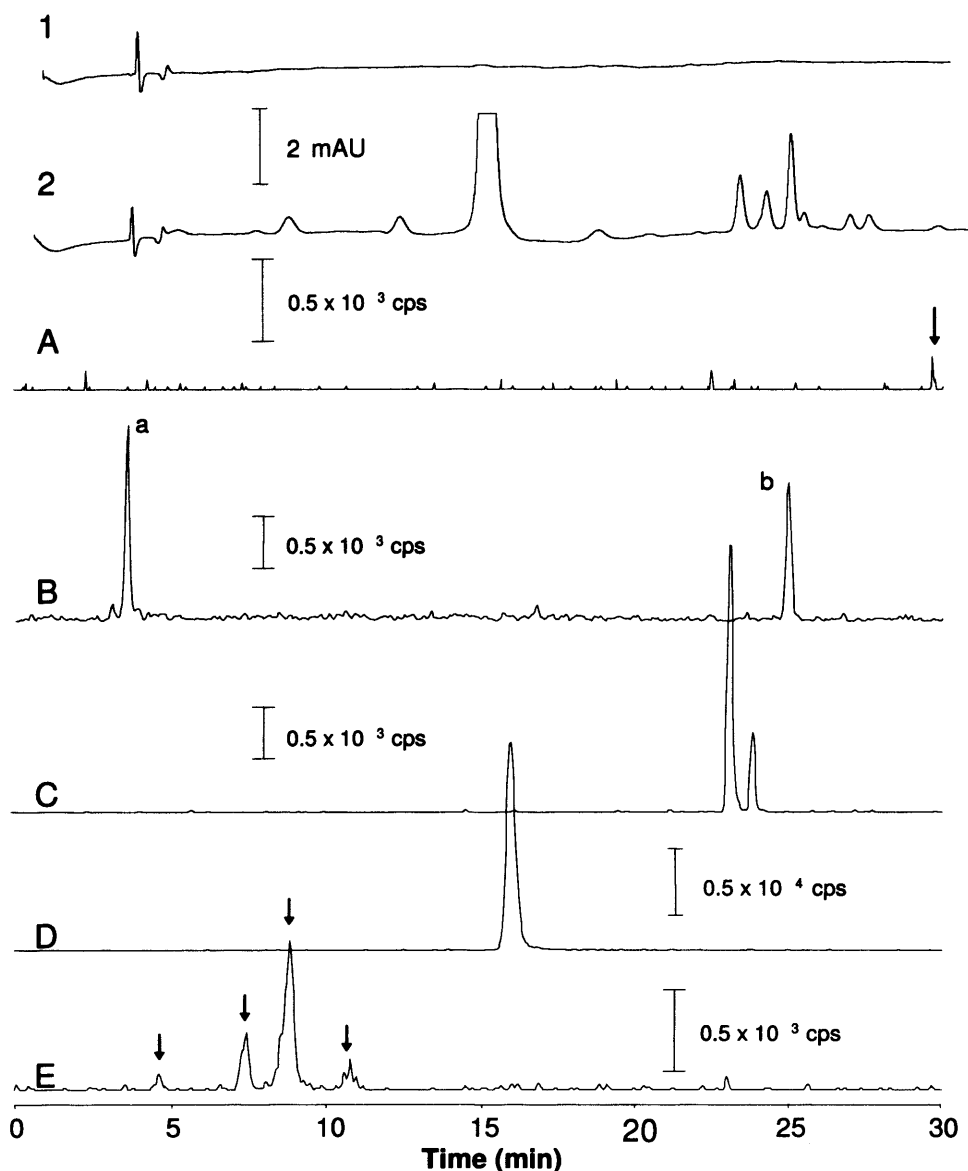


Figure 5.7: HPLC and LC/MS/MS chromatograms of mucosa from the oral bolus study (see section 5.3). 1 and 2 are HPLC chromatograms of control mucosa and mucosa 30 min after the oral bolus of C3G (T_{MAX}), respectively. Traces A - E represent individual transitions (units m/z) for a particular species: A – methyl cyanidin (peonidin, marked with arrow, $301 \rightarrow 201$), B – cyanidin aglycon transition $287 \rightarrow 137$ (b) and unknown (a) (transition $287 \rightarrow 137$), C – methyl C3G ($463 \rightarrow 301$, 2 isomers), D – C3G ($449 \rightarrow 287$), E – C3G glucuronide ($625 \rightarrow 287$, 4 isomers) (marked with arrow). Cyanidin and peonidin glucuronides were also detected, but at very low levels (not shown). Note the differing scale in D, cps = cycles per second.

Table 5.6: Identification of metabolites present in all tissues after oral bolus dose of C3G (500 mg/kg). Metabolite identification determined by LC/MS/MS analysis, using MRM transitions. Mass to charge ratio transition (m/z) for each metabolite is shown. Numbers represent the number of peaks observed for each transition. C3G observed in every tissue, so has been excluded from the table.

Metabolite	Transition	Plasma	Urine	Mucosa	Liver	Bile	Kidney	Lung	Heart	Brain	Prostate
C3G Glucuronide	625 > 287	4	4	4	3	3	3	2	-	-	3
Methylated & glucuronidated C3G	639 > 301	6	4	-	3	3	3	1	-	-	4
Cyanidin	287 > 137	-	-	1	-	-	-	-	-	-	-
Cyanidin glucuronide	463 > 287	-	1	1	-	-	-	-	-	-	-
Methylated cyanidin glucuronide	477 > 301	1	4	1	-	3	-	-	-	-	-
Methylated C3G	463 > 301	2	2	2	2	2	2	2	2	2	2
Methylated cyanidin	301 > 201	-	1	1	-	1	-	-	-	-	-
C3G Sulphate	529 > 287	-	1	-	1	-	-	-	-	-	-
Total number of metabolites		13	17	10	9	12	8	5	2	2	9

5.6 Bioavailability of Cyanidin-3-Glucoside

Bioavailability of C3G was calculated using AUC and dose after oral and I.V. administration (Tables 5.3 and 5.5, method see section 2.4.6). In order to estimate the bioavailability of total anthocyanins, the AUC for all species derived from C3G were used in the calculation, values are shown in Table 5.7.

Table 5.7: AUC and dose values necessary to calculate the bioavailability of both C3G and total anthocyanin content (TAC).

	AUC Value	C3G Dose
	(nmol.h/ml)	(mg/kg)
C3G Oral	25.051	500
C3G I.V.	3.014	1
TAC Oral	62.928	500
TAC I.V.	3.842	1

The bioavailability of C3G calculated using C3G alone and the total anthocyanin content was 1.66 and 3.28%, respectively.

5.7 Discussion

In this chapter the level of anthocyanins found in tissues and excreta after the administration of Mirtoselect or C3G and the nature of anthocyanin metabolites were investigated. Firstly, metabolism and pharmacokinetics of anthocyanins were investigated in Apc^{MIN} mice in a feeding study, followed by a second study in C57BL mice after oral and I.V. administrations of C3G. In this discussion, the measured levels are compared with results obtained by other authors, after administration of anthocyanins to either rats or pigs. The levels of anthocyanins, types of metabolites encountered and bioavailability are compared with published data. Finally, levels of anthocyanin achieved in the intestinal mucosa, the target tissue in the case of Apc^{MIN} mice, are interpreted in comparison with concentrations which elicit biochemical effects related to chemoprevention in cells *in vitro*.

5.7.1 Levels of Anthocyanins in Animals In Vivo

Talavéra *et al* (2005) fed rats a blackberry-enriched diet (1.5% w/w), which was comprised primarily of C3G, and the daily dose per rat was approximately 162 mg anthocyanins/day. The level observed in plasma for C3G was 67.2 ng/ml (Talavéra *et al.*, 2005). Mice in our study consumed less than in the Talavéra *et al* study, approximately 12 mg/mouse/day of C3G, and the highest C3G plasma concentration, 12.4 ng/ml (see section 5.2.2), was considerably lower than that observed in rats, (see 5.2.2). Analysis of liver and kidney tissue from mice consuming an AIN diet containing a blackberry extract (Talavéra *et al.*, 2005)

gave concentrations of total anthocyanin of 0.38 and 3.27 nmol/g, respectively. Levels observed in the study described here were lower than in the blackberry study, and were near or below the limit of quantitation of 0.04 nmol/g. The difference between the two studies is probably due to the fact that the dose used by Talavéra *et al* (2005) was higher than the dose used in the work described here.

The pharmacokinetic profile of C3G has been investigated previously in rats (Ichiyanagi *et al.*, 2005a and 2005b). Peak plasma levels observed for C3G by Ichiyanagi *et al* (2005a) after oral dosing of C3G (100 mg/kg) gave a C_{MAX} of 0.19 μ M. In the oral bolus experiment described in chapter 5.3 the dose used was 500 mg/kg of C3G, and the C_{MAX} for plasma was considerably higher, 14.9 μ M (section 5.3), much more than one would expect when a linear dose- C_{MAX} relationship is assumed (Ichiyanagi *et al.*, 2005a).

Ichiyanagi *et al* (2005a) observed a T_{MAX} of 15 min for C3G in the plasma of rats, whereas in the work described here a T_{MAX} of 10 min was recorded for C3G in the plasma of mice. Ichiyanagi *et al* (2005a) also observed a delay in T_{MAX} for the metabolites of C3G as compared to the T_{MAX} for parent C3G, as was seen in the work described here. The reason for this delay might be complicated. The explanation may entail several potential rate-determining processes, such as metabolism in the gut and liver, re-absorption, and further metabolism via the enterohepatic circulation, all contributing to a complex dynamic equilibrium (Table 5.6 and Ichiyanagi *et al.*, 2005a, 2005b and Fleschhut *et al.*, 2006).

5.7.2: Bioavailability of Anthocyanins

The bioavailability of C3G calculated using C3G concentration alone and total anthocyanin content were 1.66 and 3.28% of the dose, respectively. Literature reports of bioavailability of anthocyanins in mice do not exist, and the work here is novel in this respect. There are presently two studies which have been similar in design and scope to the one described here. Matsumoto *et al* (2006) conducted an oral and I.V. comparison using delphinidin-3-rutinoside in rats in which the bioavailability was 0.49% for the sum of parent anthocyanin and its metabolite. Ichibanagi *et al* also calculated bioavailability in rats, using a bilberry extract similar to Mirtoselect (Ichibanagi *et al.*, 2006). They calculated the anthocyanin bioavailability as 0.98%. The bioavailability determined here is of a similar order of magnitude as the values in the literature. Another experiment, similar to the one conducted here, but one which investigated anthocyanin bioavailability in rats was conducted by Borges *et al.*, 2007. Their study, which employed a raspberry anthocyanin extract dosed orally, measured the amount of anthocyanins excreted in urine as a percentage of the ingested dose. The bioavailability was calculated to be 1.2%, which resembles the bioavailability described here.

The literature contains several reports on the bioavailability of anthocyanins in humans (Bub *et al.*, 2001, Netzel *et al.*, 2001, Milbury *et al.*, 2002, Frank *et al.*, 2003, Felgines *et al.*, 2003 and Bitsch *et al.*, 2004). They range from 0.05% - 0.23% of the ingested dose. It is worth noting that the calculation of bioavailability in these papers has been unusual and perhaps flawed (Ichibanagi *et al.*, 2006) in that it only took the extent of anthocyanins excreted in the urine

into consideration and related it to the dose. The method more generally employed for calculating bioavailability makes use of both I.V. and oral administration, as was carried out here (see section 5.6). In my observations (Figures 5.3 and 5.4) I have demonstrated that anthocyanins are also excreted via the biliary route, and therefore using urinary excretion alone will underestimate the bioavailability. All of these values, however, show that the bioavailability of anthocyanins is low, but is similar to that of other polyphenols. Examples of polyphenols with a similar bioavailability are quercetin for which bioavailability values of 0.07 – 6.4% of the dose have been reported (Manach *et al.*, 2005), and curcumin which has been shown to have a bioavailability of <5% of the dose (Pan *et al.*, 1999). In the case of anthocyanins, the low apparent bioavailability may be due to the rapid degradation of anthocyanins in the intestinal tract by gut micro-flora (Keppler *et al.*, 2005 and Fleschhut *et al.*, 2006). The products of this degradation process (see section 1.4.5 and Figure 1.11) are not detected at 520nm, and so would not be observed by the HPLC methods employed in these studies. He *et al* reported anthocyanin losses in the faecal content were high for glucosides of cyanidin, and rapid degradation was observed after storage in faecal matter at -18°C (He *et al.*, 2005). Similarly, Felgines *et al* noted that caecal contents of rats contained low levels of parent anthocyanin or anthocyanidin, suggesting anthocyanins are unstable in this environment (Felgines *et al.*, 2002). Borges *et al.*, found almost full recovery of anthocyanins in rats 2h after dosing when the anthocyanins have passed through the stomach and duodenum/jejunum, but after 3h <50% were recovered. The loss of more than half the anthocyanins is speculated by the authors to be the consequence of colonic degradation (Borges *et al.*, 2007). Other publications have also suggested the absorption of anthocyanins is low

(Cao *et al.*, 2001 and Bub *et al.*, 2001), yet Talavéra *et al.* have shown good absorption in the stomach and small intestine despite a low urinary output (0.02% of the ingested amount) again using HPLC and LC/MS (Talavéra *et al.*, 2003, 2004 and 2005). Research into the potential cancer chemopreventive properties of anthocyanin degradation products is on-going. Kern *et al.*, determined that of the anthocyanins investigated (glycosides of delphinidin, cyanidin, peonidin, pelargonidin and malvidin) only delphinidin formed a phenolic degradation product (gallic acid) that killed cancer cells *in vitro*, and this was present in such small amounts compared to parent drug as to negate any efficacy which may be seen *in vivo* (Kern *et al.*, 2007). The concentrations of these degradation products have been suggested to be significant. Tsuda *et al.* showed that protocatechuic acid, the phenolic degradation product of cyanidin, was present in the plasma at concentrations 8 times higher than cyanidin itself, however it may be possible that other processes may produce similar agents (Tsuda *et al.*, 1999 and El Mohsen *et al.*, 2006).

5.7.3: Anthocyanin Metabolism

The range of metabolites previously observed in rats and pigs is very similar to that observed in mice in the study described here. Metabolites identified include methylated, glucuronidated species and molecules with dual-conjugation of methyl and glucuronide groups (Tsuda *et al.*, 1999, Felgines *et al.*, 2002, Talavéra *et al.*, 2003, 2004, 2005, Wu *et al.*, 2004, Ichiyanagi *et al.*, 2004, 2005a, 2005b, Matsumoto *et al.*, 2006, He *et al.*, 2006 and Felgines *et al.*, 2006).

An interesting observation by Ichiyanagi *et al* (2005a) is the difference in metabolite composition between oral and I.V. dosing. The metabolites identified were tentatively divided into hydrophilic metabolites, those eluted by HPLC with a shorter retention time than C3G and hydrophobic metabolites, eluted by HPLC after C3G i.e. at longer retention times. Ichiyanagi *et al* went on to discover that oral dosing produced 4 of the hydrophobic metabolites, whereas when a comparable dose was administered by I.V. injection, only 2 hydrophobic metabolites were produced. The metabolites produced after I.V. administration were the same as 2 of the metabolites found after oral dosing; these metabolites were identified as two methylated forms of C3G, peonidin-3-glucoside and a structural isomer, methylated at the 4' position of the B ring (see Figure 1.7). The metabolites observed only after oral administration were glucuronides of cyanidin and peonidin. In the oral bolus experiment conducted here (section 5.3, Table 5.6), the presence of these glucuronides was confirmed after oral dosing. In agreement with Ichiyanagi *et al* (2005a) these metabolites were not present in the I.V. bolus experiment completed here (section 5.4) as

adjudged by HPLC (Ichiyanagi *et al.*, 2005a). The identification of cyanidin/peonidin glucuronides is tentative evidence for the intermediate formation of anthocyanidins, the aglycons, postulated to be more pharmacologically active than the glycosides (see section 1.4.9, Table 1.5). Production of the aglycons after oral administration is likely to involve β -glucuronidase-catalysed cleavage of the glucoside. Aglycons then may rapidly undergo UDP glucuronyltransferase-catalysed glucuronidation; both enzymes exist in the mucosa (Ichiyanagi *et al.*, 2005a, 2005b and Felgines *et al.*, 2002). In contrast to this Wu *et al* speculated that the glucuronide may be formed directly from the glycoside, and thus not via the intermediary aglycon. The method for this route of glucuronidation is thought to be through the action of UDP-glucose dehydrogenase (Wu *et al.*, 2002).

Talavéra *et al* (2005) analysed kidney and liver tissues in a feeding study. The chemical nature of metabolites they detected in tissues by HPLC-ESI/MS/MS is consistent with that observed in mice here, as adjudged by retention times, as the levels observed in the study described here were too low to allow confirmation by LC/MS/MS.

Subtle structural differences between anthocyanidin molecules influence the types of metabolic modification observed, hinting at a high degree of specificity of the enzyme-substrate interaction. Where there is a catechol structure on the B ring, as with cyanidin (Figure 1.7) with phenols at the 3' and 4' position, methylation occurs, thought to be catalysed by catechol-O-methyl transferase (COMT) in the liver (Wu *et al.*, 2004 and Ichiyanagi *et al.*, 2005a and 2005b). Methylation in this molecule can occur at either the 3' or 4' position, but not at

both sites simultaneously (Wu *et al.*, 2004 and Ichiyanagi *et al.*, 2005a and 2005b). In contrast, delphinidin-3-glucoside possesses three phenols on the B-ring, at 3', 4' and 5' (Figure 1.7), forming a pyrogallol, while methylation of delphinidin-3-glucoside produces only one product (Ichiyanagi *et al.*, 2004), with a methyl on the 4' position. It is suggested that methylation of both C3G and delphinidin-3-glucoside is catalysed by COMT (Ichiyanagi *et al.*, 2004 and 2005a). The sites and extent of methylation through COMT is consistent with other flavonoids containing a catechol structure (e.g. cyanidin). Generally, the catechols get methylated at the 3' and/or 4' positions; whereas, molecules containing the pyrogallol structure (e.g. delphinidin) still get methylated by COMT, but tend to be methylated only at the 4' position (Shahrzad *et al.*, 1998, Hodgson *et al.*, 2000 and Meng *et al.*, 2001). There are no reports in the literature of the hydroxyl groups on the A-ring undergoing methylation, and similarly in the work reported here, methylation seemed to occur only on the B-ring. Cyanidin-3-glucoside which had undergone methylation on either the 3' or 4' position were detected in all tissues (Table 5.6). Glucuronidation seems to occur at any available phenolic position of C3G to produce a wide range of conjugates (Table 5.6 and Wu *et al.*, 2002 and 2004, Felgines *et al.*, 2003 and 2005, Kay *et al.*, 2004, Talavéra *et al.*, 2004 and Ichiyanagi *et al.*, 2005a and 2005b)

5.7.4: Comparison of Target Tissue Anthocyanin Levels with In Vitro Efficacy

In order to relate the adenoma-reducing ability of the anthocyanins described in Chapter 4 with tissue levels observed in the feeding study, it might be suitable

to compare concentrations in the target tissue, mucosa, with concentrations shown to be efficacious in cultured cells *in vitro*. To interpret such a comparison several assumptions have to be made. Anthocyanins engage a range of mechanisms pertinent to chemoprevention (Chapter 1, Tables 1.5 and 1.6). Focusing on colorectal cancer cells, amounts which elicit these effects range from 1 μM for down-regulation of EGFR tyrosine-kinase in A431 cells (Marko *et al.*, 2004), to 446 μM for 88% growth inhibition in HT-29 colon adenocarcinoma cells, depending on the anthocyanin molecule (Olsson *et al.*, 2004). In the following comparison, the assumption is made that effects reported for cells *in vitro* are potentially important in the observed efficacy in the Apc^{MIN} mouse (Chapter 4). Taking HT29 colon carcinoma cells as an example (Olsson *et al.*, 2004) and assuming 1 g of mucosa roughly equals one ml of aqueous media, a very tentative comparison can be made between concentrations in mucosa and cell media.

For C3G a concentration of 200 $\mu\text{g/ml}$ caused 88% growth inhibition in HT29 cells (Olsson *et al.*, 2004). Levels of anthocyanins derived from C3G detected in the mucosa of mice were much lower, 0.043 $\mu\text{g/g}$ (Section 5.2.2). This discrepancy hints at the possibility that growth inhibition was not a mechanism elicited by anthocyanins in the Apc^{MIN} mouse gastrointestinal tract. Yet there are reasons to putatively link observed efficacy in the two paradigms, Apc^{MIN} mice and HT-29 cells, despite this disparity in anthocyanin concentration. Firstly, mice in the study described here were killed throughout the day, and mice typically eat in the late evening. Therefore, the mucosal concentrations observed are steady-state levels, and post-eating levels may well be much higher. In the oral bolus study described in section 5.3, the dose was designed

to be similar to the total daily dietary intake (12 mg/mouse/day) in the feeding study described in section 5.2.2. Therefore, the levels recorded in the intestinal mucosa of mice after an oral bolus of C3G (500 mg/kg, 10 mg/mouse/day) may reflect more accurately post-eating levels of C3G. The mucosal levels of C3G detected in the bolus study (section 5.3) were 172 µg/g, much closer to the 200 µg/ml shown to inhibit growth of HT29 cells (Olsson *et al.*, 2004). However, it is unlikely that mice eat such a large dose all at once. A more accurate comparison between anthocyanin concentrations in mucosa *in vivo* and in cells *in vitro* would be provided by analysis of the respective AUC values. For mucosal anthocyanin levels the AUC is likely to increase every night post-eating and then return to steady state throughout the day. In *in vitro* experiments typically a single concentration is applied at the start, and levels decrease with time, as anthocyanins are unstable at the pH of cell medium (see section 1.4.2). Unpublished observations in our laboratory estimate the half-life of anthocyanins in cell culture media at 37 °C to be less than 4h. Furthermore, the concentrations of anthocyanins observed in the mucosa of mice should be more appropriately compared with the concentrations within HT-29 cells rather than those in the medium.

For Mirtoselect, the mucosal concentrations can be correlated with *in vitro* concentrations in a study involving a bilberry extract (Zhao *et al.*, 2004). Bilberry extract was tested in cell lines *in vitro*, and growth inhibition of HT29 cells was characterised with an IC₅₀ of 50 µg/ml (Table 1.5, Zhao *et al.*, 2004). Mucosal levels observed for anthocyanins derived from Mirtoselect in the feeding study described here were about a fifth of that value, 8.1 µg/g.

All these considerations intimate that anthocyanin concentrations measured in the mucosa of Apc^{MIN} mice, in which anthocyanins interfered with gastrointestinal carcinogenesis, are lower, but perhaps not dramatically lower than those which have been shown to engage anti-oncogenic mechanisms in cancer cells *in vitro*. One may therefore tentatively conclude that at least some of the mechanisms which have been found to affect cells *in vitro* may also be engaged to mediate anti-carcinogenesis in the Apc^{MIN} mouse model.

6. Discussion

The overall objective of the work described in this thesis was to gain information to help further the knowledge of anthocyanins and their potential role in chemoprevention. Experiments using a single anthocyanin (C3G) and a standardised mixture of 15 anthocyanins (Mirtoselect) were conducted in Apc^{MIN} mice. To help interpret any activity, HPLC and LC/MS/MS were used to identify amounts and types of anthocyanins present. M1dG – a potential biomarker for oxidative DNA damage which may be associated with cancer – was also investigated to measure any effect anthocyanins may produce.

Once the beneficial effect of anthocyanins in preventing adenoma formation was established, investigation into their absorption, metabolism, distribution and excretion (ADME) was undertaken. A comparison between oral and I.V. bolus dosing was employed. Comprehensive analysis of tissues via HPLC and LC/MS/MS gave an understanding of levels and forms of anthocyanins encountered in each tissue or biofluid, and bioavailability of C3G was also calculated.

In the following, ways are described in which the work presented here contributes to the overall body of knowledge pertaining to anthocyanins in cancer management.

6.1 Contribution to Knowledge of Efficacy

Mirtoselect and C3G significantly reduced adenoma number in the Apc^{MIN} mouse, a rodent model which has previously been shown to predict efficacy in humans of celecoxib and other NSAIDs (Jacoby *et al.*, 1996 and 2000, Baron *et al.*, 2006, Swamy *et al.*, 2006 and Yona *et al.*, 2006). This result tentatively suggests that anthocyanins may possess preventive efficacy towards adenoma occurrence and recurrence in humans. In this study (see chapter 4), C3G and Mirtoselect reduced adenoma number in the Apc^{MIN} mouse by 45 and 35%, respectively (Cooke *et al.*, 2006). Literature reports show that NSAIDs and COX-2 inhibitors reduce Apc^{MIN} mouse adenomas more efficiently than the anthocyanins studied here and at lower doses. The reductions in Apc^{MIN} mouse adenoma numbers were 88% at a dietary dose of 0.02% for piroxicam (Jacoby *et al.*, 1996) and a reduction of 70% for celecoxib at a dose of 0.03% in the diet (Swamy *et al.*, 2006). Both traditional NSAIDs and COX-2 inhibitors have toxic side-effects in the GI tract, and coxibs cause cardiovascular complications, which means their usefulness as chemopreventive agents in humans is questionable (see section 1.3.3). As a result of these side-effects, the need for novel efficacious non-toxic colorectal chemopreventive agents is clear. Other phytochemicals shown to be non-toxic which have been investigated in Apc^{MIN} mice include curcumin (0.5% w/w in diet, Perkins *et al.*, 2002) and tricetin (0.2% w/w in diet, Cai *et al.*, 2005), and these inhibited adenoma occurrence in the Apc^{MIN} mouse by 40% and 33%, respectively. These agents prevent adenoma-occurrence with a similar potency to anthocyanins, but Mirtoselect seemed more potent. Mirtoselect possessed similar efficacy at a very low dose: the 0.3% w/w dose contributes effectively 0.08% anthocyanins, which gave a 35%

reduction in adenoma number. This evidence tentatively supports the notion that anthocyanins should be considered for clinical evaluation. Another benefit of promoting Mirtoselect for potential clinical development is that it already exists as a formulation fit for human consumption (Morazzoni *et al.*, 1996).

6.2 Contribution to Knowledge of ADME

The work described in chapter 5 shows that an oral administration of anthocyanins in mice, at a dose equivalent to 1.8g in humans, leads to measurable levels in all of the tissues analysed. This is consistent with previous investigations (Miyazawa *et al.*, 1999, Bub *et al.*, 2001, Cao *et al.*, 2001, Netzel *et al.*, 2001, Wu *et al.*, 2002, Felgines *et al.*, 2003, 2005 and 2006, Ichihara *et al.*, 2004, 2005a and 2005b, Kay *et al.*, 2004 and 2005, Talavéra *et al.*, 2005). The distribution of anthocyanins throughout the body shows that at these doses anthocyanins reach a large number of tissues where one may wish to prevent cancer, and as such it may be worthwhile to consider the evaluation of anthocyanins as potential chemopreventives. However, the levels observed in all tissues, except the GI mucosa, are considerably lower than the levels shown to cause biochemical changes commensurate with chemoprevention, such as growth inhibition of cells and inhibition of signalling pathways *in vitro* (see Tables 1.5 and 1.6). With levels in the GI tract of the same order of magnitude as levels shown to elicit relevant biochemical changes in cancer cells *in vitro*, one could argue that anthocyanins should be investigated clinically for their ability to prevent GI adenoma recurrence in humans.

The bioavailability of C3G was calculated to be 1.66% for parent C3G (chapter 5), and this is consistent with bioavailability reports in the literature, albeit in rats (Matsumoto *et al.*, 2006 and Ichiyanagi *et al.*, 2006). In comparison with other phytochemicals the value is similar: curcumin, resveratrol and quercetin possessed bioavailability values in mice of <5% (Pan *et al.*, 1999), 0.07 – 6.4% (Asensi *et al.*, 2002 and Manach *et al.*, 2005) and 5.3% (Chen *et al.*, 2005), respectively. These calculated bioavailabilities can be considered low when compared to chemopreventive pharmaceuticals such as tamoxifen and aspirin, which possess bioavailabilities of 15.0% (Shin *et al.*, 2006) and 91.2% (Woodford *et al.*, 1981) respectively, considerably higher than the phytochemicals discussed here.

The difficulty associated with such a low bioavailability is achieving levels in the target tissues high enough to elicit biochemical changes related to chemoprevention. Comparing total anthocyanin content from C3G administration gives a slightly higher bioavailability (3.28%, chapter 5). The work described in chapter 4 shows administration of the mixture gave similar levels of adenoma-reducing ability, but at a lower dose, since only ~39% of the mixture consists of anthocyanins. The anthocyanin concentrations observed in the mucosa after oral administration of Mirtoselect (chapter 5) were also considerably higher than those after C3G (section 5.2.1 and 5.2.2). Therefore, administration of the mixture may be a way to improve, at least to some extent, the bioavailability. Whilst the mixture is safe, having only a low bioavailability necessitates giving high doses to achieve efficacious levels in the target tissue, the intestinal mucosa. However, this would probably only result in low levels in

the circulation and tissues, which may be a safeguard to prevent systemic toxicity.

One of the major problems associated with cancer chemoprevention trials is compliance (the extent to which the patient continues the agreed-upon treatment regime under limited supervision when faced with conflicting demands). It has been estimated that in developed countries only 50% of patients who suffer from chronic diseases adhere to treatment (Sabaté, 2003). Chemoprevention trials are especially prone to poor compliance as they normally involve healthy people taking agents over a long time for a disease they do not have. Therefore, the motivation to take the agent is low, as there is no direct immediate benefit. There are currently ways to monitor adherence, but these are not infallible. A non-invasive marker for measuring adherence is therefore desirable. In chapter 5 the steady-state urine levels in mice were easily measurable (Cooke *et al.*, 2006), and this is paralleled in humans (Cooke *et al.*, 2006a). As such, adherence may be monitored simply by sampling and analysing the subjects' urine.

The observed urine levels of C3G were 3.56 mM, the highest of any matrix analysed. In a current ongoing sister project in Leicester, the ability of Mirtoselect to inhibit the growth of bladder cancer cells is being investigated. These cells seem sensitive to the anti-proliferation effects of anthocyanins (Dr Don Jones and Dr Karen Brown, unpublished), and it is conceivable that levels of 3 – 5 mM cause growth inhibition. These preliminary results hint at the possibility that anthocyanins are a potential treatment option against superficial bladder cancer. Superficial bladder cancer is a disease with very limited

treatment options; one is surgical bladder resection (Meyer *et al.*, 2007). So it is conceivable that anthocyanins may offer a treatment role after surgical resection to help prevent any recurrence of the cancer. However, considerable further work is needed before this hypothesis can be clinically tested.

6.3 Contribution to Knowledge of Pharmacodynamics

The work described in chapter 4 tentatively suggests that M1dG in colorectal target tissue was affected by anthocyanin administration. This result is consistent with the notion that M1dG may be a biomarker of anthocyanin efficacy. Chapter 4 also showed the immuno slot-blot method developed for measuring M1dG adduct levels has numerous methodological drawbacks. As a result of this and other ongoing research, a new method for detecting M1dG adducts is being developed, using LC/MS/MS. Measurement of M1dG levels at sites remote from the target tissue, including plasma and urine, were not investigated as a surrogate biomarker for efficacy.

Whilst the direct anti-oxidant capacity of anthocyanins was not measured here, it has previously been compared to known standards *ex vivo* (see section 1.4.8). Anthocyanins have also been shown to lower the oxidative potential of mouse plasma (Ramirez-Tortosa *et al.*, 2001). M1dG is a product of oxidative DNA damage (Leuretti *et al.*, 1998 and Marnett *et al.*, 1999), and changes in oxidant status may be reflected by changes in M1dG levels. Anthocyanins have been shown to decrease murine liver concentrations of 8-oxo-dG, another product of oxidative DNA damage (Ramirez-Tortosa *et al.*, 2001). The data presented here shows the decrease in M1dG levels paralleling the decrease in

adenoma burden (see chapter 4). Therefore, determining the role of anthocyanins in affecting oxidation status may be possible using biomarkers such as M1dG or 8-oxo-dG.

6.4 Clinical Trial of Mirtoselect

Encouraged by the results observed in the Apc^{MIN} mouse intervention study (chapter 4), a phase I clinical trial has been initiated in Leicester, conducted by Sarah Thomasett. Mirtoselect is being used in this trial as it is available from Indena SpA as a formulation fit for human consumption, and as there are *a priori* no human safety concerns (Morazzoni *et al.*, 1996).

In this trial the hypothesis is being tested that when Mirtoselect is given to humans with colorectal cancer, who are waiting to undergo colectomy, anthocyanins are present at levels in colorectal tumour tissue, which are consistent with pharmacodynamic activity in cells *in vitro* and/or mucosal concentrations *in vivo* (chapter 5). The doses chosen are 1.4, 2.8 and 5.6 g of Mirtoselect per day, which equates to 360, 720 and 1440 mg of anthocyanins per day. Mirtoselect is taken as three doses throughout the day and will be taken for 7 days. Using the dose/surface area calculation to convert between species (Freireich *et al.*, 1966) the doses used in the trial encompass the 0.3% dose shown here to be efficacious in Apc^{MIN} mice. The 0.3% dose used in chapter 4 is tentatively calculated as being equivalent to 0.65 g/day in humans, with assumptions being made on the amount of diet consumed by mice and any inherent error within the body mass/area conversion (Freireich *et al.*, 1966). The endpoint of this trial is to collect pre- and post-treatment tumour biopsies,

plasma and urine from these colorectal cancer patients. These samples will be used to measure anthocyanin levels in urine, plasma and colorectal tissue. M1dG biomarker analysis of colorectal tissue and blood will also be undertaken.

Tentatively, it may be possible to predict three potential outcomes from the ongoing clinical trial. These outcomes and the potential steps following the clinical trial could be as follows:

1. The formulation is safe, low-levels or no anthocyanin compounds are detected in CRC target tissue and no pharmacodynamic biomarkers are affected. A potential follow-up procedure may be to repeat the trial, and increase the dose of Mirtoselect, or investigate different formulations of anthocyanins with enhanced bioavailability. Curcumin formulated with phosphatidylcholine has been shown to have improved systemic availability. (Marczylo *et al.*, 2007).
2. The formulation is safe; the levels of anthocyanins detected in CRC target tissue are similar to those described in chapter 5 for the Apc^{MIN} mouse, but the pharmacodynamic biomarkers are not affected by Mirtoselect. If levels of anthocyanins in CRC tissue are similar to the Apc^{MIN} mouse study (chapter 5) that would be promising, as it would show levels which inhibited adenoma development in mice can be achieved in the human G.I. tract. It is conceivable that giving Mirtoselect for only 7 days is insufficient to cause pharmacological changes. In the present study volunteers receive Mirtoselect for 7 days, whereas the mice received it for 12 weeks. Therefore, to aid with the measuring of changes in biomarker levels the study could be

repeated with the dosing period of Mirtoselect extended. One problem with this is that once patients are diagnosed with cancer the hospital is duty bound to provide treatment or surgery as soon as possible. To delay this treatment for the extension of a clinical trial would be ethically very difficult. An option would be to conduct a study where patients with no further treatment options are used as volunteers.

3. The formulation appears safe, levels detected in the CRC target tissue are similar to those observed in chapter 5 for the Apc^{MIN} mouse and the pharmacodynamic biomarkers are decreased. Assuming this outcome there would be strong evidence to support advancing Mirtoselect to the stage of adenoma prevention trials in humans.

Irrespective of the outcome of the clinical trial, the work presented here may aid interpretation of the results of the clinical trial by helping to explain the pharmacokinetics of Mirtoselect and potential pharmacodynamic biomarker changes.

7. Bibliography

- Adlercreutz, H. (1998). "Epidemiology of phytoestrogens." *Baillieres Clin Endocrinol Metab* 12(4): 605-23.
- Afaq, F., M. Saleem, C. G. Krueger, J. D. Reed and H. Mukhtar (2005). "Anthocyanin- and hydrolyzable tannin-rich pomegranate fruit extract modulates MAPK and NF-kappaB pathways and inhibits skin tumorigenesis in CD-1 mice." *Int J Cancer* 113(3): 423-33.
- Almendingen, K., X. Xie, B. Hofstad and M. H. Vatn (2004). "Dietary habits and growth and recurrence of colorectal adenomas: results from a three-year endoscopic follow-up study." *Nutr Cancer* 49(2): 131-8.
- Asensi, M., I. Medina, A. Ortega, J. Carretero, M. C. Bano, E. Obrador and J. M. Estrela (2002). "Inhibition of cancer growth by resveratrol is related to its low bioavailability." *Free Radic Biol Med* 33(3): 387-98.
- Baron, J. A., R. S. Sandler, R. S. Bresalier, H. Quan, R. Riddell, A. Lanos, J. A. Bolognese, B. Oxenius, K. Horgan, S. Loftus and D. G. Morton (2006). "A randomized trial of rofecoxib for the chemoprevention of colorectal adenomas." *Gastroenterology* 131(6): 1674-82.
- Bitsch, R., M. Netzel, S. Sonntag, G. Strass, T. Frank and I. Bitsch (2004). "Urinary Excretion of Cyanidin Glucosides and Glucuronides in Healthy

Humans After Elderberry Juice Ingestion." J Biomed Biotechnol 2004(5): 343-345.

Bjelakovic, G., A. Nagorni, D. Nikolova, R. G. Simonetti, M. Bjelakovic and C. Gluud (2006). "Meta-analysis: antioxidant supplements for primary and secondary prevention of colorectal adenoma." Aliment Pharmacol Ther 24(2): 281-91.

Blot, W. J., J. Y. Li, P. R. Taylor, W. Guo, S. Dawsey, G. Q. Wang, C. S. Yang, S. F. Zheng, M. Gail, G. Y. Li and et al. (1993). "Nutrition intervention trials in Linxian, China: supplementation with specific vitamin/mineral combinations, cancer incidence, and disease-specific mortality in the general population." J Natl Cancer Inst 85(18): 1483-92.

Bobe, G., B. Wang, N. P. Seeram, M. G. Nair and L. D. Bourquin (2006). "Dietary anthocyanin-rich tart cherry extract inhibits intestinal tumorigenesis in APC(Min) mice fed suboptimal levels of sulindac." J Agric Food Chem 54(25): 9322-8.

Borges, S., Roowi, S., Rouanet, J. M., Duthie, G. G., Lean, M. E. and A Crozier (2007). The bioavailability of raspberry anthocyanins and ellagitannins in rats." Mol Nutr Food Res 51(6): 714-25.

Borkowski, T., H. Szymusiak, A. Gliszczynska-Rwiglo, I. M. Rietjens and B. Tyrakowska (2005). "Radical scavenging capacity of wine anthocyanins is strongly pH-dependent." J Agric Food Chem 53(14): 5526-34.

- Brueggemeier, R. W., A. L. Quinn, M. L. Parrett, F. S. Joarder, R. E. Harris and F. M. Robertson (1999). "Correlation of aromatase and cyclooxygenase gene expression in human breast cancer specimens." *Cancer Lett* 140(1-2): 27-35.
- Bub, A., B. Watzl, D. Heeb, G. Rechkemmer and K. Briviba (2001). "Malvidin-3-glucoside bioavailability in humans after ingestion of red wine, dealcoholized red wine and red grape juice." *Eur J Nutr* 40(3): 113-20.
- Cabrita, L., T. Fossen and O. M. Andersen (2000). "Colour and stability of the six common anthocyanidin 3-glucosides in aqueous solutions." *Food Chemistry* 68(1): 101-107.
- Cai, H., M. Al-Fayez, R. G. Tunstall, S. Platton, P. Greaves, W. P. Steward and A. J. Gescher (2005). "The rice bran constituent tricin potently inhibits cyclooxygenase enzymes and interferes with intestinal carcinogenesis in ApcMin mice." *Mol Cancer Ther* 4(9): 1287-92.
- Cao, G., H. U. Muccitelli, C. Sanchez-Moreno and R. L. Prior (2001). "Anthocyanins are absorbed in glycated forms in elderly women: a pharmacokinetic study." *Am J Clin Nutr* 73(5): 920-6.
- Chen, X., O. Q. Yin, Z. Zuo and M. S. Chow (2005). "Pharmacokinetics and modeling of quercetin and metabolites." *Pharm Res* 22(6): 892-901.

Colditz, G. A., L. G. Branch, R. J. Lipnick, W. C. Willett, B. Rosner, B. M. Posner and C. H. Hennekens (1985). "Increased green and yellow vegetable intake and lowered cancer deaths in an elderly population." *Am J Clin Nutr* 41(1): 32-6.

Cooke, D., W. P. Steward, A. J. Gescher and T. Marczylo (2005). "Anthocyanins from fruits and vegetables--does bright colour signal cancer chemopreventive activity?" *Eur J Cancer* 41(13): 1931-40.

Cooke, D., M. Schwarz, D. Boocock, P. Winterhalter, W. P. Steward, A. J. Gescher and T. H. Marczylo (2006). "Effect of cyanidin-3-glucoside and an anthocyanin mixture from bilberry on adenoma development in the *ApcMin* mouse model of intestinal carcinogenesis--relationship with tissue anthocyanin levels." *Int J Cancer* 119(9): 2213-20.

Cooke, D. N., Thomasset, S., Boocock, D. J., Schwarz, M., Winterhalter, P., Steward, W. P., Gescher, A. J. and T.H. Marczylo (2006a). "Development of analyses by high-performance liquid chromatography and liquid chromatography/tandem mass spectrometry of bilberry (*Vaccinium myrtillus*) anthocyanins in human plasma and urine." *J. Agric. Food Chem.* 54(19):7009-13.

Cross, M. and T. M. Dexter (1991). "Growth factors in development, transformation, and tumorigenesis." *Cell* 64(2): 271-80.

- D'Agostino, L., S. Pignata, G. Tritto, G. D'Adamo, A. Contegiacomo, B. Daniele, R. Calderopoli, C. Pizzi, G. Squame and G. Mazzacca (1995). "Hypergastrinemia in rats with azoxymethane-induced colon cancers." *Int J Cancer* 61(2): 223-6.
- Detre, Z., H. Jellinek, M. Miskulin and A. M. Robert (1986). "Studies on vascular permeability in hypertension: action of anthocyanosides." *Clin Physiol Biochem* 4(2): 143-9.
- Drazen, J. M. (2005). "COX-2 inhibitors--a lesson in unexpected problems." *N Engl J Med* 352(11): 1131-2.
- Druckrey, H., R. Preussmann, F. Matzkies and S. Ivankovic (1967). "[Selective production of intestinal cancer in rats by 1,2-dimethylhydrazine]." *Naturwissenschaften* 54(11): 285-6.
- Eberhart, C. E., R. J. Coffey, A. Radhika, F. M. Giardiello, S. Ferrenbach and R. N. DuBois (1994). "Up-regulation of cyclooxygenase 2 gene expression in human colorectal adenomas and adenocarcinomas." *Gastroenterology* 107(4): 1183-8.
- El Mohsen, M. A., Marks, J., Kuhnle, G., Moore, K., Debnam, E., Kaila Srail, S., Rice-Evans, C. and J. P. Spencer (2006). "Absorption, tissue distribution and excretion of pelargonidin and its metabolites following oral administration to rats" *Br J Nutr* 95(1): 51-8.

- Esumi, H., H. Ohgaki, E. Kohzen, S. Takayama and T. Sugimura (1989). "Induction of lymphoma in CDF1 mice by the food mutagen, 2-amino-1-methyl-6-phenylimidazo[4,5-b]pyridine." *Jpn J Cancer Res* 80(12): 1176-8.
- Ethier, S. P. (2002). "Signal transduction pathways: the molecular basis for targeted therapies." *Semin Radiat Oncol* 12(3 Suppl 2): 3-10.
- Felgines, C., S. Talavera, M. P. Gonthier, O. Texier, A. Scalbert, J. L. Lamaison and C. Remesy (2003). "Strawberry anthocyanins are recovered in urine as glucuro- and sulfoconjugates in humans." *J Nutr* 133(5): 1296-301.
- Felgines, C., S. Talavera, O. Texier, C. Besson, V. Fogliano, J. L. Lamaison, L. la Fauci, G. Galvano, C. Remesy and F. Galvano (2006). "Absorption and metabolism of red orange juice anthocyanins in rats." *Br J Nutr* 95(5): 898-904.
- Felgines, C., S. Talavera, O. Texier, A. Gil-Izquierdo, J. L. Lamaison and C. Remesy (2005). "Blackberry anthocyanins are mainly recovered from urine as methylated and glucuronidated conjugates in humans." *J Agric Food Chem* 53(20): 7721-7.
- Felgines, C., O. Texier, C. Besson, D. Fraisse, J. L. Lamaison and C. Remesy (2002). "Blackberry anthocyanins are slightly bioavailable in rats." *J Nutr* 132(6): 1249-53.

Fimognari, C., F. Berti, G. Cantelli-Forti and P. Hrelia (2004a). "Effect of cyanidin 3-O-beta-glucopyranoside on micronucleus induction in cultured human lymphocytes by four different mutagens." *Environ Mol Mutagen* 43(1): 45-52.

Fimognari, C., F. Berti, M. Nusse, G. Cantelli-Forti and P. Hrelia (2004b). "Induction of apoptosis in two human leukemia cell lines as well as differentiation in human promyelocytic cells by cyanidin-3-O-beta-glucopyranoside." *Biochem Pharmacol* 67(11): 2047-56.

Fleschhut, J., F. Kratzer, G. Rechkemmer and S. E. Kulling (2006). "Stability and biotransformation of various dietary anthocyanins in vitro." *Eur J Nutr* 45(1): 7-18.

Fodde, R., W. Edelmann, K. Yang, C. van Leeuwen, C. Carlson, B. Renault, C. Breukel, E. Alt, M. Lipkin, P. M. Khan and et al. (1994). "A targeted chain-termination mutation in the mouse Apc gene results in multiple intestinal tumors." *Proc Natl Acad Sci U S A* 91(19): 8969-73.

Fodde, R., R. Smits and H. Clevers (2001). "APC, signal transduction and genetic instability in colorectal cancer." *Nat Rev Cancer* 1(1): 55-67.

Frank, T., M. Netzel, G. Strass, R. Bitsch and I. Bitsch (2003). "Bioavailability of anthocyanidin-3-glucosides following consumption of red wine and red grape juice." *Can J Physiol Pharmacol* 81(5): 423-35.

- Freireich, E. J., E. A. Gehan, D. P. Rall, L. H. Schmidt and H. E. Skipper (1966).
"Quantitative comparison of toxicity of anticancer agents in mouse, rat,
hamster, dog, monkey, and man." *Cancer Chemother Rep* 50(4): 219-44.
- Galvano, F., L. La Fauci, G. Lazzarino, V. Fogliano, A. Ritieni, S. Ciappellano,
N. C. Battistini, B. Tavazzi and G. Galvano (2004). "Cyanidins:
metabolism and biological properties." *J Nutr Biochem* 15(1): 2-11.
- Garcia-Alonso, M., G. Rimbach, J. C. Rivas-Gonzalo and S. De Pascual-Teresa
(2004). "Antioxidant and cellular activities of anthocyanins and their
corresponding vitisins A--studies in platelets, monocytes, and human
endothelial cells." *J Agric Food Chem* 52(11): 3378-84.
- Gescher, A., U. Pastorino, S. M. Plummer and M. M. Manson (1998).
"Suppression of tumour development by substances derived from the
diet--mechanisms and clinical implications." *Br J Clin Pharmacol* 45(1): 1-
12.
- Glauert, H. P. and J. A. Weeks (1989). "Dose- and time-response of colon
carcinogenesis in Fischer-344 rats after a single dose of 1,2-
dimethylhydrazine." *Toxicol Lett* 48(3): 283-7.
- Goodlad, R. A., A. J. Ryan, S. R. Wedge, I. T. Pyrah, D. Alferez, R. Poulsom, N.
R. Smith, N. Mandir, A. J. Watkins and R. W. Wilkinson (2006).
"Inhibiting vascular endothelial growth factor receptor-2 signaling reduces

tumor burden in the ApcMin/+ mouse model of early intestinal cancer." *Carcinogenesis* 27(10): 2133-9.

Gustafson-Svard, C., I. Lilja, O. Hallbook and R. Sjodahl (1997). "Cyclooxygenase and colon cancer: clues to the aspirin effect?" *Ann Med* 29(3): 247-52.

Hagiwara, A., K. Miyashita, T. Nakanishi, M. Sano, S. Tamano, T. Kadota, T. Koda, M. Nakamura, K. Imaida, N. Ito and T. Shirai (2001). "Pronounced inhibition by a natural anthocyanin, purple corn color, of 2-amino-1-methyl-6-phenylimidazo[4,5-b]pyridine (PhIP)-associated colorectal carcinogenesis in male F344 rats pretreated with 1,2-dimethylhydrazine." *Cancer Lett* 171(1): 17-25.

Hagiwara, A., H. Yoshino, T. Ichihara, M. Kawabe, S. Tamano, H. Aoki, T. Koda, M. Nakamura, K. Imaida, N. Ito and T. Shirai (2002). "Prevention by natural food anthocyanins, purple sweet potato color and red cabbage color, of 2-amino-1-methyl-6-phenylimidazo[4,5-b]pyridine (PhIP)-associated colorectal carcinogenesis in rats initiated with 1,2-dimethylhydrazine." *J Toxicol Sci* 27(1): 57-68.

Harris, G. K., A. Gupta, R. G. Nines, L. A. Kresty, S. G. Habib, W. L. Frankel, K. LaPerle, D. D. Gallaher, S. J. Schwartz and G. D. Stoner (2001). "Effects of lyophilized black raspberries on azoxymethane-induced colon cancer and 8-hydroxy-2'-deoxyguanosine levels in the Fischer 344 rat." *Nutr Cancer* 40(2): 125-33.

He, J., B. A. Magnuson and M. M. Giusti (2005). "Analysis of anthocyanins in rat intestinal contents--impact of anthocyanin chemical structure on fecal excretion." *J Agric Food Chem* 53(8): 2859-66.

He, J., B. A. Magnuson, G. Lala, Q. Tian, S. J. Schwartz and M. M. Giusti (2006). "Intact anthocyanins and metabolites in rat urine and plasma after 3 months of anthocyanin supplementation." *Nutr Cancer* 54(1): 3-12.

Heinonen (1994). "The effect of vitamin E and beta carotene on the incidence of lung cancer and other cancers in male smokers. The Alpha-Tocopherol, Beta Carotene Cancer Prevention Study Group." *N Engl J Med* 330(15): 1029-35.

Hennekens, C. H., J. E. Buring, J. E. Manson, M. Stampfer, B. Rosner, N. R. Cook, C. Belanger, F. LaMotte, J. M. Gaziano, P. M. Ridker, W. Willett and R. Peto (1996). "Lack of effect of long-term supplementation with beta carotene on the incidence of malignant neoplasms and cardiovascular disease." *N Engl J Med* 334(18): 1145-9.

Heo, H. J. and C. Y. Lee (2005). "Strawberry and its anthocyanins reduce oxidative stress-induced apoptosis in PC12 cells." *J Agric Food Chem* 53(6): 1984-9.

Herbst, R. S. (2004). "Review of epidermal growth factor receptor biology." *Int J Radiat Oncol Biol Phys* 59(2 Suppl): 21-6.

Herbst, R. S. and C. J. Langer (2002). "Epidermal growth factor receptors as a target for cancer treatment: the emerging role of IMC-C225 in the treatment of lung and head and neck cancers." *Semin Oncol* 29(1 Suppl 4): 27-36.

Herschman, H. R. (1996). "Prostaglandin synthase 2." *Biochim Biophys Acta* 1299(1): 125-40.

Hertog, M. G., P. C. Hollman, M. B. Katan and D. Kromhout (1993). "Intake of potentially anticarcinogenic flavonoids and their determinants in adults in The Netherlands." *Nutr Cancer* 20(1): 21-9.

Heyer, J., K. Yang, M. Lipkin, W. Edelmann and R. Kucherlapati (1999). "Mouse models for colorectal cancer." *Oncogene* 18(38): 5325-33.

Hida, T., Y. Yatabe, H. Achiwa, H. Muramatsu, K. Kozaki, S. Nakamura, M. Ogawa, T. Mitsudomi, T. Sugiura and T. Takahashi (1998). "Increased expression of cyclooxygenase 2 occurs frequently in human lung cancers, specifically in adenocarcinomas." *Cancer Res* 58(17): 3761-4.

Hilmi, I. and K. L. Goh (2006). "Chemoprevention of colorectal cancer with nonsteroidal anti-inflammatory drugs." *Chin J Dig Dis* 7(1): 1-6.

- Hodgson, J. M., L. W. Morton, I. B. Puddey, L. J. Beilin and K. D. Croft (2000). "Gallic acid metabolites are markers of black tea intake in humans." *J Agric Food Chem* 48(6): 2276-80.
- Hou, D. X., M. Fujii, N. Terahara and M. Yoshimoto (2004a). "Molecular Mechanisms Behind the Chemopreventive Effects of Anthocyanidins." *J Biomed Biotechnol* 2004(5): 321-325.
- Hou, D. X., K. Kai, J. J. Li, S. Lin, N. Terahara, M. Wakamatsu, M. Fujii, M. R. Young and N. Colburn (2004b). "Anthocyanidins inhibit activator protein 1 activity and cell transformation: structure-activity relationship and molecular mechanisms." *Carcinogenesis* 25(1): 29-36.
- Hou, D. X., T. Ose, S. Lin, K. Harazoro, I. Imamura, M. Kubo, T. Uto, N. Terahara, M. Yoshimoto and M. Fujii (2003). "Anthocyanidins induce apoptosis in human promyelocytic leukemia cells: structure-activity relationship and mechanisms involved." *Int J Oncol* 23(3): 705-12.
- Hsu, T. C., M. R. Young, J. Cmarik and N. H. Colburn (2000). "Activator protein 1 (AP-1)- and nuclear factor kappaB (NF-kappaB)-dependent transcriptional events in carcinogenesis." *Free Radic Biol Med* 28(9): 1338-48.
- Hyun, J. W. and H. S. Chung (2004). "Cyanidin and Malvidin from *Oryza sativa* cv. Heugjinjubyeo mediate cytotoxicity against human monocytic

leukemia cells by arrest of G(2)/M phase and induction of apoptosis." J Agric Food Chem 52(8): 2213-7.

ICH (1996). "Guidance for Industry Q2B Validation of Analytical Procedures: Methodology." International Conference on Harmonisation of Technical Requirements for Registration of Pharmaceuticals for Human Use.

Ichibanagi, T., M. M. Rahman, Y. Kashiwada, Y. Ikeshiro, Y. Shida, Y. Hatano, H. Matsumoto, M. Hirayama, T. Tsuda and T. Konishi (2004). "Absorption and metabolism of delphinidin 3-O-beta-D-glucopyranoside in rats." Free Radic Biol Med 36(7): 930-7.

Ichibanagi, T., Y. Shida, M. M. Rahman, Y. Hatano and T. Konishi (2005b). "Extended glucuronidation is another major path of cyanidin 3-O-beta-D-glucopyranoside metabolism in rats." J Agric Food Chem 53(18): 7312-9.

Ichibanagi, T., Y. Shida, M. M. Rahman, Y. Hatano and T. Konishi (2006). "Bioavailability and tissue distribution of anthocyanins in bilberry (*Vaccinium myrtillus* L.) extract in rats." J Agric Food Chem 54(18): 6578-87.

Ichibanagi, T., Y. Shida, M. M. Rahman, Y. Hatano, H. Matsumoto, M. Hirayama and T. Konishi (2005a). "Metabolic pathway of cyanidin 3-O-beta-D-glucopyranoside in rats." J Agric Food Chem 53(1): 145-50.

- Ito, N., R. Hasegawa, K. Imaida, S. Tamano, A. Hagiwara, M. Hirose and T. Shirai (1997). "Carcinogenicity of 2-amino-1-methyl-6-phenylimidazo[4,5-b]pyridine (PhIP) in the rat." *Mutat Res* 376(1-2): 107-14.
- Jacoby, R. F., D. J. Marshall, M. A. Newton, K. Novakovic, K. Tutsch, C. E. Cole, R. A. Lubet, G. J. Kelloff, A. Verma, A. R. Moser and W. F. Dove (1996). "Chemoprevention of spontaneous intestinal adenomas in the Apc Min mouse model by the nonsteroidal anti-inflammatory drug piroxicam." *Cancer Res* 56(4): 710-4.
- Jacoby, R. F., K. Seibert, C. E. Cole, G. Kelloff and R. A. Lubet (2000). "The cyclooxygenase-2 inhibitor celecoxib is a potent preventive and therapeutic agent in the min mouse model of adenomatous polyposis." *Cancer Res* 60(18): 5040-4.
- Jen, J., S. M. Powell, N. Papadopoulos, K. J. Smith, S. R. Hamilton, B. Vogelstein and K. W. Kinzler (1994). "Molecular determinants of dysplasia in colorectal lesions." *Cancer Res* 54(21): 5523-6.
- Kang, S. Y., N. P. Seeram, M. G. Nair and L. D. Bourquin (2003). "Tart cherry anthocyanins inhibit tumor development in Apc(Min) mice and reduce proliferation of human colon cancer cells." *Cancer Lett* 194(1): 13-9.
- Katsube, N., K. Iwashita, T. Tsushida, K. Yamaki and M. Kobori (2003). "Induction of apoptosis in cancer cells by Bilberry (*Vaccinium myrtillus*) and the anthocyanins." *J Agric Food Chem* 51(1): 68-75.

- Kay, C. D., G. Mazza, B. J. Holub and J. Wang (2004). "Anthocyanin metabolites in human urine and serum." *Br J Nutr* 91(6): 933-42.
- Kay, C. D., G. J. Mazza and B. J. Holub (2005). "Anthocyanins exist in the circulation primarily as metabolites in adult men." *J Nutr* 135(11): 2582-8.
- Kelley, D. J., J. R. Mestre, K. Subbaramaiah, P. G. Sacks, S. P. Schantz, T. Tanabe, H. Inoue, J. T. Ramonetti and A. J. Dannenberg (1997). "Benzo[a]pyrene up-regulates cyclooxygenase-2 gene expression in oral epithelial cells." *Carcinogenesis* 18(4): 795-9.
- Keppler, K. and H. U. Humpf (2005). "Metabolism of anthocyanins and their phenolic degradation products by the intestinal microflora." *Bioorg Med Chem* 13(17): 5195-205.
- Kern, M., Fridrich, D., Reichert, J., Skrbek, S., Nussner, A., Hofem, S., Pahlke, G., Rufer, C and D Marko (2007) "Limited stability in cell culture medium and hydrogen peroxide formation affect the growth inhibitory properties of delphinidin and its degradation product gallic acid." *Mol Nutr Food Res* 51(9): 1163-72
- Kinzler, K. W. and B. Vogelstein (1996). "Lessons from hereditary colorectal cancer." *Cell* 87(2): 159-70.
- Kobaek-Larsen, M., I. Thorup, A. Diederichsen, C. Fenger and M. R. Hoitinga (2000). "Review of colorectal cancer and its metastases in rodent

models: comparative aspects with those in humans." *Comp Med* 50(1): 16-26.

Koide, T., H. Kamei, Y. Hashimoto, T. Kojima and M. Hasegawa (1996). "Antitumor effect of hydrolyzed anthocyanin from grape rinds and red rice." *Cancer Biother Radiopharm* 11(4): 273-7.

Kutchera, W., D. A. Jones, N. Matsunami, J. Groden, T. M. McIntyre, G. A. Zimmerman, R. L. White and S. M. Prescott (1996). "Prostaglandin H synthase 2 is expressed abnormally in human colon cancer: evidence for a transcriptional effect." *Proc Natl Acad Sci U S A* 93(10): 4816-20.

Lala, G., M. Malik, C. Zhao, J. He, Y. Kwon, M. M. Giusti and B. A. Magnuson (2006). "Anthocyanin-rich extracts inhibit multiple biomarkers of colon cancer in rats." *Nutr Cancer* 54(1): 84-93.

Lamprecht, S. A. and M. Lipkin (2002). "Migrating colonic crypt epithelial cells: primary targets for transformation." *Carcinogenesis* 23(11): 1777-80.

Lapidot, T., S. Harel, B. Akiri, R. Granit and J. Kanner (1999). "PH-dependent forms of red wine anthocyanins as antioxidants." *J Agric Food Chem* 47(1): 67-70.

Laquer, G. (1964). "Carcinogen effect of cycad meal and cycasin methylazoxymethanol glycoside, in rats and effects of cycasin in germ-free rats." *Fed. Proc.* 23(23): 1386 1387.

- Lazze, M. C., M. Savio, R. Pizzala, O. Cazzalini, P. Perucca, A. I. Scovassi, L. A. Stivala and L. Bianchi (2004). "Anthocyanins induce cell cycle perturbations and apoptosis in different human cell lines." *Carcinogenesis* 25(8): 1427-33.
- Leaver, D. D., P. F. Swann and P. N. Magee (1969). "The induction of tumours in the rat by a single oral dose of N-nitrosomethylurea." *Br J Cancer* 23(1): 177-87.
- Lee, I. M., N. R. Cook, J. E. Manson, J. E. Buring and C. H. Hennekens (1999). "Beta-carotene supplementation and incidence of cancer and cardiovascular disease: the Women's Health Study." *J Natl Cancer Inst* 91(24): 2102-6.
- Leuratti, C., R. Singh, C. Lagneau, P. B. Farmer, J. P. Plastaras, L. J. Marnett and D. E. Shuker (1998). "Determination of malondialdehyde-induced DNA damage in human tissues using an immunoslot blot assay." *Carcinogenesis* 19(11): 1919-24.
- Lorenz, E. a. S., H L (1941). "Intestinal carcinoma and other lesions in mice following oral administration of 1, 2, 5, 6-dibenzanthracene and 20-methylcholanthracene." *J. Natl. Cancer Inst.* 1:17-40.
- Magnuson, B. A. C. Z., Geeta Lala, YoungJoo Kwon, Tao Yu, Jonathan Friedman, Chika Obele, Minnie Malik (2003). "Anthocyanin-Rich Extracts

Inhibit Growth of Human Colon Cancer Cells and Azoxymethane-Induced Colon Aberrant Crypts in Rats: Implications for Colon Cancer Chemoprevention." AACR 2003 Cancer Epidemiology Biomarkers & Prevention AACR Poster: 1323s - 1324s.

Manach, C., G. Williamson, C. Morand, A. Scalbert and C. Remesy (2005).

"Bioavailability and bioefficacy of polyphenols in humans. I. Review of 97 bioavailability studies." Am J Clin Nutr 81(1 Suppl): 230S-242S.

Mandel, J. S., J. H. Bond, T. R. Church, D. C. Snover, G. M. Bradley, L. M.

Schuman and F. Ederer (1993). "Reducing mortality from colorectal cancer by screening for fecal occult blood. Minnesota Colon Cancer Control Study." N Engl J Med 328(19): 1365-71.

Manson, M. M. (2003). "Cancer prevention -- the potential for diet to modulate molecular signalling." Trends Mol Med 9(1): 11-8.

Marczylo, T. H., R. D. Verschoyle, D. N. Cooke, P. Morazzoni, W. P. Steward

and A. J. Gescher (2007). "Comparison of systemic availability of curcumin with that of curcumin formulated with phosphatidylcholine." Cancer Chemother Pharmacol 60(2): 171-7.

Marko, D., N. Puppel, Z. Tjaden, S. Jakobs and G. Pahlke (2004). "The

substitution pattern of anthocyanidins affects different cellular signaling cascades regulating cell proliferation." Mol Nutr Food Res 48(4): 318-25.

- Marnett, L. J. (1999). "Lipid peroxidation-DNA damage by malondialdehyde." *Mutat Res* 424(1-2): 83-95.
- Maskens, A. P. (1976). "Histogenesis and growth pattern of 1,2-dimethylhydrazine-induced rat colon adenocarcinoma." *Cancer Res* 36(5): 1585-92.
- Matsumoto, H., T. Ichiyanagi, H. Iida, K. Ito, T. Tsuda, M. Hirayama and T. Konishi (2006). "Ingested delphinidin-3-rutinoside is primarily excreted to urine as the intact form and to bile as the methylated form in rats." *J Agric Food Chem* 54(2): 578-82.
- Matsumoto, H., H. Inaba, M. Kishi, S. Tominaga, M. Hirayama and T. Tsuda (2001). "Orally administered delphinidin 3-rutinoside and cyanidin 3-rutinoside are directly absorbed in rats and humans and appear in the blood as the intact forms." *J Agric Food Chem* 49(3): 1546-51.
- Mazza, G., C. D. Kay, T. Cottrell and B. J. Holub (2002). "Absorption of anthocyanins from blueberries and serum antioxidant status in human subjects." *J Agric Food Chem* 50(26): 7731-7.
- McLellan, E. A., A. Medline and R. P. Bird (1991). "Sequential analyses of the growth and morphological characteristics of aberrant crypt foci: putative preneoplastic lesions." *Cancer Res* 51(19): 5270-4.

Meiers, S., M. Kemeny, U. Weyand, R. Gastpar, E. von Angerer and D. Marko (2001). "The anthocyanidins cyanidin and delphinidin are potent inhibitors of the epidermal growth-factor receptor." *J Agric Food Chem* 49(2): 958-62.

Meng, X., M. J. Lee, C. Li, S. Sheng, N. Zhu, S. Sang, C. T. Ho and C. S. Yang (2001). "Formation and identification of 4'-O-methyl-(-)-epigallocatechin in humans." *Drug Metab Dispos* 29(6): 789-93.

Mestre, J. R., G. Chan, F. Zhang, E. K. Yang, P. G. Sacks, J. O. Boyle, J. P. Shah, D. Edelstein, K. Subbaramaiah and A. J. Dannenberg (1999). "Inhibition of cyclooxygenase-2 expression. An approach to preventing head and neck cancer." *Ann N Y Acad Sci* 889: 62-71.

Meyer, D., H. P. Schmid and D. S. Engeler (2007). "[Therapy and follow-up of bladder cancer.]." *Wien Med Wochenschr* 157(7-8): 162-9.

Milbury, P. E., G. Cao, R. L. Prior and J. Blumberg (2002). "Bioavailability of elderberry anthocyanins." *Mech Ageing Dev* 123(8): 997-1006.

Milner, J. A., S. S. McDonald, D. E. Anderson and P. Greenwald (2001). "Molecular targets for nutrients involved with cancer prevention." *Nutr Cancer* 41(1-2): 1-16.

Miyazawa, T., K. Nakagawa, M. Kudo, K. Muraishi and K. Someya (1999). "Direct intestinal absorption of red fruit anthocyanins, cyanidin-3-

glucoside and cyanidin-3,5-diglucoside, into rats and humans." *J Agric Food Chem* 47(3): 1083-91.

Morazzoni, P. (1996). *Fitoterapia* LXVII - N.1.

Moser, A. R., H. C. Pitot and W. F. Dove (1990). "A dominant mutation that predisposes to multiple intestinal neoplasia in the mouse." *Science* 247(4940): 322-4.

Netzel, M., G. Strass, M. Janssen, I. Bitsch and R. Bitsch (2001). "Bioactive anthocyanins detected in human urine after ingestion of blackcurrant juice." *J Environ Pathol Toxicol Oncol* 20(2): 89-95.

Nielsen, I. L., L. O. Dragsted, G. Ravn-Haren, R. Freese and S. E. Rasmussen (2003b). "Absorption and excretion of black currant anthocyanins in humans and watanabe heritable hyperlipidemic rabbits." *J Agric Food Chem* 51(9): 2813-20.

Nielsen, I. L., G. R. Haren, E. L. Magnussen, L. O. Dragsted and S. E. Rasmussen (2003a). "Quantification of anthocyanins in commercial black currant juices by simple high-performance liquid chromatography. Investigation of their pH stability and antioxidative potency." *J Agric Food Chem* 51(20): 5861-6.

Noda, Y., T. Kaneyuki, A. Mori and L. Packer (2002). "Antioxidant activities of pomegranate fruit extract and its anthocyanidins: delphinidin, cyanidin, and pelargonidin." *J Agric Food Chem* 50(1): 166-71.

Nordlinger, B., Y. Panis, J. P. Puts, J. P. Herve, R. Delelo and F. Ballet (1991).

"Experimental model of colon cancer: recurrences after surgery alone or associated with intraperitoneal 5-fluorouracil chemotherapy." *Dis Colon Rectum* 34(8): 658-63.

Nyman, N. A. and J. T. Kumpulainen (2001). "Determination of anthocyanidins in berries and red wine by high-performance liquid chromatography." *J Agric Food Chem* 49(9): 4183-7.

Olsson, M. E., K. E. Gustavsson, S. Andersson, A. Nilsson and R. D. Duan (2004). "Inhibition of cancer cell proliferation in vitro by fruit and berry extracts and correlations with antioxidant levels." *J Agric Food Chem* 52(24): 7264-71.

Omenn, G. S., G. Goodman, M. Thornquist, J. Grizzle, L. Rosenstock, S. Barnhart, J. Balmes, M. G. Cherniack, M. R. Cullen, A. Glass and et al. (1994). "The beta-carotene and retinol efficacy trial (CARET) for chemoprevention of lung cancer in high risk populations: smokers and asbestos-exposed workers." *Cancer Res* 54(7 Suppl): 2038s-2043s.

Orner, G. A., W. M. Dashwood, C. A. Blum, G. D. Diaz, Q. Li and R. H. Dashwood (2003). "Suppression of tumorigenesis in the Apc(min) mouse: down-regulation of beta-catenin signaling by a combination of tea plus sulindac." *Carcinogenesis* 24(2): 263-7.

- Oshima, M., J. E. Dinchuk, S. L. Kargman, H. Oshima, B. Hancock, E. Kwong, J. M. Trzaskos, J. F. Evans and M. M. Taketo (1996b). "Suppression of intestinal polyposis in Apc delta716 knockout mice by inhibition of cyclooxygenase 2 (COX-2)." *Cell* 87(5): 803-9.
- Oshima, M., H. Oshima, M. Tsutsumi, S. Nishimura, T. Sugimura, M. Nagao and M. M. Taketo (1996a). "Effects of 2-amino-1-methyl-6-phenylimidazo[4,5-b]pyridine on intestinal polyp development in Apc delta 716 knockout mice." *Mol Carcinog* 15(1): 11-7.
- Ozturk, O., T. Isbir, I. Yaylim, C. I. Kocaturk and A. Gurses (2003). "GST M1 and CYP1A1 gene polymorphism and daily fruit consumption in Turkish patients with non-small cell lung carcinomas." *In Vivo* 17(6): 625-32.
- Pan, M. H., T. M. Huang and J. K. Lin (1999). "Biotransformation of curcumin through reduction and glucuronidation in mice." *Drug Metab Dispos* 27(4): 486-94.
- Passamonti, S., U. Vrhovsek and F. Mattivi (2002). "The interaction of anthocyanins with bilitranslocase." *Biochem Biophys Res Commun* 296(3): 631-6.
- Perkins, S., R. D. Verschoyle, K. Hill, I. Parveen, M. D. Threadgill, R. A. Sharma, M. L. Williams, W. P. Steward and A. J. Gescher (2002). "Chemopreventive efficacy and pharmacokinetics of curcumin in the

min/+ mouse, a model of familial adenomatous polyposis." *Cancer Epidemiol Biomarkers Prev* 11(6): 535-40.

Pretlow, T. P., M. A. O'Riordan, T. G. Pretlow and T. A. Stellato (1992). "Aberrant crypts in human colonic mucosa: putative preneoplastic lesions." *J Cell Biochem Suppl* 16G: 55-62.

Ramirez-Tortosa, C., O. M. Andersen, P. T. Gardner, P. C. Morrice, S. G. Wood, S. J. Duthie, A. R. Collins and G. G. Duthie (2001). "Anthocyanin-rich extract decreases indices of lipid peroxidation and DNA damage in vitamin E-depleted rats." *Free Radic Biol Med* 31(9): 1033-7.

Rao, C. V., T. Kawamori, R. Hamid and B. S. Reddy (1999). "Chemoprevention of colonic aberrant crypt foci by an inducible nitric oxide synthase-selective inhibitor." *Carcinogenesis* 20(4): 641-4.

Rice-Evans, C. A., N. J. Miller and G. Paganga (1996). "Structure-antioxidant activity relationships of flavonoids and phenolic acids." *Free Radic Biol Med* 20(7): 933-56.

Ristimaki, A., N. Honkanen, H. Jankala, P. Sipponen and M. Harkonen (1997). "Expression of cyclooxygenase-2 in human gastric carcinoma." *Cancer Res* 57(7): 1276-80.

Rubinfeld, B., B. Souza, I. Albert, O. Muller, S. H. Chamberlain, F. R. Masiarz, S. Munemitsu and P. Polakis (1993). "Association of the APC gene product with beta-catenin." *Science* 262(5140): 1731-4.

Rubio, C. A. and S. Takayama (1994). "Difference in histology and size in colonic tumors of rats receiving two different carcinogens." *J Environ Pathol Toxicol Oncol* 13(3): 191-7.

Sabaté, E. (2003). "Adherence to long-term therapies : evidence for action " World health Organization: 196.

Sardas, S. (2003). "The role of antioxidants in cancer prevention and treatment." *Indoor Built Environ* 12: 401-404.

Schwarz, M., S. Hillebrand, S. Habben, A. Degenhardt and P. Winterhalter (2003). "Application of high-speed countercurrent chromatography to the large-scale isolation of anthocyanins." *Biochemical Engineering Journal* 14(3): 179-189.

Seeram, N. P., R. A. Momin, M. G. Nair and L. D. Bourquin (2001). "Cyclooxygenase inhibitory and antioxidant cyanidin glycosides in cherries and berries." *Phytomedicine* 8(5): 362-9.

Seeram, N. P. and M. G. Nair (2002). "Inhibition of lipid peroxidation and structure-activity-related studies of the dietary constituents anthocyanins, anthocyanidins, and catechins." *J Agric Food Chem* 50(19): 5308-12.

- Seeram, N. P., Y. Zhang and M. G. Nair (2003). "Inhibition of proliferation of human cancer cells and cyclooxygenase enzymes by anthocyanidins and catechins." *Nutr Cancer* 46(1): 101-6.
- Shahrzad, S. and I. Bitsch (1998). "Determination of gallic acid and its metabolites in human plasma and urine by high-performance liquid chromatography." *J Chromatogr B Biomed Sci Appl* 705(1): 87-95.
- Shamsuddin, A. K. and B. F. Trump (1981). "Colon epithelium. II. In vivo studies of colon carcinogenesis. Light microscopic, histochemical, and ultrastructural studies of histogenesis of azoxymethane-induced colon carcinomas in Fischer 344 rats." *J Natl Cancer Inst* 66(2): 389-401.
- Sharma, R. A. and P. B. Farmer (2004). "Biological relevance of adduct detection to the chemoprevention of cancer." *Clin Cancer Res* 10(15): 4901-12.
- Shin, S. C., J. S. Choi and X. Li (2006). "Enhanced bioavailability of tamoxifen after oral administration of tamoxifen with quercetin in rats." *Int J Pharm* 313(1-2): 144-9.
- Singh, R., C. Leuratti, S. Josyula, M. A. Sipowicz, B. A. Diwan, K. S. Kasprzak, H. A. Schut, L. J. Marnett, L. M. Anderson and D. E. Shuker (2001). "Lobe-specific increases in malondialdehyde DNA adduct formation in the livers of mice following infection with *Helicobacter hepaticus*." *Carcinogenesis* 22(8): 1281-7.

Singletary, K. W., M. J. Stansbury, M. Giusti, R. B. Van Breemen, M. Wallig and A. Rimando (2003). "Inhibition of rat mammary tumorigenesis by concord grape juice constituents." J Agric Food Chem 51(25): 7280-6.

Sorensen, I. K., E. Kristiansen, A. Mortensen, H. van Kranen, C. van Kreijl, R. Fodde and S. S. Thorgeirsson (1997). "Short-term carcinogenicity testing of a potent murine intestinal mutagen, 2-amino-1-methyl-6-phenylimidazo(4,5-b)pyridine (PhIP), in Apc1638N transgenic mice." Carcinogenesis 18(4): 777-81.

Sporn, M. B. and K. T. Liby (2005). "Cancer chemoprevention: scientific promise, clinical uncertainty." Nat Clin Pract Oncol 2(10): 518-25.

Sporn, M. B. and N. Suh (2000). "Chemoprevention of cancer." Carcinogenesis 21(3): 525-30.

Stoner, G. D., C. Sardo, G. Apseloff, D. Mullet, W. Wargo, V. Pound, A. Singh, J. Sanders, R. Aziz, B. Casto and X. Sun (2005). "Pharmacokinetics of anthocyanins and ellagic acid in healthy volunteers fed freeze-dried black raspberries daily for 7 days." J Clin Pharmacol 45(10): 1153-64.

Su, L. K., K. W. Kinzler, B. Vogelstein, A. C. Preisinger, A. R. Moser, C. Luongo, K. A. Gould and W. F. Dove (1992). "Multiple intestinal neoplasia caused by a mutation in the murine homolog of the APC gene." Science 256(5057): 668-70.

Su, L. K., B. Vogelstein and K. W. Kinzler (1993). "Association of the APC tumor suppressor protein with catenins." *Science* 262(5140): 1734-7.

Subbaramaiah, K., N. Telang, J. T. Ramonetti, R. Araki, B. DeVito, B. B. Weksler and A. J. Dannenberg (1996). "Transcription of cyclooxygenase-2 is enhanced in transformed mammary epithelial cells." *Cancer Res* 56(19): 4424-9.

Sugimura, T. (1997). "Overview of carcinogenic heterocyclic amines." *Mutat Res* 376(1-2): 211-9.

Surh, Y. J. (2003). "Cancer chemoprevention with dietary phytochemicals." *Nat Rev Cancer* 3(10): 768-80.

Swamy, M. V., J. M. Patlolla, V. E. Steele, L. Kopelovich, B. S. Reddy and C. V. Rao (2006). "Chemoprevention of familial adenomatous polyposis by low doses of atorvastatin and celecoxib given individually and in combination to APCMin mice." *Cancer Res* 66(14): 7370-7.

Takaku, K., M. Oshima, H. Miyoshi, M. Matsui, M. F. Seldin and M. M. Taketo (1998). "Intestinal tumorigenesis in compound mutant mice of both Dpc4 (Smad4) and Apc genes." *Cell* 92(5): 645-56.

Taketo, M. M. (1998). "Cyclooxygenase-2 inhibitors in tumorigenesis (Part II)." *J Natl Cancer Inst* 90(21): 1609-20.

Taketo, M. M. and K. Takaku (2000). "Gastro-intestinal tumorigenesis in Smad4 mutant mice." Cytokine Growth Factor Rev 11(1-2): 147-57.

Talavera, S., C. Felgines, O. Texier, C. Besson, A. Gil-Izquierdo, J. L. Lamaison and C. Remesy (2005). "Anthocyanin metabolism in rats and their distribution to digestive area, kidney, and brain." J Agric Food Chem 53(10): 3902-8.

Talavera, S., C. Felgines, O. Texier, C. Besson, J. L. Lamaison and C. Remesy (2003). "Anthocyanins are efficiently absorbed from the stomach in anesthetized rats." J Nutr 133(12): 4178-82.

Talavera, S., C. Felgines, O. Texier, C. Besson, C. Manach, J. L. Lamaison and C. Remesy (2004). "Anthocyanins are efficiently absorbed from the small intestine in rats." J Nutr 134(9): 2275-9.

Thorup, I., O. Meyer and E. Kristiansen (1992). "Effect of a dietary fiber (beet fiber) on dimethylhydrazine-induced colon cancer in Wistar rats." Nutr Cancer 17(3): 251-61.

Thorup, I., O. Meyer and E. Kristiansen (1994). "Influence of a dietary fiber on development of dimethylhydrazine-induced aberrant crypt foci and colon tumor incidence in Wistar rats." Nutr Cancer 21(2): 177-82.

Tsao, A. S., E. S. Kim and W. K. Hong (2004). "Chemoprevention of cancer."
CA Cancer J Clin 54(3): 150-80.

Tsuda, T., F. Horio and T. Osawa (1999). "Absorption and metabolism of
cyanidin 3-O-beta-D-glucoside in rats." FEBS Lett 449(2-3): 179-82.

Tsuda, T., M. Watanabe, K. Ohshima, S. Norinobu, S. Choi, S. Kawakshi and T.
Osawa (1994). "Antioxidative activity of the anthocyanin pigments
cyanidin-3-O-Beta-d-glucoside and cyanidin." J. Agric. Food Chem.
42(11): 2407 - 2410.

Tsunoda, A., M. Shibusawa, Y. Tsunoda, N. Yasuda and T. Koike (1992).
"Reduced growth rate of dimethylhydrazine-induced colon tumors in
rats." Cancer Res 52(3): 696-700.

Verschoye, R. D., Greaves, P., Cai, H., Edwards, R. E., Steward, W. P., and A.
J. Gescher (2007). "Evaluation of the cancer chemopreventive efficacy
of rice bran in genetic mouse models of breast, prostate and intestinal
carcinogenesis." Br J Cancer 96(2): 248-54

Vogelstein, B., E. R. Fearon, S. R. Hamilton, S. E. Kern, A. C. Preisinger, M.
Leppert, Y. Nakamura, R. White, A. M. Smits and J. L. Bos (1988).
"Genetic alterations during colorectal-tumor development." N Engl J Med
319(9): 525-32.

Waddell, W. R. and R. W. Loughry (1983). "Sulindac for polyposis of the colon."
J Surg Oncol 24(1): 83-7.

Wakabayashi, K., M. Nagao, H. Esumi and T. Sugimura (1992). "Food-derived
mutagens and carcinogens." Cancer Res 52(7 Suppl): 2092s-2098s.

Wang, H., M. G. Nair, G. M. Strasburg, Y. C. Chang, A. M. Booren, J. I. Gray
and D. L. DeWitt (1999). "Antioxidant and antiinflammatory activities of
anthocyanins and their aglycon, cyanidin, from tart cherries." J Nat Prod
62(2): 294-6.

Wattenberg, L. W. (1972). "Inhibition of carcinogenic and toxic effects of
polycyclic hydrocarbons by phenolic antioxidants and ethoxyquin." J Natl
Cancer Inst 48(5): 1425-30.

Wattenberg, L. W. (1983). "Inhibition of neoplasia by minor dietary
constituents." Cancer Res 43(5 Suppl): 2448s-2453s.

Wattenberg, L. W. (1985). "Chemoprevention of cancer." Cancer Res 45(1): 1-
8.

Weinberg, R. A. (2006). "The Biology of Cancer." Garland Science.

Woodford, D. W. and L. J. Lesko (1981). "Relative bioavailability of aspirin
gum." J Pharm Sci 70(12): 1341-3.

- Wu, X., G. Cao and R. L. Prior (2002). "Absorption and metabolism of anthocyanins in elderly women after consumption of elderberry or blueberry." *J Nutr* 132(7): 1865-71.
- Wu, X., H. E. Pittman, 3rd and R. L. Prior (2004). "Pelargonidin is absorbed and metabolized differently than cyanidin after marionberry consumption in pigs." *J Nutr* 134(10): 2603-10.
- Wu, X. and R. L. Prior (2005). "Identification and characterization of anthocyanins by high-performance liquid chromatography-electrospray ionization-tandem mass spectrometry in common foods in the United States: vegetables, nuts, and grains." *J Agric Food Chem* 53(8): 3101-13.
- Yang, J., N. Shikata, H. Mizuoka and A. Tsubura (1996). "Colon carcinogenesis in shrews by intrarectal infusion of N-methyl-N-nitrosourea." *Cancer Lett* 110(1-2): 105-12.
- Yang, K., W. Edelmann, K. Fan, K. Lau, V. R. Kolli, R. Fodde, P. M. Khan, R. Kucherlapati and M. Lipkin (1997). "A mouse model of human familial adenomatous polyposis." *J Exp Zool* 277(3): 245-54.
- Yona, D. and N. Arber (2006). "Coxibs and cancer prevention." *J Cardiovasc Pharmacol* 47 Suppl 1: S76-81.

- Zhang, Y., S. K. Vareed and M. G. Nair (2005). "Human tumor cell growth inhibition by nontoxic anthocyanidins, the pigments in fruits and vegetables." *Life Sci* 76(13): 1465-72.
- Zhao, C., M. M. Giusti, M. Malik, M. P. Moyer and B. A. Magnuson (2004). "Effects of commercial anthocyanin-rich extracts on colonic cancer and nontumorigenic colonic cell growth." *J Agric Food Chem* 52(20): 6122-8.
- Zheng, W. and S. Y. Wang (2003). "Oxygen radical absorbing capacity of phenolics in blueberries, cranberries, chokeberries, and lingonberries." *J Agric Food Chem* 51(2): 502-9.
- Zingirian, M., M. T. Dorigo and E. Gandolfo (1990). "Contribution of manual and computerized perimetry to the differential diagnosis of optic neuropathies." *Metab Pediatr Syst Ophthalmol* 13(2-4): 50-4.
- Zusman, I., A. Zimmer and A. Nyska (1991). "Role of morphological methods in the analysis of chemically induced colon cancer in rats." *Acta Anat (Basel)* 142(4): 351-6.